MATHEMATICAL MODELING OF
BLOOD PRESSURE AND CEREBRAL BLOOD FLOW USING
PHOTOPLETHYSMOGRAPHY SIGNAL

by

ARMIN SOLTAN ZADI

DISSERTATION

Submitted in partial fulfillment of the requirements
for the degree of Doctor of Philosophy at
The University of Texas at Arlington
May, 2019

Arlington, Texas

Supervising Committee:

Dr. George Alexandrakis
Dr. Khosrow Behbehani, Supervising
Dr. Hanli Liu
Dr. Rong Zhang

ABSTRACT

Mathematical Modeling of

Blood Pressure and Cerebral Blood Flow

from Photoplethysmography Signal

Armin Soltan zadi, Ph.D.

The University of Texas at Arlington, 20XX

Supervising Professor: Khosrow Behbehani

Continuous and non-invasive monitoring of blood pressure (BP) and cerebral blood flow (CBF) has numerous clinical and health maintenance applications. Of particular interest is monitoring of BP and CBF during events that stress the cardiovascular system such as cessation of breathing during sleep apnea. Current means and methods of continuous measurement of these signals are either invasive or require expensive equipment. Therefore, investigation of new methods of continuous estimation of the BP and CBF are of high interest. One attractive alternative is to use photoplethysmography (PPG) technique to estimate BP and CBF, as PPG is shown to be able to detect blood volume changes in peripheral vasculature. This study aims to investigate the feasibility of estimating key parameters of BP and CBF using PPG. Specifically, it is hypothesized that apnea-induced fluctuations in blood pressure and cerebral blood flow can be estimated using photoplethysmography.

We propose a new method for the continuous estimation of systolic and diastolic values as well as peaks and troughs of cerebral blood flow. The estimates are obtained from a

photoplethysmography signal as input to a fifth order autoregressive moving average (ARMA) models. The ARMA models are suited for physiological modeling because they are dynamic. They integrate past and present samples of input as well as past samples of the estimated output to estimate the present value of the output. Further, ARMA models accommodate pure time delays that are often present in physiological system response.

To test the said hypothesis using the proposed ARMA modeling approach, we performed two studies: 1) breath-hold (BH) maneuver was used as a means of simulating apnea to elicit changes in both BP and CBF, and 2) polysomnography sleep (PSG) study of patients suspected of having obstructive sleep apnea (OSA) was conducted. During both studies, concurrent measurement of BP, CBF, and PPG was made. BH protocol consisted of 5 consecutive BH with 90 seconds normal breathing (NB) interval in between and 60 seconds of NB at the beginning and at the end. For BH study, beat-to-beat full-wave BP and CBF of 15 subjects (8 males, 7 females, aged 28.9 ± 5.0 years, BMI 24.1 ± 4.8 kg/m^2) with no known cardiovascular disorder were recorded. For sleep study, same measurements of 15 OSA patients (10 males, 5 females, aged 53.8 ± 7.4 years, BMI 34.2 ± 7.2 kg/m^2) were recorded during PSG study. From each subject's dataset 6 longest apneas were selected to keep the statistical analysis as consistent as possible to the BH study. Each BH/NB interval, or apnea episode in case of sleep study, was evaluated with all other congruent intervals to ascertain the accuracy of the models and resulted in both modeling and validation errors which were further used to calculate means, standard deviations and rMSE.

For BH study, the mean of model residuals for was less than 3 mmHg for BP modeling and less than 4 cm/s for CBF modeling and the root mean squared (rMSE) of the ARMA model residuals, was less than 8 mmHg during the study for modeling BP and less than 11 cm/s for CBF. Also, maximum standard deviation was calculated to be less than 9 mmHG for the BP modeling

and less than 13 cm/s for CBF modeling. For the sleep apnea study, mean of residuals for BP was less than 8 mmHG and the rMSE of the model residuals was less than 22 mmHG. Further, for this study, the mean of residuals for CBF estimates was less than 13 cm/s and their rMSE values was less than 15 cm/s. Standard deviation of the errors were all less than 34 mmHG with average of 15.83 mmHg for BP modeling and 20 cm/s with average of 7.28 cm/s for CBF modeling.

BH modeling results indicate that ARMA model can provide estimates with adequate accuracy to be of practical use in estimating BP and CBF values. In contrast, for PSG study, further development, including better feature selection and possibly non-linear modeling may be needed to increase the accuracy of the estimates. Results of both studies suggest that with further development, it may be possible to get reasonable estimates of key features of blood pressure or cerebral blood flow from PPG, creating opportunities for improvement in monitoring cerebrovascular and cardiovascular system health. One such opportunity is the ability to nocturnally measure blood pressure and cerebral blood flow using now widely available and reasonably-priced pulse oximeter systems, as they are capable of delivering PPG signal.

ACKNOWLEDGEMENTS

First and foremost I would like to express my sincere gratitude to my advisor Professor Khosrow Behbehani. It has been an honor to be his Ph.D. student. I appreciate all his contributions of time, ideas, and funding to make my Ph.D. experience productive and stimulating. The joy and enthusiasm he has for his research was contagious and motivational for me, even during tough times in the Ph.D. pursuit. I am also thankful for the excellent example he has provided by his respectful character and personality. Besides my advisor, I would like to thank the rest of my dissertation committee members (Dr. Rong Zhang, Dr. Hanli Liu and Dr. George Alexandrakis) for their insightful comments and invaluable advice. I am also thankful to Dr. Donald Watenpaugh, from Sleep Consultants Inc., for materializing my study by subject recruitment.

I am also grateful to my fellow colleagues at Bio-signal processing lab, Raichel M. Alex, Ahmad F. Turki and Mahrshi B. Jani for extending their help and support in all possible ways.

My gratitude goes to the faculty and staff of Bioengineering department for their support throughout my PhD study. Special thanks to Ms. Julia Rockow for all her help and encouragement from the day I arrived at UTA to the last day.

April 25, 2019

DEDICATION

I dedicate this thesis to my family and friends for their unwavering support. A special feeling of gratitude to my loving parents, Pooran and Ghasem, whose words of encouragement and push for tenacity ring in my ears. All my childhood memories are full of sweet things you did for me. I appreciate how you raised me and all the extra love that you gave me.

I also dedicate this work to my lovely wife, Farnaz, who has always accepted me for me and supported my hustle, drive and ambition. You have been my inspiration and my soul mate.

At the end, I would like to thank my sister Atena and all my friends whose encouragement made me able to achieve such success and honor.

Armin Soltan zadi

April 25, 2019

TABLE OF CONTENTS

LIST OF FIGURES

LIST OF TABLES

CHAPTER 1

Introduction

1.1 Sleep apnea

The temporary and intermittent cessation or reduction of airflow for more than 10 seconds during sleep is called sleep apnea [1]. Sleep apnea causes arterial oxygen concentration reduction (hypoxia) and CO2 accumulation (hypercapnia) which is usually followed by micro-arousals to resume the breathing [2]. In patients with severe apnea, apnea can occur hundreds of times during a single night sleep. These frequent pauses can lead to sleep fragmentation and deprivation of quality of sleep [3]. It is of high importance to timely diagnose and treat sleep apnea because of its association with serious diseases such as hypertension, stroke, cognitive impairment, cerebrovascular and neurological morbidities and mortalities as well as other metabolic complications [4].

1.1.1 Types and pathogenesis of sleep apnea types

Sleep apnea can be categorized into two major types based on the cause of the apnea: 1) obstructive sleep apnea (OSA), and 2) central sleep apnea (CSA) [5]. The obstructive sleep apnea (OSA) is by far the most common type and it is believed that the relaxation of soft palate at the base of tongue due to lack of muscle tone during sleep mediates it. It causes recurrent episodes of partial (Hypopnea) or complete (Apnea) blockage of the upper airway, followed by sleep arousal and excessive respiratory effort to overcome the obstruction. The symptoms of OSA include loud snoring, abnormal pattern of breathing with gasps and pauses, morning headaches, and excessive daytime sleepiness. The other type of apnea is called central sleep apnea, believed to be caused by failure of the respiratory center in brainstem to regulate the respiratory muscles during sleep.

Therefore, there will be no inspiratory effort and abdominal movement distinguishing it from OSA. The risk factors for sleep apnea are known to be age, sex, obesity, smoking, heart failure and alcohol consumption [6].

1.1.2 Epidemiology, diagnosis and treatment of OSA

Severity of sleep apnea can be represented by Apnea-Hypopnea Index (AHI), which is defined as the average number of apnea and hypopnea per hour of sleep. An AHI of less than 5 is considered as normal, between 5 to 14 as mild OSA, between 15 to 29 as moderate OSA and equal and greater than 30 as severe OSA [7].

As mentioned earlier, OSA is the more common form of sleep apnea syndrome whose prevalence in the U.S. is comparable to asthma, type 2 diabetes and coronary artery disease [8]. Eighty four percent of the sleep disordered breathing patients have OSA [9]. OSA prevalence in the U.S. is most likely to rise up to three folds in the future as its risk factors like obesity and older age are increasing [10]. An earlier study in the U.S. called Wisconsin cohort study showed that the estimated prevalence of OSA in middle-aged adults (between 30 and 60) is 9% for women and 24% for men (AHI>5) [11] [1]. The prevalence in 1741 subjects from Pennsylvania cohort turned out to be 17% in men and 5% in women (AHI>5) [12]. Other studies from Australia [13], Spain [14], Korea [15] and India [16] have reported comparable rates. These results indeed highlight the importance of non-obesity factors contributing to OSA as the overall BMI is much lower in Europe and Asia.

The gold standard sleep-disordered breathing (SDB) diagnosis test is polysomnography (PSG) that is performed in a sleep laboratory. PSG consists of an overnight recording of electrocardiogram (ECG), electroencephalogram (EEG), photoplethysmogram (PPG), electrooculogram (EOG), electromyogram (EMG), nasal airflow and chest and abdominal

plethysmogram. Due to the PSG cost and limited availability in all locations, OSA syndrome is usually under-diagnosed.

The most common and optimal treatment for OSA is known to be continuous positive airway pressure (CPAP) machine [17]. In this method, a nasal and/or oral mask is used to apply pressurized air with either a constant (CPAP) or varying (BiPAP or APAP) pressure levels to the airway to prevent its collapse during sleep. Other types of treatments for those who cannot tolerate this form of therapy, include oral appliances [18], medical drugs and surgery [19].

1.1.3   Physiological premises and consequences

Airway patency dynamic alterations has been modeled previously as a function of transmural pressure (intrathoracic pressure) and dilation force from pharyngeal dilator muscle tone [20] [21]. Therefore, pharyngeal collapse in OSA is a product of both sleep-related decrement in pharyngeal dilator muscle activity and abnormal airway anatomy [22]. During the sleep, upper airway muscle activity falls, which results in increased upper airway compliance. On the other hand, pharyngeal neuro-compensatory reflexes, which are triggered by negative intrathoracic pressure, are reduced. Therefore it is usually difficult to identify if the collapse is primarily due to muscle tone loss or altered neural control or both [23].

In OSA patients, neuro-reflexes are mainly controlled by peripheral and central chemoreceptors, which are in turn respondents to hypoxia and hypercapnia respectively. Both of these, activate the sympathetic nerve activity, and thereby increase heart rate, blood pressure and vasoconstriction. In contrast, negative intrathoracic pressure reduces the stimulation of pulmonary stretch receptors, which in turn diminishes the vagal nerve activation and consequently sympathetic nerve activity and heart rate are reduced. Due to opposing behavior of these effects, neurocirculatory response to OSA can vary depending on which can overcome the other.

3

OSA has many physiological impacts on cerebrovascular system by inducing neurocirculatory modulations [24]. Repetitive chemoreflex stimulations by hypoxia-hypercapnia, lead to a rise in sympathetic nerve activity [25]. Surge in sympathetic nerve activity together with stress hormone, adrenaline, cause constriction of peripheral blood vessels leading to increase in blood pressure. Further, recurring hypoxia followed by reoxygenation can form oxidative stress which in turn results in systemic inflammation and endothelial dysfunction [26] [27]. The increased oxidative stress together with elevated blood pressure can lead to disruption of cerebral autoregulation [24] [28]. Moreover, this repetitive hypoxia and hypercapnia caused by apnea during the sleep can lead to stroke, irreversible brain damage and cognitive impairments [29].

1.1.4   *Cardiovascular comorbidities*

OSA may induce, promote or amplify hypertension, coronary artery disease, heart failure and stroke through chemical, autonomic, mechanical and inflammatory mechanisms [26]. Repetitive hypoxia-hypercapnia cycles elicit oscillations in sympathetic nervous activity, which directly affect heart rate [27]. These intermittent cycles can also promote oxidation of lipoproteins, hence increase oxidative stress hormones. They can also contribute to increased expression of adhesion molecules, monocyte adherence to endothelial cells, and vascular smooth-muscle proliferation.

Decreased intrathoracic pressure leads to an increase in left ventricular transmural pressure and afterload. OSA patients also experience oscillations in blood pressure and heart rate which affects shear stress on the vascular endothelium. This combined with recurrent hypoxia can lead to endothelial dysfunction [5]. Additionally, chronic left ventricular afterload in combination with oxidative stress hormone release can lead to hypertension [30]. Simultaneously, the repetitive

hypoxia and hypercapnia caused by apnea during the sleep can lead to stroke, irreversible brain damage, and cognitive impairments [29].

It has also been reported that intermittent hypoxia-hypercapnia oscillations stimulate chemoreflex. Since chemoreceptors are strong modulator of the sympathetic nerve activity, they will eventually promote release of stress hormone, adrenaline. Increased sympathetic nerve activity with stress hormone leads to constriction of peripheral blood arteries causing blood pressure to raise [31].

1.1.5 *Cerebrovascular comorbidities*

Researchers have shown that cerebral autoregulation (CA) mechanism is affected in patients with obstructive sleep apnea (OSA) [32] [33]. Further, a recent study has reported that apnea-induced hypoxia occurring during sleep apnea episodes causes a rapid rise in BP which can overwhelm the CA and induce significant oscillations in CBF [34]. In OSA patients, CA impairment increases the risk of stroke, independent of other known vascular risk factors [32]. Also, neurocognitive deficits including impairments of short-term and long term memory, working memory and executive functions has been observed in OSA patients [35] [36]. OSA is shown to be associated with altered structure of brain such as the loss of gray and white matter as well as the neurocognitive malfunction [37] [38] [39].

1.2 Research objectives

1.2.1 *Significance of research*

As detailed in the preceding sections of this chapter, it has been shown that OSA elicits systemic hemodynamic perturbations. Further, there is strong evidence in the literature that CA autoregulation mechanism gets overwhelmed during apnea episodes resulting in sizeable oscillations in cerebral blood flow velocity. This, of course, is driven by large oscillations in BP

due to apnea. Considering the possible serious consequences of cerebral hemodynamic oscillations, it is of importance to measure and quantify the level of oscillations in BP and CBF.

1.2.1.1 Direct nocturnal measurement of BP and associated challenges

Direct continuous blood pressure measurements using cuff-based methods are robust and reliable, but they work discontinuously requiring a few minutes for each measurement [40]. Such a method is likely to disrupt sleep due to application of pressure to upper arm for BP measurements. Some of the indirect continuous blood pressure monitoring devices apply auscultation and/or oscillation, but also perform intermittently [41]. Most widely used methods are based on vascular unloading proposed by Penaz 40 years ago [42]. A Finapres machine works by applying varying pressure via a small finger cuff and using a fast servomotor to react to changes in blood volume measured by a photoplethysmograph (PPG) [43]. However, even after several improvements by others [44] [45] [46] [47], it still suffers from frequent interruptions for calibration which can be a major drawback, especially if it happens during transient changes in BP. An alternative method of measuring BP continuously is the use of tonometry. Tonometry devices use piezoelectric crystals to sense oscillations [48] [49] and are able to measure the blood pressure continuously. While they do not suffer from disadvantages of using in line cuffs, a review of 22 studies has shown that there is substantial room for improvement [50]. Both tonometry and auscultatory methods are also subject to fixation and highly sensitive to motion artifacts. Overall, the cost of the measurement of blood pressure in the labs and even more so at home has prevented the inclusion of such measurements for sleep studies.

1.2.1.2 Direct nocturnal measurement of CBF and associated challenges

Ultrasound Transcranial Doppler (TCD) blood flow sensor is a non-invasive and sensitive means that can help monitor cerebral hemodynamics with high temporal resolution [51]. TCD

6

makes continuous recording of cerebral blood flow velocity with high temporal resolution [52] [53]. Measurement of instantaneous blood flow velocity in the medial cerebral artery using TCD allows estimating the cerebral blood flow, because the diameter of medial cerebral artery remains approximately constant. Using TCD, the relationship between systemic blood pressure (BP) and CBF has been investigated in several experimental studies [54] [55] [56].

While direct continuous CBF measurement using TCD is robust and reliable, it is also challenging, particularly during sleep. It requires experience for a trained person to determine the proper position for the TCD sensor on the temple and proper angle for aiming the TCD ultrasound beam to properly measure CBF. However, usually sleep technicians who perform sleep studies are not trained to make such measurements, and equipping sleep labs with TCD equipment is quite costly. Further, sleeping with the TCD sensor attached is somewhat uncomfortable for the sleep disorder patient. Because of these limitations, it is important to find alternative ways of monitoring the oscillations in CBF BP due to apnea episodes. The combination of the cost of TCD and difficulty of application makes it impractical to make direct measurement of CBF during sleep. Therefore, indirect measurement of CBF using inexpensive and easy to use devices can make it accessible to all patients.

1.2.1.3   Potential promise of photoplethysmography for estimating BP and CBF

One possible method of monitoring sleep-apnea induced BP and CBF oscillations is to use data from other easy-to-apply sensing devices to estimate the changes in CBF. One such device that is commonly in use for sleep studies both in the laboratories and also home-based sleep study is oximeter [57]. Many oximeters provide a photoplethysmography (PPG) signal which is a pulsatile waveform resulting from beat to beat cardiac cycle and contains significant information about blood volume change in microvessels. The use of PPG—alone or in conjunction with

electrocardiogram recording—as a surrogate measure for estimating systolic, diastolic and mean arterial blood pressure has been previously reported by our laboratory and others [58] [59] [60] [61] [62] [63]. In this study, we investigated the possibility of quantitatively describing the relationship between BP and PPG. Given the interrelationship between the rise in BP and CBF response, we further opted to explore the possibility of estimating changes in CBF due to an apnea episode from PPG.

1.2.1.3.1   Advantages of PPG

Photoplethysmography is a low-cost noninvasive method that uses optical sensors with two different wavelengths to detect the blood volume change in microvessels typically from finger. The PPG waveform shows a pulsatile waveform attributed to cardiac synchronous changes in blood volume and a slow frequency baseline which is varying due to sympathetic nervous system response, respiration and thermoregulation [64] [65]. PPG sensors are inexpensive and are already implemented into the existing sleep study protocols. It is non-invasive, non-disruptive and easily available which makes it most suitable device to be used in hospitals or even at home.

In this study we will try to formulate a descriptive model for the relationship between these signals and systemic response during the OSA.

One such opportunity is the ability to nocturnally measure blood pressure and cerebral blood flow as part of now widely available and reasonably-priced pulse oximeter systems. As mentioned, there are significant oscillations in nocturnal blood pressure and cerebral blood flow due to obstructive sleep apnea [66]. However, due to cost and complexity, the current technology makes direct measurement of BP and CBF during multiple nights at home impractical. A PPG-derived BP/CBF measurement can provide for multiple-night or long-term measurement of these

vital signals and might prove to be a valuable means for assessing the efficacy of therapy and/or medication for control of BP in sleep apnea patients.

Development of such methods has a high potential for implementation in wearable health monitoring devices. Such implementation could bring about a positive impact for near-continuous monitoring of BP and CBF in a large sector of the population ranging from athletes to hypertensive patients. Among many possible applications, such as the examples mentioned here, methodology for person-specific model calculation and validation need to be developed. This is likely to be an essential part of such applications, as it is unlikely that a single model would be able to estimate BP and/or CBF for members of all population sectors from the PPG variations. The likely need for person-specific models stems from the fact that there is a wide variation in the physiological systems involved in the control of blood pressure which includes responsiveness of the sympathetic nervous system, mechanical, fluid mechanics, dynamical properties of the cardiovascular system, and metabolic rate.

1.2.1.4   Benefits/importance of measuring nocturnal blood pressure in OSA patients

Hypertension is one of the major risk factors contributing to cardiovascular morbidity and mortality of patients [67]. Noninvasive, continuous blood pressure (BP) monitoring has been shown to be a superior detector of mortality than clinical measurements [68]. Many studies have demonstrated that nocturnal BP is a better predictor of cardiovascular risk than is daytime BP [69]. On the other hand, scientific evidence for a link between obstructive sleep apnea and hypertension is compelling [70]. A large community-based study has shown that the odds of having hypertension is 37% greater in persons with obstructive sleep apnea. It indicates that SDB is associated with systemic hypertension in middle-aged and older individuals [71].

1.2.1.5 Benefits/importance of measuring nocturnal cerebral blood flow in OSA patients

Sufficiency of the CBF peaks and troughs as a predictor of mortality has been shown in several studies [72] [73] [74]. In particular, it has shown that cerebral autoregulation mechanism is affected in patients with obstructive sleep apnea (OSA) [32] [33]. Further, a recent study has shown that apnea-induced hypoxia occurring during sleep apnea episodes causes a rapid rise in BP which can overwhelm the CA and induce significant oscillations in CBF [34]. In sleep apnea patients, CA impairment increases the risk of stroke, independent of other known vascular risk factors [32]. Therefore, monitoring CBF oscillations caused by apnea is important.

1.2.2 *Aims and Hypothesis*

We propose to mine photoplethysmography PPG signal, which is part of nocturnal polysomnography (PSG) data, to estimate CBF and BP during apnea episodes. We investigate formulating a descriptive mathematical model to estimate episodic apnea-induced changes in BP using PPG signal. Additionally, we will explore the possibility of estimating the variations in CBF during apnea episodes from PPG signal. For this purpose, we have formulated two hypotheses to be investigated and some specific aims for each hypothesis described as follows:

Hypothesis1: Apnea induced blood pressure variations can be modeled using photoplethysmography signal features.

Aim 1.1: Using a breath hold maneuver as a means of simulating apnea, develop dynamic mathematical models to estimate the elicited temporal changes in systolic, diastolic, and mean arterial BP from concurrently recorded PPG signal

Aim 1.2: Development dynamic mathematical models to estimate apnea-induced changes in systolic, diastolic, and mean arterial BP using concurrently recorded PPG signal during OSA episodes.

**Hypothesis 2**: Apnea induced cerebral blood flow oscillations can be estimated from PPG signal

Aim 2.1: Using a breath hold maneuver, develop dynamic mathematical models to estimate the elicited temporal changes in CBF from concurrently recorded PPG signal

Aim 2.2: Development dynamic mathematical models to estimate apnea-induced changes in systolic, diastolic, and mean arterial BP using concurrently recorded PPG signal during OSA episodes.

1.2.3 Innovations

Based on the proposed specific aims and stated hypotheses, the top 4 innovations listed below are those that with the successful achievement of the aims will bring about and contribute to new knowledge:

I. Relating cerebral blood flow to PPG signal:

There are a few studies that have explored the apnea induced cerebrovascular variations during nocturnal study [75] [35] [76], yet no study is found which has investigated the possibility of estimating changes in CBF from PPG.

II. Estimating BP variations from PPG without the need for any additional measures such as ECG:

The ability to estimate BP from PPG with any need to measure ECG can be advantageous, as it reduces the number of instruments needed which in turn can facilitate measurement of BP, this important physiological indicator of cardiovascular health.

III. Exploring concurrent dynamics of PPG and CBF during apnea:

Overcoming the difficulties of measuring CBF during apnea episodes, would enable clinicians to better assess the effect apnea on the brain.

IV.   Discovering possible difference in breath hold dynamic and sleep apnea:

Although breath hold and many other perturbation methods have been used widely to simulate apnea and investigate the effect of sleep apnea on hemodynamic system, there may be some differences in systemic response to hypoxia arisen from voluntarily holding breath versus one elicited by sleep apnea episodes. Our models may be able to reveal any difference between simulated and real sleep apnea.

CHAPTER 2

Measurement of Physiological Response to OSA

2.1 Photoplethysmography

Photoplethysmography (PPG) is a low-cost noninvasive method that uses optical sensors to detect the blood volume change in microvessels typically from finger. This blood volume change can be detected at different wavelengths and combined to calculate the oxygen saturation of the blood. This is done by maximizing the difference between the absorption coefficients of oxyhemoglobin (HbO) and deoxyhemoglobin (Hb). The PPG waveform shows a pulsatile waveform resulting from beat to beat cardiac cycle and a slow frequency baseline which is varying due to sympathetic nervous system response, respiration and thermoregulation [64] [65].

2.1.1 Principle of operation

Pulse oximetry is performed using of two small LEDs in red and IR range, typically 670 nm and 940 nm in a device called pulse oximeter. It is designed to be attached to an optically translucent part of the human body, usually finger or earlobe. Combined information of the reflected or transmitted light from these LEDs can be then used to extract useful information including SpO2 or blood oxygen saturation. The pulsatile waveform of reflected/transmitted light either from red or IR sensor can also be used as PPG signal with its typical waveform shown in Figure 1. PPG detects the arterial volumetric changes by sensing the changes in infrared light transmission through the finger. PPG works based on the Beer-Lambert law, which indicates that the absorption of light depends only on path length, absorption of components in tissue and concentration of each of those components.
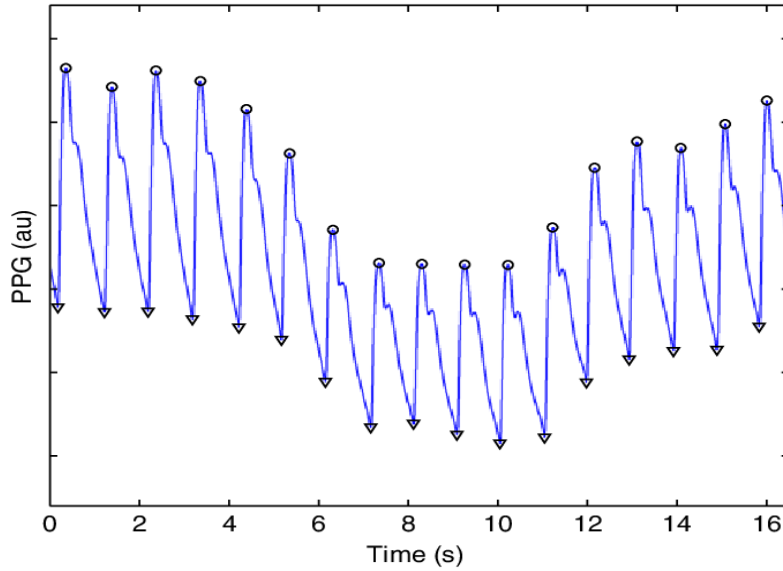
Figure 1- PPG signal with its peaks and troughs detected and labeled

2.1.2 Advantages and benefits

PPG signal is a non-invasive and non-disruptive method, which is also easy to use, convenient, simple and low-cost. It has been used for many years and nowadays many pulse oximeters can provide the PPG signal as an output [77]. Considering the fact that the pulse oximeters are now commonly in use in all sleep laboratories, obtaining PPG signal is one of the easiest way of monitoring heart rate via sensing blood volume change at the periphery. Since PPG uses light which has no or minimal direct effect on human body. It is also fast and can be used for real time monitoring. Pulse oximetry is also very helpful in situations where the patient's blood oxygenation is not stable like intensive care or surgery and emergency settings. Due to their simplicity and their ability to provide real-time and continuous measurement of blood volume and oxygen saturation, they are an inevitable part of the emergency rooms. The photoplethysmography technology has also been recently used in wide range of commercially wearable devices to calculate health-related parameters including heart rate [65]. For this study, the

14

photoplethysmography signal was acquired using Nellcor OxiMax N-600x monitor (Medtronic, Minneapolis, USA). A finger probe has been attached to the N-600x monitor which houses both red and IR LEDs together with the photodetectors. Accuracy of OxiMax N-600x has been previously shown to be between ±2 to ±3 percent over the range of 60 to 100 percent of oxygen saturation [78] [79].

2.1.3   *Physiological link between CBF and BP with PPG*

Both arterial and venous blood volume at the site of PPG affect the sensed PPG. Of course, the cardiac system as well as the respiratory and autonomic systems influence the movement of arterial and venous blood. Hence, the frequencies present in PPG are associated with the modulation frequencies of these three physiological systems [80]. Further, that cardiac frequencies make up the higher frequencies in PPG and respiratory, sympathetic, and thermoregulation comprise the lower frequencies present in PPG. As stated in a recent review paper, the PPG waveform is a complex signal, not well understood, and still subject of active research [81].

It is well known that the cardiac component of the PPG waveform comes from the site of the maximum pulsation within the arteriolar vessels, where pulsatile energy is converted to smooth flow, just before the level of the capillaries [82]. The aorta can be considered as a capacitance that enables transformation of the "on-off" blood-flow characteristics of the left ventricle into a less pulsatile flow in distal vessels [80]. Therefore, a smooth blood-flow pattern is achieved at capillary level. Arterial wall stiffness determines the degree of energy absorbed by the elastic aorta and its recoil in diastole. Hence, the more compliant the aorta is, the smaller pulse pressure will be achieved. In contrast, the complex network of small arteries and arterioles represents the resistance vasculature [83].

With each cardiac cycle, heart pumps the blood into the peripheral arteries and causes the volumetric changes, which can be detected using PPG sensors. Hence, the pulsatile waveform of the PPG is the reflection of the peripheral pressure wave causing the volume change in the interrogation field of the PPG sensor that is percutaneously attached near a distal vessel. Applying Poiseuille's law (Eq.1), vascular resistance depends on lumen radius (R) of individual vessels, on length of vessels (L) or on rarefaction (number of vessels connected in parallel) and also on the viscosity of the fluid (μ) [84].

$$\Delta P = \frac{8\mu LQ}{\pi R^4} \tag{1}$$

Eq. 1 describes the relationship between the pressure drop (ΔP) in a long stiff cylindrical pipe of constant cross sectional area and the volumetric flow rate (Q). The pressure drop (ΔP) is the difference between aortic pulse pressure and peripheral pulse pressure. Therefore, the flow being sensed at finger probe (Q) is a function of this pressure drop, which emphasizes the contribution of cardiac pulse pressure in volumetric change in small arterioles. Additionally, it is worth mentioning that though the Poiseuille's law is applicable for stiff pipe with constant diameter but in literature it has been used to approximate the relation between flow and resistance in vessels [84]. It has been done assuming short lengths of vessels having the same stiffness and further integration over the length of the vessels.

As explained, both blood pressure and blood volumetric changes detected that are by PPG sensor have characteristic features which can vary with changes in peripheral circulation and have inter-relationship which is useful for extraction of diagnostic information. Due to complexity of modeling the relationship between PPG and the elements that contribute to its formation, particularly the contribution of cardiac system via blood pressure, the researchers have opted to explore models that do not explicitly model the physiological effects. Specifically, there are

numerous studies investigating relationship between BP and PPG by applying a variety of models, from studying the complex non-linear and time varying properties of blood pressure and microvascular blood flow changes [85] [86] to lumped parameter models comprising resistance and compliance including multiple regression models [87], Windkessel models [88] [89], and also the neural network models [90]. One of the simplest equation to study relationship between BP and PPG is proposed in [91] where they use an individual transfer function in frequency domain by applying fast Fourier transform to the waveforms of each individual:

$$ITF = FFT(BP)/FFT(V) \tag{2}$$

where V is the volumetric changes detected by PPG. They reported RMS error of around 5 mmHg between reconstructed BP and measured BP by recruiting 12 men healthy subjects.

Heneghan et.al. [92] used a simple linear regression method to describe the relationship between systolic blood pressure and PPG amplitude using the following equation:

$$SBP = b_0 + b_1.AMP \tag{3}$$

where AMP is the amplitude of PPG signal (i.e., the difference between the peak and trough of a PPG pulse) b_0 is the intercept, b_1 is the slope, and SBP is the systolic blood pressure. They recruited 18 young healthy subjects and reported the correlation coefficient of around 0.6 between Pulse amplitude and SBP and SD of regression residuals to be around 3 mmHg.

2.2 Non-invasive blood pressure monitoring

Due to the high importance of both hypertension and hypotension in impairment of vital organs, it is critical to closely monitor the arterial blood pressure [93]. Conventional non-invasive blood pressure measurements can broadly be divided into two categories: intermittent methods and continuous methods. The intermittent methods such as cuff-based methods are robust and reliable, but they work discontinuously and are not suitable for sleep study where the changes are

17

abrupt and suddenly [94]. The continuous methods provide full wave blood pressure, and can be further categorized into arterial applanation tonometry and volume clamp methods. The volume clamp method that is also recognized as vascular unloading technology is based on the work by Czech physiologist Jan Penaz [95]. One of the most advanced machines that is operating based on this method is Finapres blood pressure NOVA monitor (Finapres Medical Systems, Enschede, Netherlands) which is used in this study to collect blood pressure data.

It is noted that the direct and invasive measurement of blood pressure through arterial cannulation is considered to be the most accurate and gold standard method. However, since this method is invasive and has risks associated with it, it usually is applied only in intensive care units and operating rooms. Further, it increases the risk of bleeding, vessel or nerve lesion and embolism [96]. Therefore, non-invasive measurement of blood pressure seems vital. Following sections will cover the conventional methods, current non-invasive method and its advantages and deficiencies.

2.2.1 *Finapres monitor and its method of operation*

Finapres Nova monitor works based on the "unloaded arterial wall" principle introduced by Penaz [97]. In this method, the blood pulsation in finger is optically detected by PPG sensor, which is mounted in a small inflatable cuff placed on a finger. No preference on the selected finger is reported in literature. The cuff is secured to the finger using a Velcro strip. The detected PPG signal is used as a feedback to a servomotor, which rapidly varies the cuff pressure to cancel out the blood pressure pulsations in the finger. In this manner, the cuff pressure becomes equal and opposite of intra-arteriole pressure. The arteriole transmural pressure which is the superposition of external and internal pressures approaches zero. In this way, the artery always remains in a semi-open situation. The oscillation in the cuff are then considered to resemble the arterial blood pressure [98]. For Finapress Nova, the servomotor is adjusted 1000 times per seconds allowing the

feedback to be as close as possible to the actual blood pressure. This method has been validated by comparing its measurements to invasive blood pressure monitoring and proved to have reasonable accuracy [99] with high within subject precision [100].

2.2.2 *Capabilities and limitations of Finapres*

The advantage of the volume clamp method is that it can provide full-wave blood pressure measurement. The Finapres machine can provide continuous measurements of BP for up to 24 hours. BP measurements using Finapres machine can be done in sleep and in partial ambulatory mode (e.g., on a treadmill or stationary bike). It can also reconstruct the brachial artery pressure waveform via generalized waveform inverse model [101]. Finapres has an integrated heart level compensation system, which takes into account any hydrostatic pressure differential caused by difference in heart level and the finger to which the sensor is attached [102].

However, this machine needs to be calibrated rather frequently during the measurement which cause loss of BP signal over short intervals. Moreover, in some subjects, it can result in finger numbness because of continuous pressure applied by the cuff. This limitation, however, can be somewhat avoided by having two sensors attached to 2 fingers and switch between them every few minutes, a feature that newer Nova models have.

2.3 Cerebral Blood flow monitor

Cerebral autoregulation is a homeostatic mechanism that aims to maintain stable cerebral blood flow (CBF) despite blood pressure fluctuations. Previous studies have convincingly documented that in normotensive adults, when mean arterial blood pressure is within the range of 60-160 mmHg, CBF level ranges between 50mL per 100g of brain tissue per minute [103] [104] [105].

Sufficiency of the CBF peaks and troughs as a predictor of mortality has been shown in several studies [72] [73] [74]. In particular, it has shown that cerebral autoregulation mechanism is affected in patients with obstructive sleep apnea (OSA) [32] [33]. Further, a recent study has shown that apnea-induced hypoxia occurring during sleep apnea episodes causes a rapid rise in BP which can overwhelm the CA and induce significant oscillations in CBF [34]. In sleep apnea patients, CA impairment increases the risk of stroke, independent of other known vascular risk factors [32]. Therefore, monitoring CBF oscillations caused by apnea is important.

Based on the above findings by our group and others, it is possible to investigate modeling of BP from PPG [34] [63]. Further, as stated above, investigators have shown that CBF can be mathematically related to BP and then BP can be modeled using PPG. Hence, it is reasonable to expect that one can model CBF from PPG. The modeling expected to be more feasible during apnea, when the strength of the sympathetic nervous response to apnea overwhelms the cerebral autoregulation mechanism. Therefore, the CBF becomes closely coupled and directly affected by BP, without the oscillation damping effects that CA introduces during normal breathing. Hence, there may be higher congruence between BP and CBF during apnea and that would make modeling CBF from PPG more plausible. It is expected that this will result in higher correlation between BP and CBF changes, significantly increasing the likelihood of success in modeling of CBF using PPG [106].

2.3.1 Transcranial Doppler

Ultrasound Transcranial Doppler (TCD) blood flow sensor is a non-invasive and sensitive means that can help monitor cerebral hemodynamics with high temporal resolution [51]. TCD has made continuous recording of cerebral blood flow velocity with high temporal resolution possible [52] [53]. TCD can be used to measure blood flow velocity in many arteries including middle

cerebral artery (MCA), posterior cerebral artery (PCA), etc. However, measurement of instantaneous blood flow velocity in the medial cerebral artery using TCD allows estimating the cerebral blood flow, because the diameter of medial cerebral artery remains approximately constant.

2.3.1.1 Principles of operation of TCD

Transcranial Doppler (TCD) ultrasound is a non-invasive, sensitive and portable machine that uses pulsed ultrasound waves and the Doppler effect to assess the intracerebral blood flow velocity. The ultrasound waves are transmitted through the skull and reflected off of blood cells moving within the cerebral blood vessels. The difference between emitted and reflected wave wavelength is called Doppler shift and is directly proportional to blood flow velocity. The formula describing this relationship is the following:

$$V(Flow\ velocity) = \frac{f_d \times c}{2 \times f_t \times \cos\theta} \tag{1}$$

where c is the propagation speed or the speed of ultrasound in tissue (approximately 1541 m/s), θ (theta) is the angle between emitted wave direction and blood vessel, f_d is the Doppler shift (Hz) and f_t is the emitted beam frequency (Hz). It is recommended to minimize the angle θ to less than 30 degrees to have highest possible reading. The basic assumption for CBF measurements is the diameter of the vessel under test does not change during acquisition [107].

TCD can work in two modes: continuous mode and pulsed mode. In continuous mode two separate transducers will be used, one as emitter and the other one as receiver. There will be no temporal information retrieved in this mode as ultrasound waves are being sent continuously. In pulsed mode, however, only one transducer will be used to emit and receive the pulses. In this way, the time between emitted pulse and received pulse can be detected and that is directly related to the distance between sensor probe and artery. This information is further used to create a signal

called M-mode either that gives information about various depths and the direction of blood flow, toward the probe or away.

2.3.1.2 TCD capabilities and limitations

While direct continuous CBF measurement using TCD is robust and reliable, it is also challenging, particularly during sleep. It requires acquiring significant level of experience for a trained person to determine the proper position for the TCD sensor on the temple and proper angle for aiming the TCD ultrasound beam toward MCA to measure CBF. Currently, sleep technicians who perform sleep studies are not usually trained to make such measurements, and equipping sleep labs with TCD equipment is quite costly. Further, sleeping with the TCD sensor attached is somewhat uncomfortable for patients. Because of these limitations, it is highly desirable to find alternative ways of monitoring the oscillations in CBF due to apnea episodes.

2.4 Experimental setup

Rigorous assessment of the systemic and cerebral hemodynamics usually needs a step disturbance (stimulus) to be applied to BP to perturb the BP and monitoring the response of BP and CBF to such a perturbation [108]. Many procedures such as the Kety-Schmidt technique [109], Xe measurements and [110] manipulation of blood pressure using vasoactive medications [111] , and the Valsalva maneuver [112] have been used to provide such perturbations. For this study, we opted to use two protocols to perturb the systemic hemodynamic and monitor the dynamic changes in desired signals: 1) Breath-hold maneuver which simulated apnea (Breath-hold Study) 2) Apneic episodes in obstructive sleep apnea patients (Apnea Study). Each of these are explained in detail in following sections.

2.4.1 *Breath hold maneuver*

The breath-hold maneuver protocol was selected as it simulates sleep apnea and elicits the same physiological responses as sleep apnea events, such as drop in oxygen saturation and rise in carbon dioxide. Indeed, these changes stimulate the chemoreceptors that in turn trigger the sympathetic nervous system to increase arterial blood pressure and in turn, cerebral blood flow.

2.4.1.1 Study protocol and patient population

The protocol and written subject consent form for testing subjects were approved by The University of Texas at Arlington (UTA) Human Subject Institutional Review Board. Fifteen subjects (8 males, 7 females, aged 28.9 ± 5.0 years, BMI 24.1 ± 4.8 kg/m^2) with no known medical conditions volunteered for this study and signed the consent form. None of the subjects showed hypertension based on evaluation of their baseline data and comparison with the published values by the Centers for Disease Control and Prevention (CDC, an official U.S. government public health monitoring agency). The subjects were asked to avoid any caffeine intake for six hours before the experiments. They were tested in supine position, performing a sequence of breath-holding maneuvers. The sequence of the maneuvers is shown in Figure 2. At the start, while lying down on a bed, each subject was asked to breathe normally for 60 s to obtain baseline data. Subsequently, each subject performed a series of five breath-hold maneuvers. During each breath-hold (BH), subjects were instructed to hold their breath for as long as they could. This resulted in varying durations for each breath-hold, depending on the ability of the subject to hold breathing. Inter-breath-hold intervals were fixed at 90 seconds to provide adequate recovery time between consecutive breath-holds. At the conclusion of the fifth breath-hold maneuver, the subject remained in the supine position and resumed breathing normally for 60 seconds. Data was collected for the entire duration, from the initial baseline through the final ending NB period.
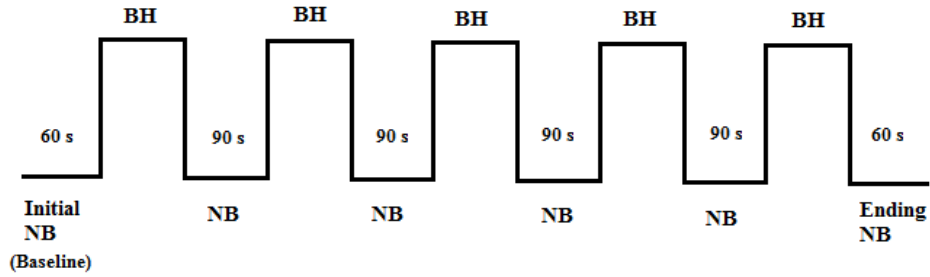
Figure 2- Sequence and timing of the breath-hold (BH) maneuvers and normal breathing (NB) intervals

2.4.1.2 Instrumentation

In this study, we used a Finapres blood pressure NOVA monitor (Finapres Medical Systems, Enschede, Netherlands) [102]. To measure CBF, we used a DWL TCD "Doppler box" (DWL, Compumedics Germany GmbH, Singen, Germany), this method has been validated and widely used [113] [114]. The photoplethysmography signal was acquired using Nellcor OxiMax N-600x monitor (Medtronic, Minneapolis, USA). All CBF, BP and PPG signals were acquired at 1000 samples per second. However, for the purposes of this study the data were down-sampled to 100 samples per seconds, as the lower sample rate was sufficient for the modeling of the signals of interest. This point is further elaborated in Chapter 3 of this dissertation. The signals were clean and no noise reduction were necessary to be applied.

2.4.1.3 Dataset

Each subject performed 5 breath-hold and 6 normal breathing intervals, 4 between breath-holds, one at the beginning and one at the end. A circuit with start and stop button switch was used to mark the beginning and end of each breath-hold and generate a two-level electrical signal which went high (5 Volts) whenever subject holds his/her breath and zero whenever he/she continued to breathe normally. This signal was saved in 6th channel of DAQ and is called "Marker". This provide a convenient and accurate method of identify the beginning and end of each maneuver

and, for processing, it facilitated the clipping other CBF, BP and PPG signals into segments of breath-holds and normal breathings.

2.4.2   *Sleep study*

OSA has significant effect on both systemic and cerebrovascular hemodynamic. To investigate effect of OSA and estimate BP and CBF during the sleep apnea, we conducted 6 to 8 hours of nocturnal polysomnography on 15 patients. The protocol, subject selection and data acquisition are discussed in detail in following subsections.

2.4.2.1   Study protocol and patient population

The protocol and written subject consent form for testing subjects were approved by UTA Human Subject Institutional Review Board. Fifteen subjects (10 males, 5 females, aged 53.8 ± 7.4 years, BMI $34.2 \pm 7.2 \, kg/m^2$) signed the informed consent form. These subjects were selected from those who were suspected of having OSA and referred for diagnosis. The patients were instrumented with the standard polysomnography and additional instruments together with some other instruments and monitored during 8 hours of sleep in sleep laboratory.

Upon completion of the sleep study, a certified technician - blind to the objectives of the study - scored the polysomnography data obtained during Apnea Study to ascertain if the patient indeed had OSA. Then we processed the data from the PPG, blood pressure, as well as cerebral blood flow for modeling and estimation during the episodes of apnea.

2.4.2.2   Polysomnography

Polysomnography (PSG) is a standard clinical multi-parametric test performed while the subject sleeps. It consists of simultaneous recording of several physiological signals and is considered to be the gold standard in detection of sleep disorders. For our study, PSG included attachment of electrocardiogram (ECG), electrooculogram (EOG), and electromyogram (EMG)

25

electrodes. As part of this standard clinical setup, chest and abdominal inductance plethysmography bands (to monitor the respiratory efforts) and electroencephalogram (EEG), as well as a flow sensor were attached to the chest, abdomen, scalp and nostril of the patient, respectively.

2.4.2.3 Instrumentation for measurement of BP, CBF, and PPG

In addition to the standard clinical polysomnography instruments, for the present study we also connected the following sensors to the patient: 1) A Doppler ultrasonic transducer small probe that is mounted on one side of the head near the temple to measure brain blood flow (Compumedics DWL, Singen, Germany); 2) A finger cuff was placed on either middle or ring finger to continuously measure blood pressure from finger (Nexfin monitor, BMEYE, Amsterdam, Netherlands); 3) Finger or forehead probe to measure percent oxygen saturation of the blood and photoplethysmography signal (Nellcor N-600X Bedside Pulse Oximetry Monitor; Dublin, Ireland). Additional measurements of end tidal CO_2, brain tissue oxygenation were made for other analysis, but are not pertinent to the analysis presented in this dissertation. The output from all these extra sensors were fed to the computer where the data were digitally collected and stored. The data was collected by a dedicated computer using LabVIEW software and data acquisition card (National Instruments, Austin, TX).

2.4.2.4 Data acquisition and synchronization

Polysomnography data was recorded on the sleep lab computer using a sleep diagnostic system (Digital 32+ Amplifier, Embla, Broomfield, CO) integrated with Sandman Elite software (Embla, Broomfield, CO). Another computer was used to acquire the added sensor channels via DAQ including PPG, BP and CBF signal. LabVIEW programming environment was used to generate a synchronization signal that was fed Embla system as well as the second data acquisition

system. This signal was generated by taking the computer time and producing a pulse train which has 3 consecutive pulses whose amplitude were proportional to second, minute and hour. This signal was used for post-data collection synchronizations of the data stored in Sandman and DAQ. A representative plot of the synchronization signal can be seen in Appendix A.

2.4.2.5   Dataset

As mentioned, data from Sandman were scored by a sleep technician who was blind to the purpose of our study. A synthetic signal similar to "Marker" in breath-hold study was generated based on the respiratory events scored by technician. Arbitrarily, this signal was designed to have the following values to denote different respiratory conditions, as scored by the sleep technician. Specifically, the normal breathing assigned to be 10 (AU), Hypopnea as 4, CSA as 3, mixed apnea as 2 and OSA as 1. Figure 3 illustrates an example of this respiratory event file.
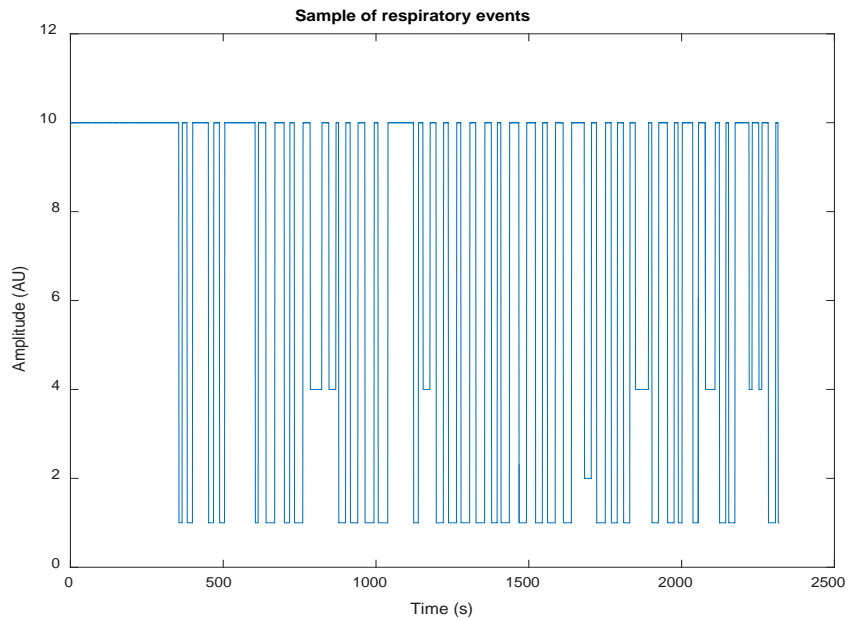
Figure 3- A respiratory event marking signal displaying various breathing states: apneas (values of 1), hypopneas (values of 4), normal breathing (values of 10), and mixed apnea (value of 2). Time value of 0 reflects the start time of the recording.

27

To facilitate comparison of the results between the Breath-hold Study and Apnea Study, we analyzed 6 longest obstructive apnea events for each subject.

CHAPTER 3

Estimation of BP and CBF during OSA episodes

3.1 Estimation method

In this study, we investigated formulating a descriptive model to relate the rise in BP due physiological perturbation of breath hold as well as obstructive sleep apnea to concurrently recorded PPG. Further, we also explored the possibility of relating the changes in CBF due to same physiological perturbations to PPG. Specifically, an ARMA model was examined as the mathematical means for this investigation.

3.1.1 *ARMA models*

An autoregressive moving average (ARMA) model provides a means of mathematically relating the dynamic relationship between PPG as input and either BP or CBF as output. The general form of an ARMA model for a single-input-single-output, time-invariant, and causal system can be represented as:

$$y(m) + a_1 y(m - 1) + \ldots + a_{n_a} y(m - n_a) = b_1 u(m - n_k) + \ldots + b_{n_b} u(m - n_b - n_k + 1) + e(m) \qquad (2)$$

where, m is the sample number, y is the output, u is the input, and e stands for the modeling error, a_i for $i = 1,2 \ldots, n_a$ and b_j for $j = 1,2, \ldots, n_b$ are the model parameters that need to be computed, n_a is the model order, n_b signifies the number of previous input values used in the model, and n_k is the number of pure-time delay samples.

By incorporating possible influences of the present and previous values of the input as well as previous values of the output on the current value of the output, ARMA model is capable of

modeling of dynamics of physiological responses. Further, ARMA modeling accommodates pure time delays that may be present in the process of relating input to output, a rather common phenomenon in physiological systems [115]. Researchers have applied ARMA models in multiple physiological applications such as modeling of cardiovascular and respiratory responses [116] [117] [118] [119].

For the purposes of this study, we employed a single input (i.e. a PPG feature) and a single output (i.e. a CBF feature) model. Mathematically, Model orders

A major decision in developing an effective ARMA model is the selection of the order of the model and any pure-time delay that may be involved. Investigators developing ARMA models have proposed guidelines for selecting the critical model parameters of $n_a,$ $n_b,$ and n_k [120] [121] [122]. In our study, we limited the model orders to be less than or equal to 5. This upper limit for the model order was selected based on examining MSE for models of various orders derived from a few randomly selected experimental settings (i.e. breath hold and normal breathing records), which showed that model orders higher than 5 did not produce significant improvement in MSE.

3.1.2   *Delay determination*

Another challenge in ARMA modeling is determination of delay between input and output. To find the delay between PPG and BP/CBF, we analyzed some random intervals (both NB and BH) by calculating cross-correlation between input (i.e. PPG peaks or PPG troughs) and output (i.e. systolic, diastolic, CBFP, CBFT). All the cross correlations turned out to have maximum in range of 5 samples delay between input and output. A sample of cross-correlation between PPG peaks and systolic values are shown in Figure 4.
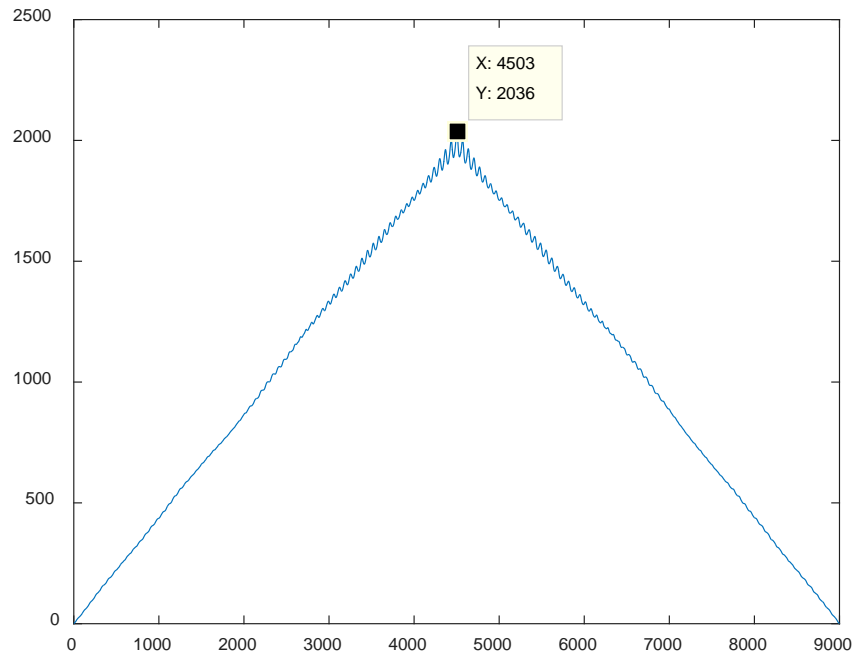
Figure 4- Cross correlation between PPG peaks and systolic BP in a BH interval from a randomly selected subject data. This is a representative plot of the cross correlation values obtained for other sample records.

Therefore, we opted to set the delay to range from 0 to 5 samples. It is worth mentioning that the delay and model order are important factors that affect the accuracy and goodness of fit fo the model, so careful selection of these values can result in better accuracy and performance of the model.

3.1.3   Coefficient calculation

Once the upper limit for the model orders is selected, the next step is to estimate the 'a's and 'b's coefficients in the model. In this study, we opted to apply the principle of parsimony and model adequacy to find the least mean square error in a certain range of orders. Orders were set from 1 to 5, and delay ranged from 0 to 5 for our study. Then, the ARMA model parameters were estimated by applying MATLAB *ARMA* identification algorithm which uses a least square method based on QR-factorization to minimize the model error for selected maximum values of n_a, n_b, and

n_k [123]. Based on the selected maximum values for n_a and n_b and n_k, all models resulting from the possible permutations of these upper limits were generated and compared using their residual rMSE using following equation:

$$rMSE = \sqrt{\frac{\sum_{t=1}^{n}(\hat{y}_t - y_t)^2}{n}} \tag{3}$$

where, y_t is the tth sample of the measured output, $\hat{y}_t$ is the tth estimated value of the estimated output by the model, and n is the number of samples in the interval being modeled.

The lowest MSE was selected as an optimum model generated for the specified maximum values for n_a and n_b and n_k. We also used Akaike's information criterion (AIC) [120] [124] to find an optimum model, but it does not necessarily give the lowest MSE. The AIC finds the best model based on both parsimony and goodness of fit.

3.1.4   Advantages and limitations of ARMA models

Autoregressive models are suitable for modeling physiological phenomena as they incorporate dynamic behavior of a system by including prior values of input and output in estimating the present value of the output. Further, they provide a capability for including pure-time delay term in the model, which can be used to model a frequently observed delay in physiological systems. On contrary, they are poor in long-term prediction as they depend on previous values to estimate future output [125]. Dealing with outliers and multiple predictors are some other factors that need to be taken into consideration when dealing with ARMA models.

3.1.5   MATLAB algorithms

After synchronization (as described in 2.4.2.4) and preprocessing, peaks and troughs of PPG, BP and CBF are detected using the *findpeak* algorithm provided by MATLAB (version R2016b by MathWorks Inc., Natick, MA, USA) [126]. Since the application of the ARMA model requires

equidistant sampling of both the input and output data, we used cubic spline interpolation to interpolate BP/CBF peak and BP/CBF trough values as well as the PPG peaks and troughs at the same sampling rate of the BP/CBF and PPG signals, i.e. 100 Hz. Then, ARMA models for each of clip (5 BH and 6 NB intervals in case of breath-hold study, 6 apnea episodes in case of sleep study) were calculated separately for input (i.e. PPG peaks or PPG troughs) and output (i.e. systolic, diastolic, CBFP, CBFT, respectively) for all subjects.

To implement ARMA models in MATLAB, we used *arx* command with 'simulation' option for this command from the MATLAB system identification toolbox. To evaluate performance of the models, we used *compare* command, but since compare uses information of both input and output to calculate initial condition, it cannot be directly used for validation. Therefore, we wrote our parametric function based on the ARMA equation (Equation 2) using initial condition from *compare* command, with validation input and modeling output as dataset given to it. The initial condition is computed using output data that was used for constructing the model together with the input coming from the interval we want to predict. This is more realistic as we do not use the measured output that needs to be predicted for the computing initial condition.

3.2   Application of estimation method

Using ARMA model, we separately investigated the relationship between PPG and BP as well as the relationship between PPG and CBF. While the approach for these investigations are described in sections 3.3 and 3.4, the steps for preparation of the data for these investigations are presented in this section.

3.2.1   Data preprocessing

To determine proper sampling rate for the modeling, PPG, BP and CBF data was initially analyzed for power spectrum density (PSD). We observed that almost all the energy is below 50

Hz. Therefore, to minimize the complexity of the system and reduce processing time, we down-sampled all signals from 100 Hz to 100 Hz. A sample plot of PSD for PPG signal in a breath-hold interval can be seen in Figure 5.
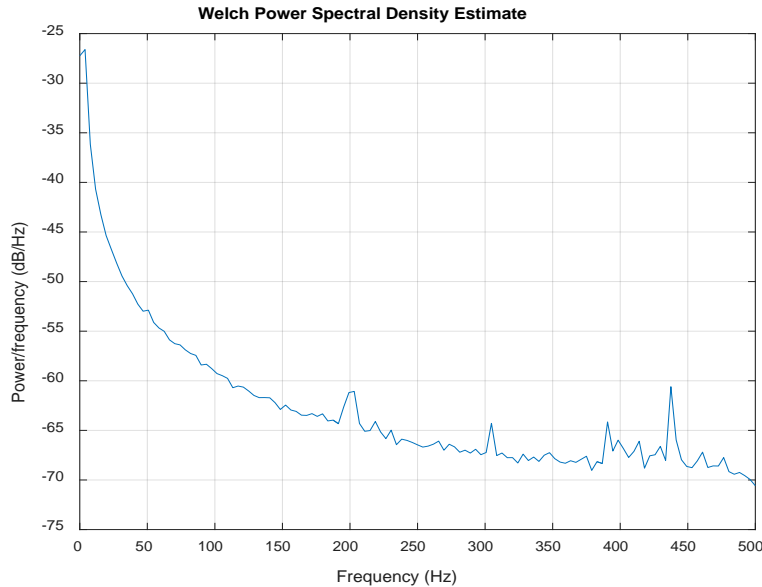
Figure 5- A sample plot of PSD (from PPG of BH2 for Subject number 6)

After down-sampling to 100 Hz and clipping the signal for desired interval, all signals including PPG, BP and CBF were analyzed for their peaks and troughs. It is worth mentioning that the signals from BH studies were free of high frequency noise and no noise reduction was necessary to be applied. However, the CBF signals collected during sleep study had motion artifacts which was removed by applying a moving average filter with window of size 7 samples. As mentioned, we used *findpeak* command to detect peaks. *'MinPeakProminence'* were chosen to be 0.1 volts for PPG, 10 cm/s for CBF and 15 mmHg for BP peak detection. *'MinPeakDistance'* were set as 20 samples for PPG and CBF but 40 samples for BP, and 'MinPeakHeight' were set to be 0.15 volts for PPG, 15 cm/s for CBF and 15 mmHg for BP. These values are chosen before multiplication factor, which is 100 to convert voltage to actual value, is applied.

34

The BP and CBF waveforms were scanned over the interval between each two consecutive peaks to detect the minimum value and was set as the troughs of the signals. Then, all the peaks and troughs were interpolated and resampled at 100 samples/s to have equidistance samples. A representative plot of PPG and BP signal together with their peaks and troughs interpolated for a NB interval are displayed in Figure 6 below. It is the interpolated peaks of the input (i.e. PPG signal) and interpolated peaks of the output (i.e., BP or CBF) that were used for the modeling.
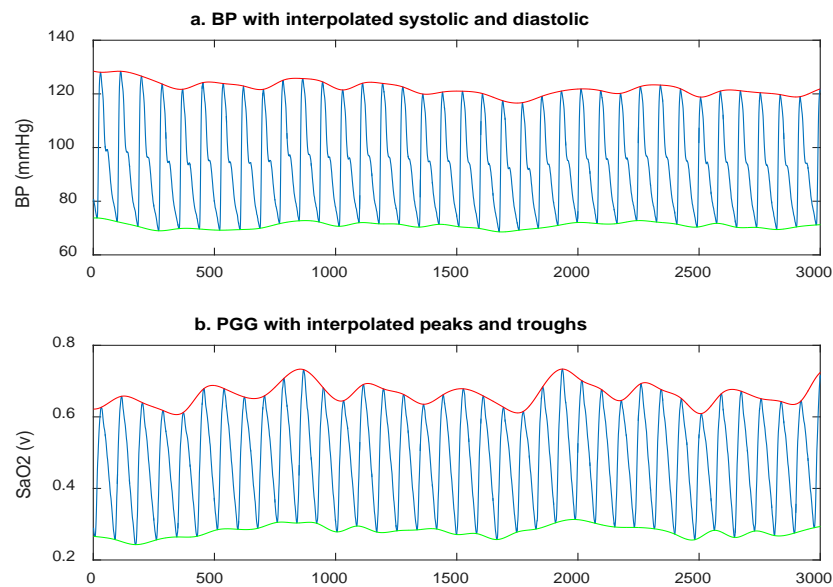
Figure 6- PPG and BP signal with their peaks and troughs interpolated using a cubic spline interpolation and sampled at 100 samples/s.

The procedure of detecting peaks and troughs explained above was the same for extracting the input (i.e., PPG) and the output (i.e., BP and CBF) signals in both BH and sleep apnea studies. These peaks and troughs are then used with the *arx* function of the MATLAB to estimate the models.

3.2.2   Data segmentation

In BH study, "marker" signal (Figure 6) was used to determine when the subject starts or ends each breath-hold or normal breathing interval. However, the modeling investigation, we used the time point where BP reached its maximum value due to breath hold. This point often fell beyond the end of the BH interval, as there is an inherent delay in the physiological response to restoration of normal breathing at the conclusion of the BH maneuver.

The same procedure was followed for sleep study, except that the "EVENT" signal (Figure 3) was used to determine the intervals. As in the case of BH, for modeling purposes, the end of an event was taken to be when the BP (or CBF) surge due to apnea reached a maximum value.

3.3   ARMA modeling of blood pressure from photoplethysmogram

A typical blood pressure and PPG signals during a BH maneuver are shown in Figure 7.
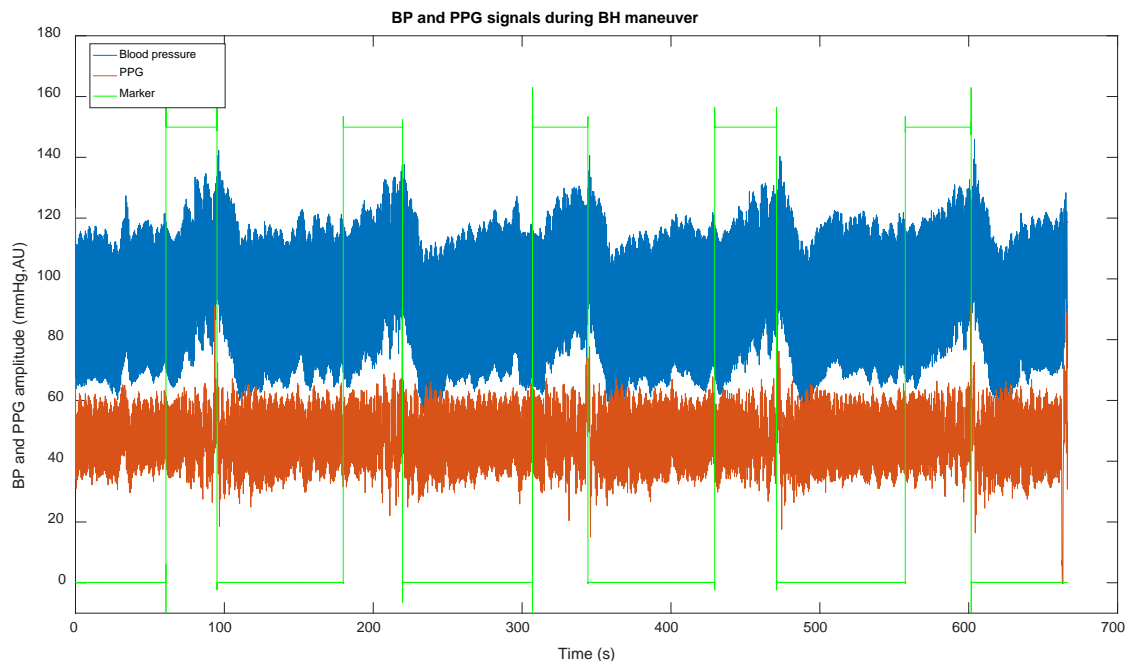
Figure 7- Recorded blood pressure (blue) and PPG (red) signals during BH maneuver. The green line shows the breath-hold maneuvers (BH, high values) and normal breathing (NB, low values) intervals.

The high values of the green line designates the intervals during which the subject is holding breath. At its low values, the subject is breathing normally. Figure 8 illustrates the zoomed-in view of a single BH interval to demonstrate how BP and PPG respond to breath-hold.
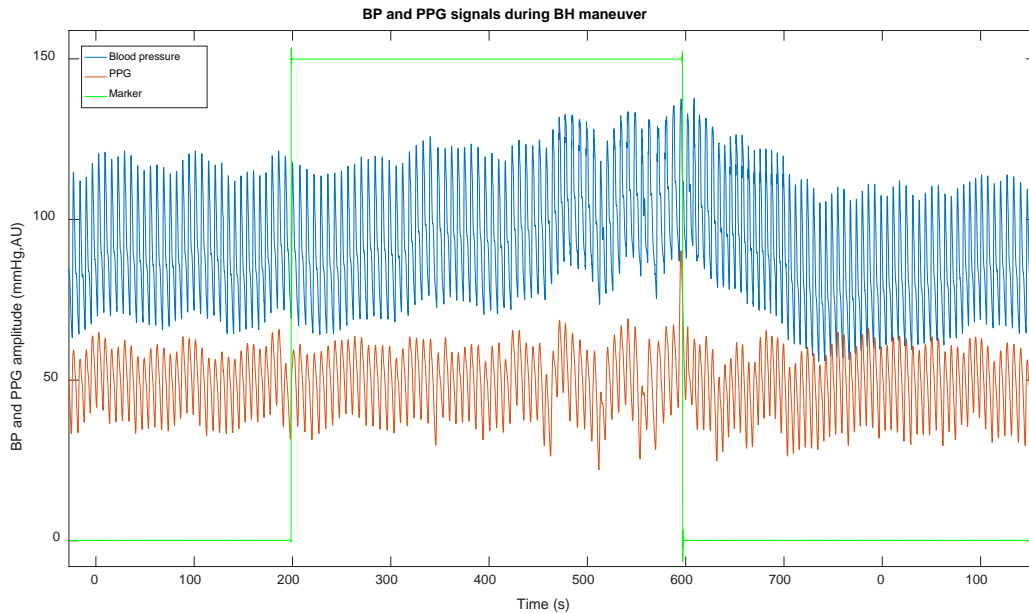
Figure 8- Recorded blood pressure (blue) and PPG (red) signals during BH maneuver. The green line shows the breath-hold maneuvers (BH, high values) and normal breathing (NB, low values) intervals.

As shown, the blood pressure exhibits a rising trend during BHs, so does the PPG amplitude, be it delayed and shorter in duration. It is noted that irrespective of the duration of each breath hold, the blood pressure and the level of PPG tend to rise and reach the highest level when BH is ended or shortly afterwards. The rise in PPG may be attributable to a greater volume of blood reaching to the peripheral vasculature, as the blood pressure rises. The same discussion applies to apnea intervals where the physiological responses are elicited by apnea, such as the drop in oxygen saturation and the rise in carbon dioxide. Indeed, the same rise in BP can be seen in apnea events. A sample of BP and PPG during apnea intervals are illustrated in Figure 9 and its zoomed view in a few apnea episodes can be seen in Figure 10.

37
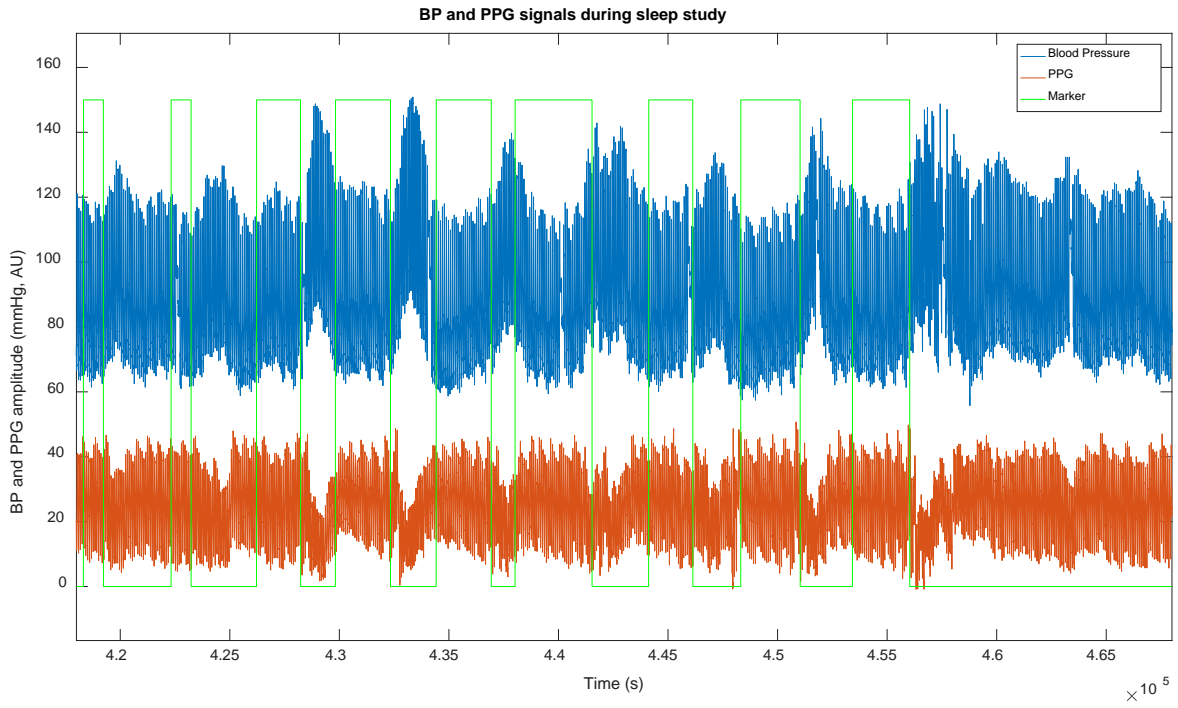
Figure 9-Recorded blood pressure (blue) and PPG (red) signals during sleep study. The green line shows the apnea marker (apnea, high values) and normal breathing (NB, low values) intervals. Identification of the apnea events was done by a certified sleep technician blind to the objectives of this research.
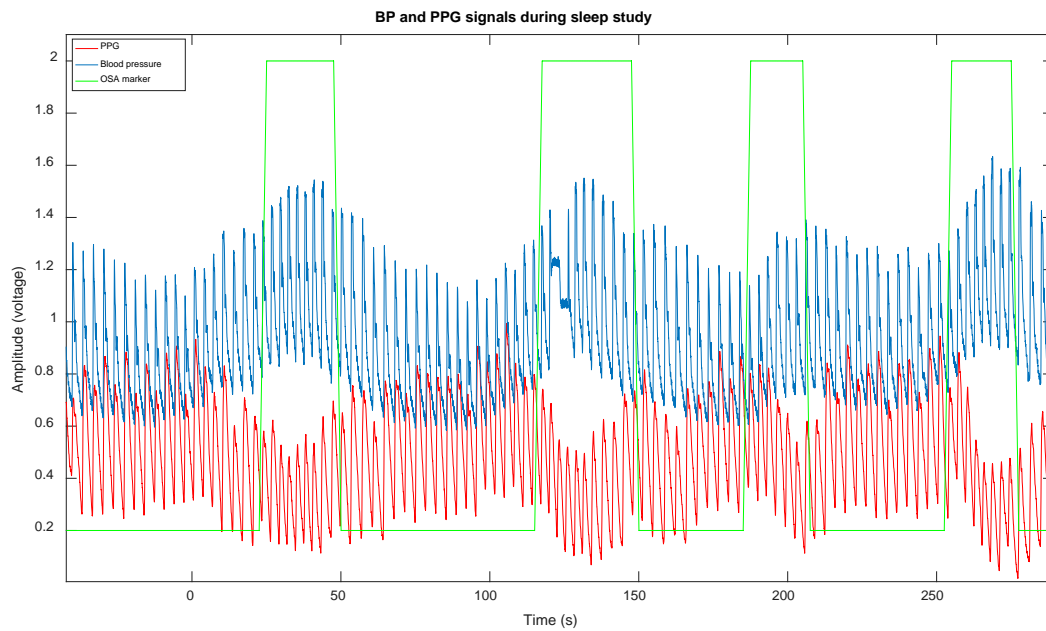
Figure 10- Zoomed blood pressure (blue) and PPG (red) signals during sleep study. The green line shows the apnea marker (apnea, high values) and normal breathing (NB, low values) intervals.

3.3.1   Systolic, Diastolic and MAP modeling

Applying ARMA model with the peaks of the PPG signal as input and SBP as output, we obtained the model parameters for estimating SBP (labeled as $\widehat{SBP}$) from PPG signal. Similarly, by using troughs of PPG as input and DBP as output, we obtained the model parameters for estimating DBP (labeled as $\widehat{DBP}$) from PPG signal. Then, for both measured MAP and estimated MAP (labeled as $\widehat{MAP}$), we applied equation (3) by using respective measured (i.e., SBP, DBP) and estimated values (i.e., $\widehat{SBP}$ and $\widehat{DBP}$).

$$MAP = \frac{2 \times DBP + SBP}{3} \tag{4}$$

Of course, estimated MAP is to reflect the measured MAP which can be computed using an equation (Figure 1) by substituting the measured values of SBP and DBP that are obtained from the blood pressure monitor (i.e., Finapres).

In breath-hold study, ARMA models for each of the five BH and six NB intervals were calculated separately for both systolic and diastolic BP for all 15 subjects. In other words, we obtained 11 SBP models and 11 DBP models for each subject.

On the other hand, in sleep study, we obtained a separate model in each of the 6 selected apnea intervals for both systolic and diastolic BP in all 15 subjects. Therefore, for each subject, we end up having 6 models for each SDB and DBP.

3.4   ARMA modeling of cerebral blood flow from photoplethysmogram

The rise in BP due to apnea as well as breath hold may mediate a rise in CBF, depending on the severity of rise in the BP and efficacy of cerebral autoregulation. Given this interrelationship between the rise in BP and CBF response, we opted to explore the possibility of estimating changes in CBF due to an apnea episode or breath-hold interval from PPG. Based on this paradigm, we investigated the modeling of CBF from PPG when hypoxia is present and acts as a perturbation to

39

the blood pressure physiological control system. The aim was to establish whether it is possible to accurately estimate and track apnea-driven changes in CBF from PPG. Specifically, similar modeling was performed to estimate the focal points of CBF signal from PPG peaks and troughs.

An important consideration is, however, the effect of cerebral autoregulation (CA) which attempts to minimize the CBF fluctuations when BP changes. Usually, CA is impaired in SDB patients, which in turn results in CBF fluctuation [32] [33]. This enables us to dynamically model the CBF since the baseline of CBF is following a rising trend as illustrated in following figures. If CA is not impaired during apnea episodes, it may not be possible to estimate CBF values from PPG as the CA minimizes such changes. A typical CBF and PPG signal during BH study are shown in Figure 11. For this specific subject, it is obvious that CA did not stop the CBF from rising at the end of the breath-hold intervals. Magnified figure of a sample BH interval is displayed in Figure 12 to illustrate the concurrent response of PPG and CBF to breath-hold.
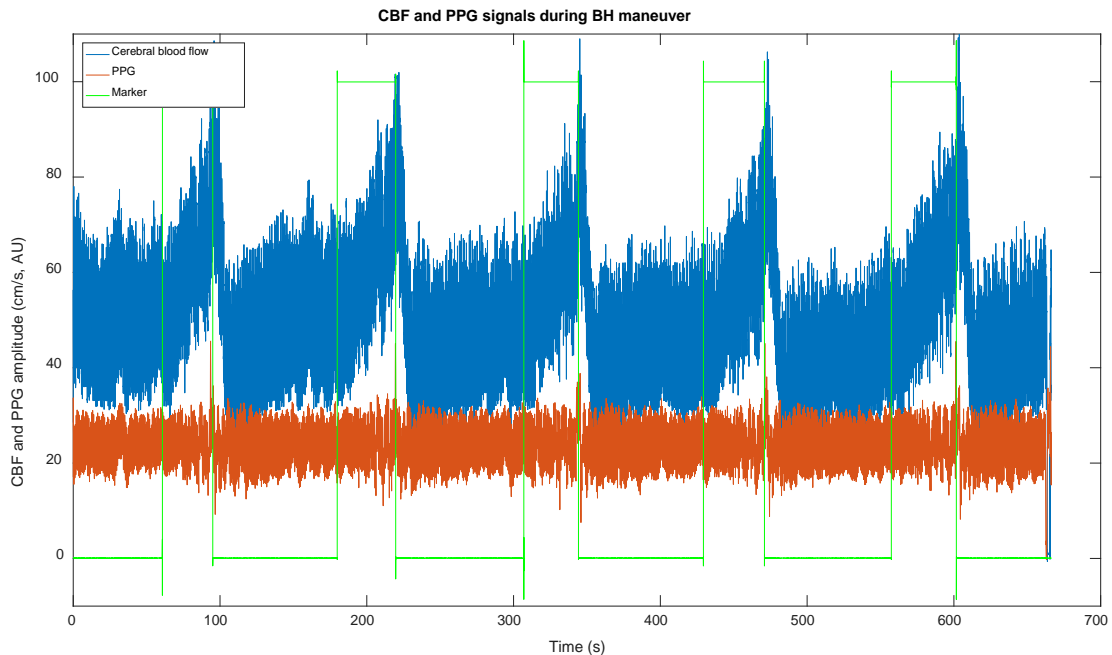
Figure 11- Recorded cerebral blood flow (orange) and PPG (blue) signals during BH maneuver. The green line is the marker for the breath-hold maneuvers (BH, high level) and normal breathing (NB, low level) intervals.
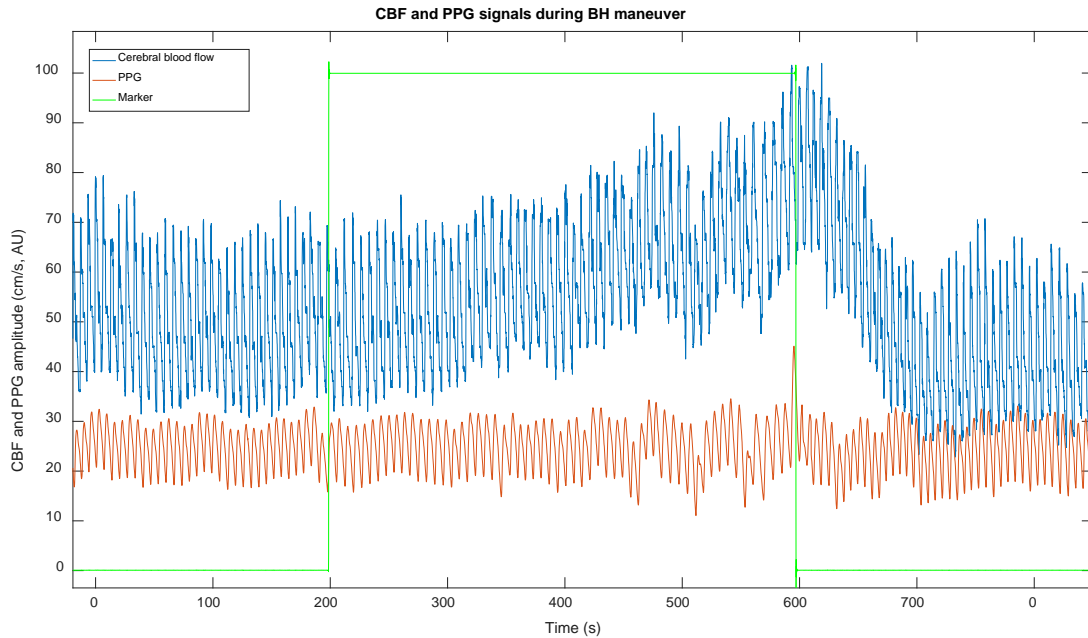
Figure 12- zoomed-in view of cerebral blood flow (orange) and PPG (blue) signals during BH maneuver. The green line is the marker for the breath-hold maneuvers (BH, high level) and normal breathing (NB, low level) intervals.

A sample of CBF and PPG signal during sleep study is displayed in Figure 13. The zoomed view of a few apnea intervals can be seen in Figure 14 as well, illustrating the detail of how the PPG and CBF are changing in response to apnea event.
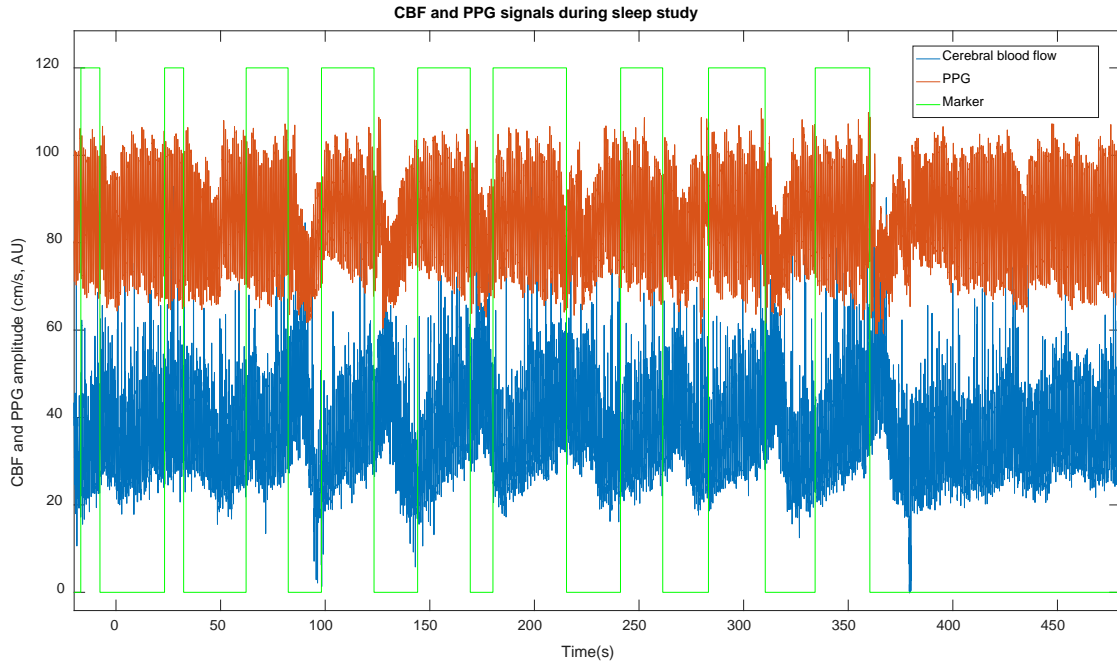
Figure 13- Recorded cerebral blood flow (orange) and PPG (blue) signals during BH maneuver. The green line is the marker for the breath-hold maneuvers (BH, high level) and normal breathing (NB, low level) intervals. Identification of the apnea events was done by a certified sleep technician blind to the objectives of this research.

Figure 14- zoomed-in view of cerebral blood flow (orange) and PPG (blue) signals during BH maneuver. The green line is the marker for the breath-hold maneuvers (BH, high level) and normal breathing (NB, low level) intervals.

3.4.1 Cerebral blood flow peaks and troughs modeling

Similar to BP modeling, ARMA models are estimated using peaks of the PPG signal as input and peaks of CBF (CBFP) as output, we obtained the model parameters for estimating CBFP (i.e.,$\widehat{CBFP}$) from PPG signal and by using troughs of PPG as input and CBFT (CBF troughs) as output, we obtained the model parameters for estimating CBFT (i.e., $\widehat{CBFT}$) from PPG signal. Again, in a similar way, 5 models for each CBFP and CBFT were obtained in breath-hold intervals and 6 models for each in normal breathing intervals. Altogether, we obtained 22 models for both CBFP and CBFT in all normal breathing and breath-hold intervals. Likewise, for the sleep study, we obtained 6 models relating CBFP to PPG peaks and 6 models relating CBFT to PPG troughs, a total of 12 models.

3.5 Evaluation

3.5.1 Metrics

To ascertain the accuracy of the models, once the model parameters (i.e. a_i's, b_j's, n_a, n_b, and n_k in Eq. 2) for each experimental setting (i.e. BH1, BH2… BH5 and NB1, NB2… NB5) were determined, they were kept constant and used to compute the sample-by-sample difference between the model estimated CBF features (i.e., $\widehat{CBFP}$ and $\widehat{CBFT}$) and the measured CBF features values (i.e., CBFP and CBFT respectively). We refer to this difference as *model error*, as they reflect how well the model fits the experimental data for each experimental setting. Further, for each experimental setting, for each CBF feature, and for all subjects combined, we aggregated the *model error* values by computing the root mean square of the errors using the following equation:

$$rMSE = \sqrt{\frac{\sum_{t=1}^{n}(\hat{y}_t - y_t)^2}{n}} \tag{4}$$

where, y_t is the tth sample of the measured CBF feature, $\hat{y}_t$ is the tth estimated value of the CBF feature by the model, and n is the number of samples in the CBF feature time series.

We also computed mean and standard deviation of the errors for each interval to help us quantitatively assess the performance of the modeling. They can reveal another level of accuracy of the model and dispersion of the errors.

3.5.2   *Modeling and validation errors*

Explicitly, when applying Eq. 3, the values of $\hat{y}_t$ and their corresponding y_t values for each experimental setting, each CBF feature, and all subjects combined were used to compute the rMSE values for modeling that feature. That is, under our experimental design, for each experimental setting and for each CBF feature, there are 15 subject datasets of *model error* values that were used. Therefore, all *model error* values obtained from all subjects contributed to computation of the rMSE values for *model error*. It is noted that in computing the values of $\hat{y}_t$, the initial values for the model output were estimated using the Compare command provided by MATLAB which uses an optimization routine that utilizes the measured input and output to estimate the optimum initial values for the output (i.e., the first n_a plus n_k values of $\hat{y}_t$).

We also assessed the accuracy of each model that was derived from measured data for a subject and for a given experimental setting in predicting the measured values of CBF features for other congruent experimental settings. For example, for each subject, we applied the model that was derived from estimating CBFP during BH1 to predict CBFP for BH2, BH3… and BH5 and repeated the same for the model derived from BH2 data to predict CBFP for BH1, BH3, BH4, and BH5 and so on. This resulted in 20 prediction evaluation cases per each subject. With this method, the prediction accuracy was assessed for all combinations of the congruent experimental settings. We refer to the difference between each sample of predicted CBF feature and its measured value

as *validation error*. To establish an aggregate representation of the *validation error* values, we applied Eq. 3 to all corresponding *validation error* values obtained from all subjects. Hence, for each CBF feature and each experimental setting, the *validation error* values obtained for all subjects contributed to computation of the corresponding rMSE values of the *validation error*.

As in the case of computing the rMSE values for *model error*, the initial values of the estimated output (i.e., the first n_a plus n_k values) were computed using the optimization routine of *compare* command provided by MATLAB. However, in this case for computing the *prediction error*, we assumed that the values of the output that are going to be predicted are not available for computing the optimized initial values. Hence, we applied the available output values that were used in obtaining the model parameters to optimize the initial conditions.

CHAPTER 4

Results

In this chapter, we will present the results obtained from modeling and evaluation of both studies, breath-hold and sleep study. The breath-hold study BP modeling from PPG will be presented first followed by the modeling of the CBF from PPG during breath-hold study. Next, the results of modeling BP using PPG as input in sleep study will be presented. After that, the findings from the modeling of CBF using PPG as input in sleep study will be described.

4.1 Breath-hold modeling

The ARMA models for each of the five BH and six NB intervals were calculated separately for estimating of the beat-to-beat systolic BP and diastolic BP from PPG for all 15 subjects.

4.1.1 Blood pressure modeling results in Breath-hold study

Figure 15 shows a sample of computed $\hat{SBP}$ superimposed on their respective measured values of SBP in both BH and NB intervals from the same subject (subject No. 6).

(a)   (b)
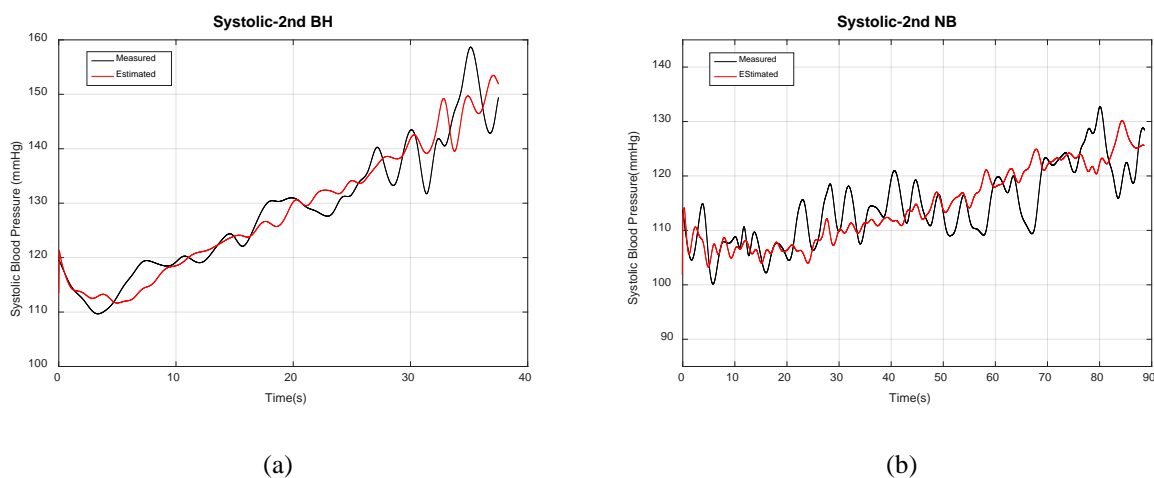
Figure 15- Measured SBP signal versus estimated SBP ($\hat{SBP}$) from modeling: figure (a) shows example of breath-hold model and figure (b) shows example of normal breathing model. Both plots are from Subject No. 6 results.

46

Similarly, plots for DB̂P and MÂP can be seen in Figure 16 and Figure 17 where computed DB̂P and MÂP are superimposed on measured DBP and MAP (again from subject No. 6).

(a)

(b)
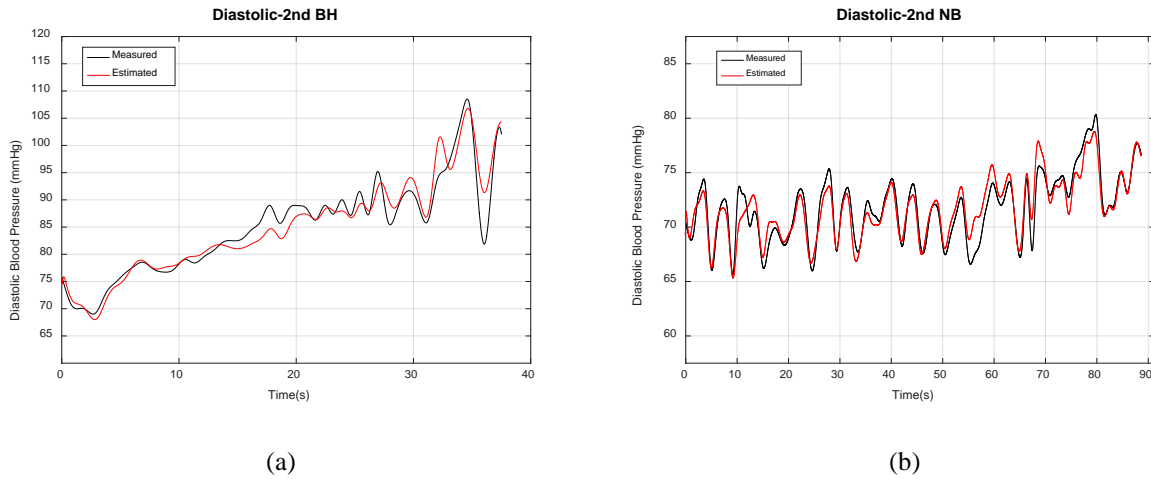
Figure 16- Measured DBP signal versus estimated DBP ($D\hat{B}P$) from modeling: figure (a) shows an example of breath-hold model and figure (b) shows an example of normal breathing model. Both plots are from Subject No. 6 results.

(a)

(b)
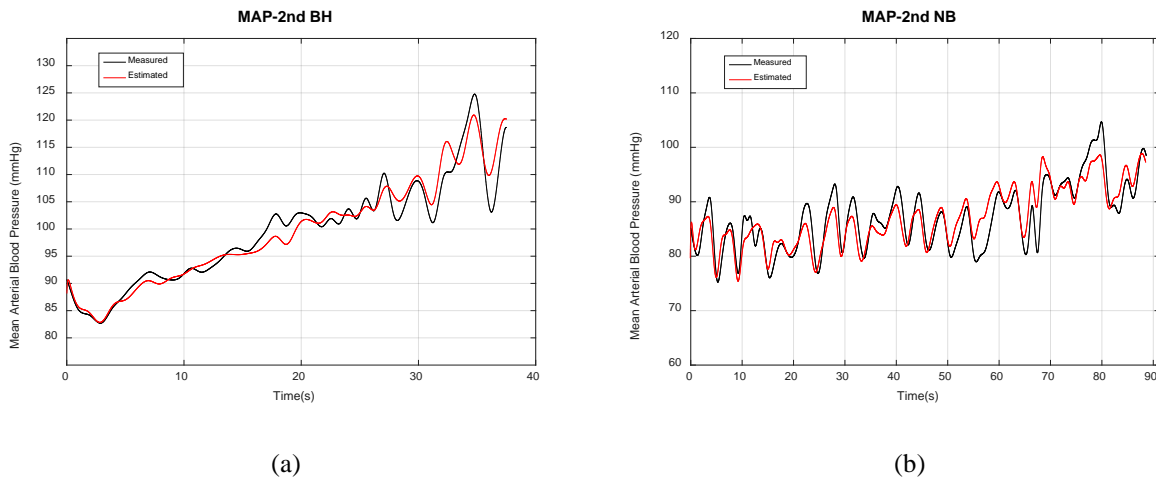
Figure 17- Measured MBP signal versus estimated MAP (MÂP) from modeling: figure (a) shows an example of breath-hold model and figure (b) shows an example of normal breathing model. Both plots are from Subject No. 6 results.

Figure 18 throughFigure 20 show the mean of the Model Errors as well as the mean of the Validation Errors – as defined in section 3.5.2- for systolic, diastolic and MAP in breath-hold study. Means of these measures (i.e., Model Errors and Predictions) are calculated across the all 15 subjects.

Error means and standard deviations are calculated for each combination of the model intervals with validation intervals. For instance, for BH1 it has been validated with BH2 across all the 15 subjects and mean of the error is reported at location where the model comes from BH1 and validation interval comes from BH2. In this manner, in these figures, the values at the intersection of the same breath-hold or normal breathing intervals on the x and y axes represent the modeling error means.

(a)   (b)
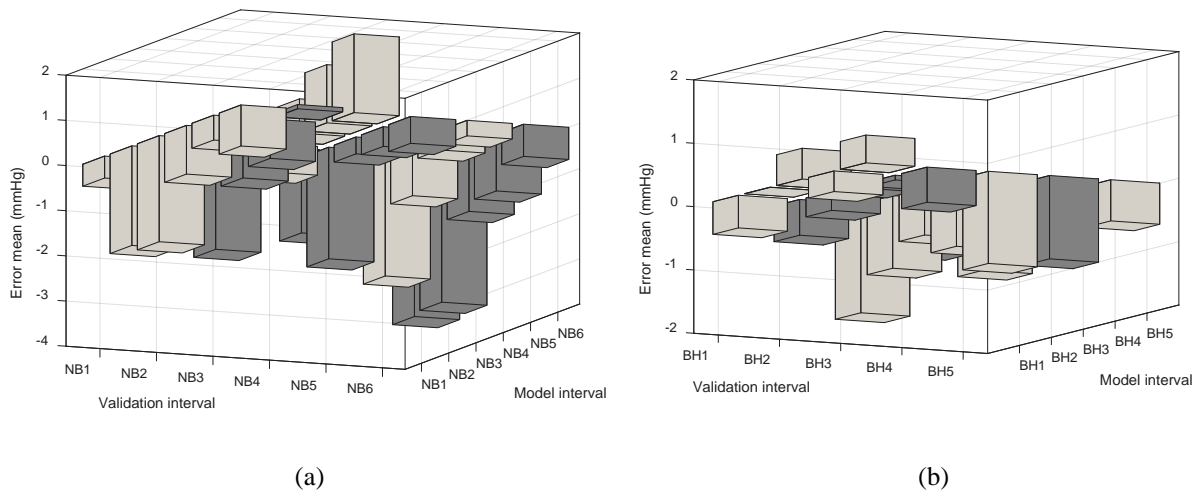
Figure 18- Mean of errors for SBP in a) NB intervals b) BH intervals

48
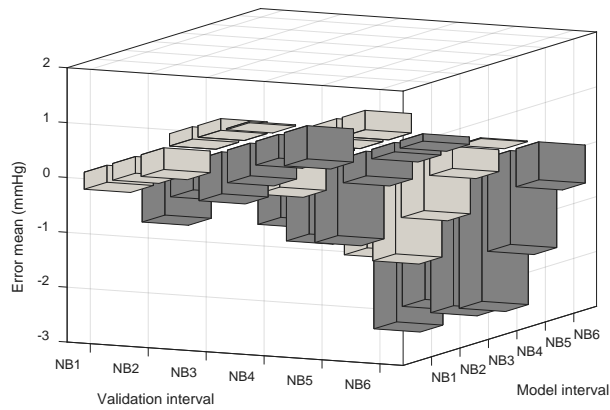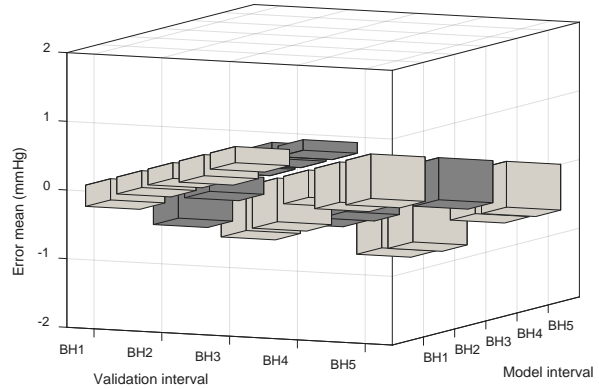
(a)   (b)

Figure 19- Mean of errors for DBP in a) NB intervals b) BH intervals
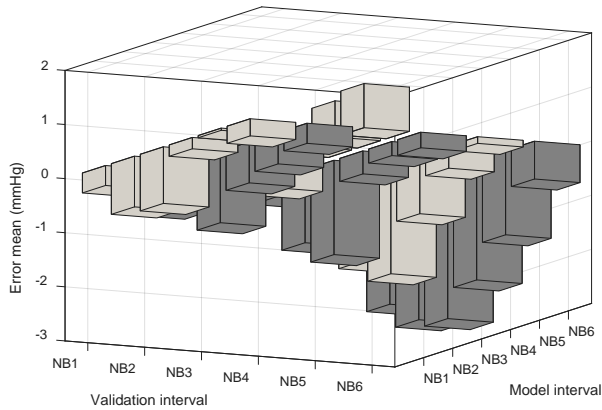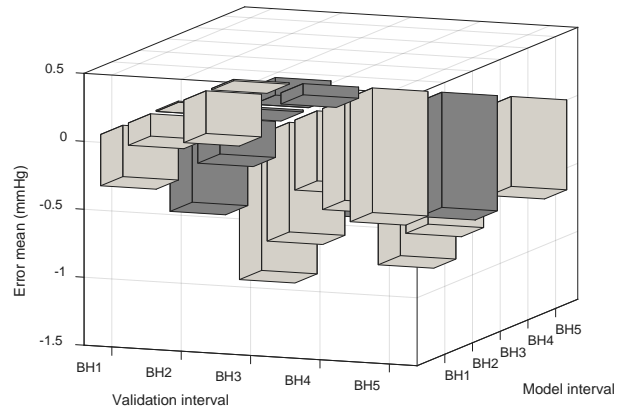
(a)   (b)

Figure 20- Mean of errors for MAP in a) NB intervals b) BH intervals

Figure 21 through Figure 23 display the standard deviation of the Model Errors and Prediction Errors reflecting the level of dispersion in these errors around their mean values. Each color represents separate validation interval, while each model is displayed at each corner. For example, consider the standard deviation of the residual of the models derived from the data associated with BH2. These are shown with the red color in Figure 16b. It can be seen that when

49

these models were used to estimate SBP for the BH2 intervals, the standard deviation of the Model

Errors (i.e., the residuals of predicting SBP from the model that was derived from the same dataset)

was at its lowest value of 4 mmHg. However, when these models were used to estimate SBP for

another interval such as BH1, the standard deviation of the Predication Errors was approximately

8 mmHg.   In this way, the standard deviation of each model when evaluated with all intervals are

reported.

(a)   (b)
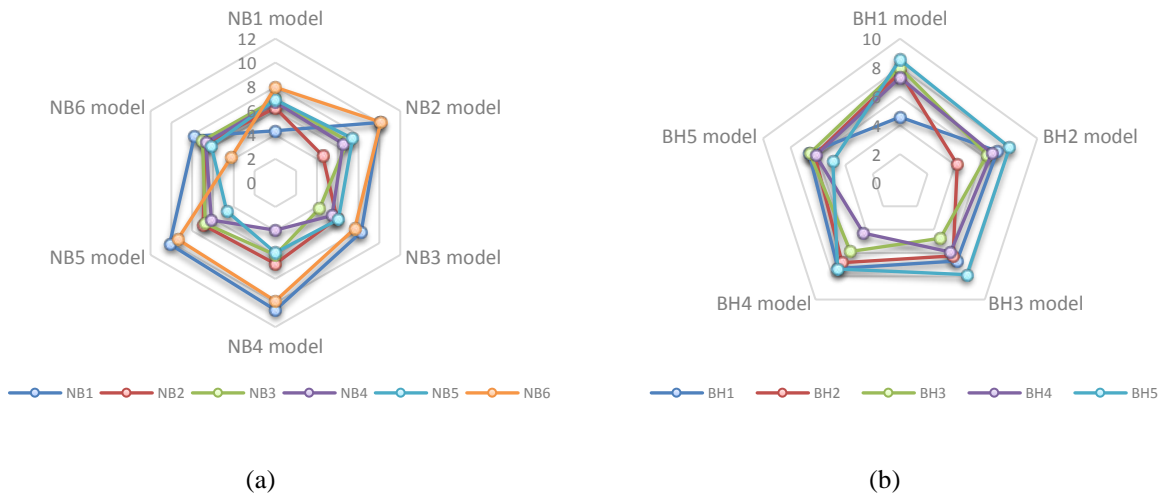
Figure 21- Standard deviation of errors for SBP in a) NB intervals b) BH intervals

(a)   (b)
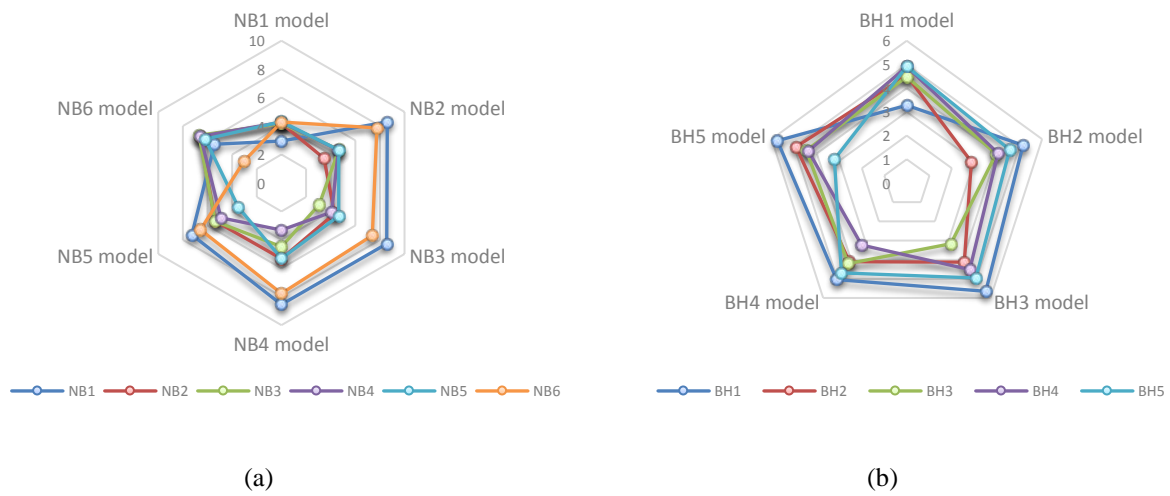
Figure 22- Standard deviation of errors for DBP in a) NB intervals b) BH intervals

(a)   (b)
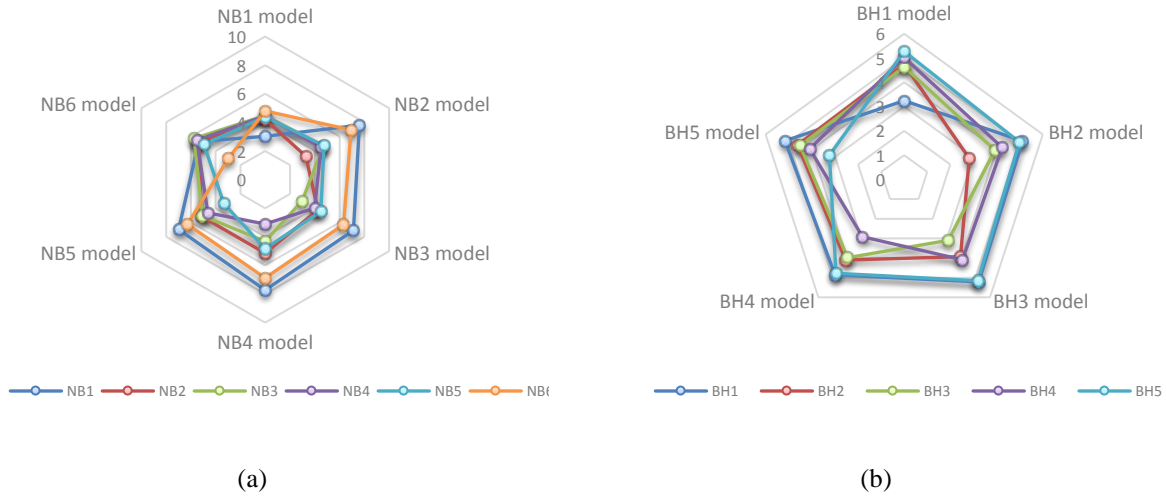
Figure 23- Standard deviation of errors for MAP in a) NB intervals b) BH intervals

To estimate the accuracy of the values of $\hat{SBP}$, $\hat{DBP}$, and $\hat{MAP}$ obtained from each model, the root mean square error (rMSE) for the model errors for both BH and NB intervals were computed using equation 4. The results of averaging the rMSE values derived from the model errors for all subjects and for BH and NB intervals are tabulated in tables 1 and 2, respectively. To assess how a model developed from the data of one interval (e.g., BH1) predicts the corresponding BP measures (i.e., SBP, DBP or MAP) of another congruent interval, we computed the rMSE of the prediction errors for NB and BH and tabulated them in tables 3 and 4.

Table 1- rMSEs for models errors of NB intervals (mmHg)

	1st NB	2nd NB	3rd NB	4th NB	5th NB	6th NB
Systolic	4.39	4.58	4.29	3.95	4.69	4.26
Diastolic	2.97	3.50	3.10	3.35	3.49	3.12
MAP	3.07	3.32	3.04	3.14	3.35	3.03

Table 2- rMSEs for model errors of BH intervals (mmHg)

	1st BH	2nd BH	3rd BH	4th BH	5th BH
Systolic	4.60	4.19	4.81	4.35	4.94
Diastolic	3.29	2.88	3.19	3.26	3.24
MAP	3.27	2.84	3.14	2.94	3.27

Table 3- rMSE of prediction errors of models identified for each NB interval and applied to estimating BP features for other NB intervals (mmHg)

	1st NB	2nd NB	3rd NB	4th NB	5th NB	6th NB
Systolic	6.58	8.14	6.68	7.88	7.94	6.76
Diastolic	4.01	6.25	6.03	6.44	5.89	6.09
MAP	4.22	5.74	5.27	5.85	5.64	5.32

Table 4- rMSE of prediction errors of models identified for each BH interval and applied to estimating BP features for other BH intervals (mmHg)

	1st BH	2nd BH	3rd BH	4th BH	5th BH
Systolic	7.38	6.63	6.48	6.49	7.94
Diastolic	4.48	4.24	4.63	4.33	4.65
MAP	4.66	4.36	4.46	4.22	4.41

4.1.2 *Cerebral blood flow modeling results in Breath-hold study*

For modeling CBF, we also obtained models for estimating CBF during the breath hold maneuvers and normal breathing intervals. Specifically, we modeled the changes in CBF peaks which are associate with the systolic part of the cardiac cycle and separately we modeled the troughs of CBF which are associated with the diastolic part of the cardiac cycle. In all, we obtained

11 CBFP/systolic models and 11 CBFT/diastolic models for each subject. Figure 24 illustrates a sample of compute $\widehat{CBFP}$ superimposed on their respective measured values of CBFP in both BH and NB intervals taken from the same subject (subject No. 4).

(a)   (b)
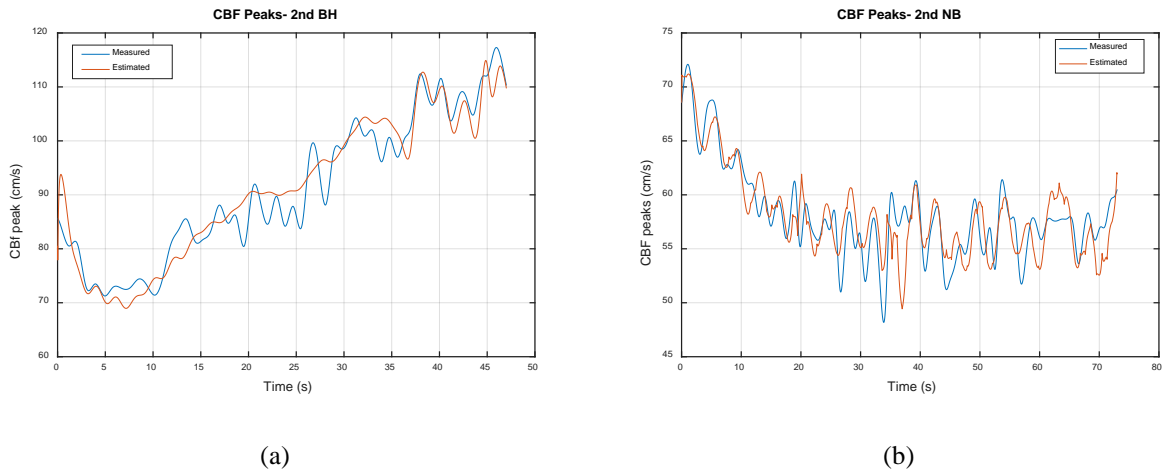
Figure 24- Measured CBFP signal versus estimated CBFP from modeling: figure (a) shows example of breath-hold model and figure (b) shows example of normal breathing model

Likewise, estimated values and measured values for CBFT are displayed in Figure 25 for both NB and BH intervals from the same subject (subject No. 4).

(a)   (b)
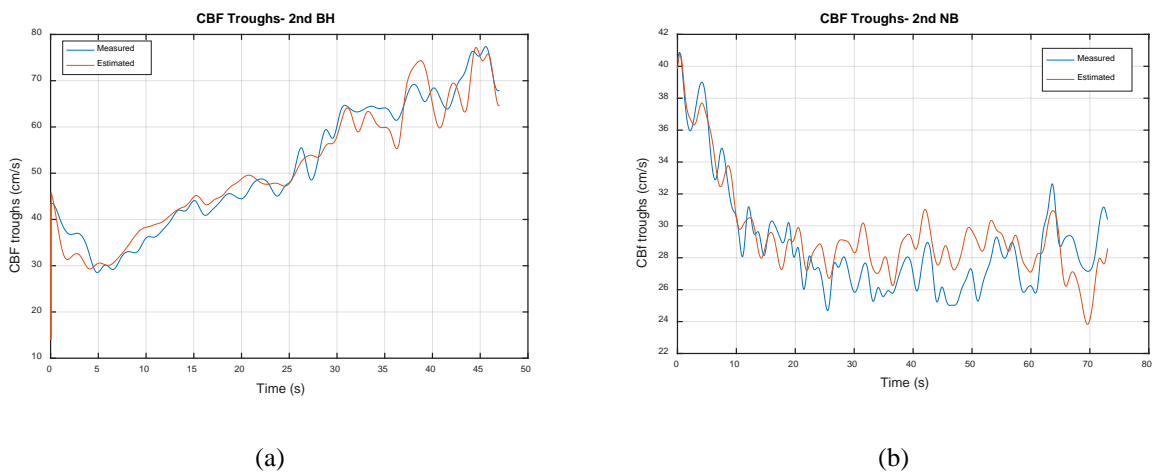
Figure 25- Measured CBFT signal versus estimated CBFT from modeling: figure (a) shows example of breath-hold model and figure (b) shows example of normal breathing model

Figure 26 and Figure 27 show the mean of the Model Errors as well as the mean of the Prediction Errors for CBFP and CBFT in breath-hold study. Means of errors are calculated across all the subjects.

(a)   (b)
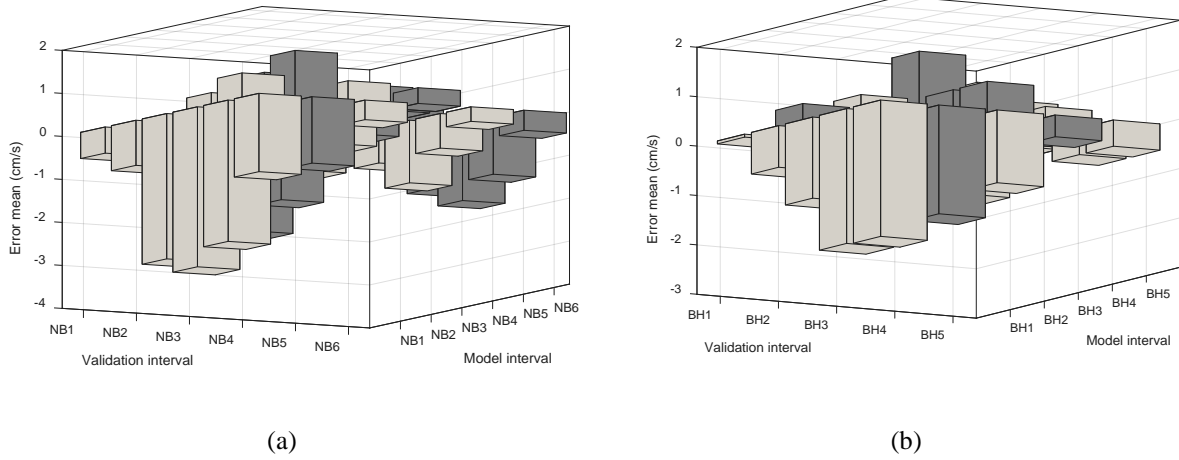
Figure 26- Mean of errors for CBFP in a) NB intervals b) BH intervals

(a)   (b)
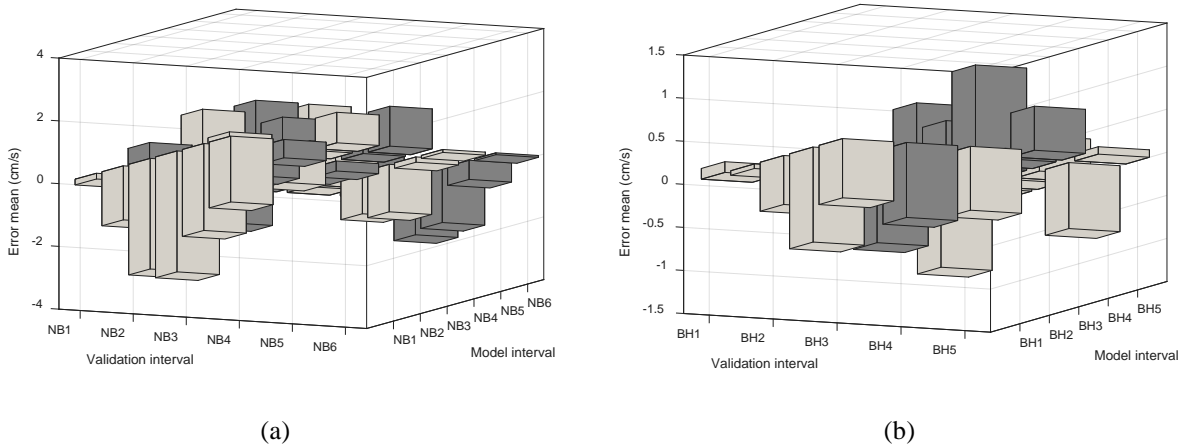
Figure 27- Mean of errors for CBFT in a) NB intervals b) BH intervals

Figure 28 and Figure 29 display the standard deviation of the Model Errors and Prediction Errors reflecting the level of dispersion in these errors around their mean values.

(a)   (b)
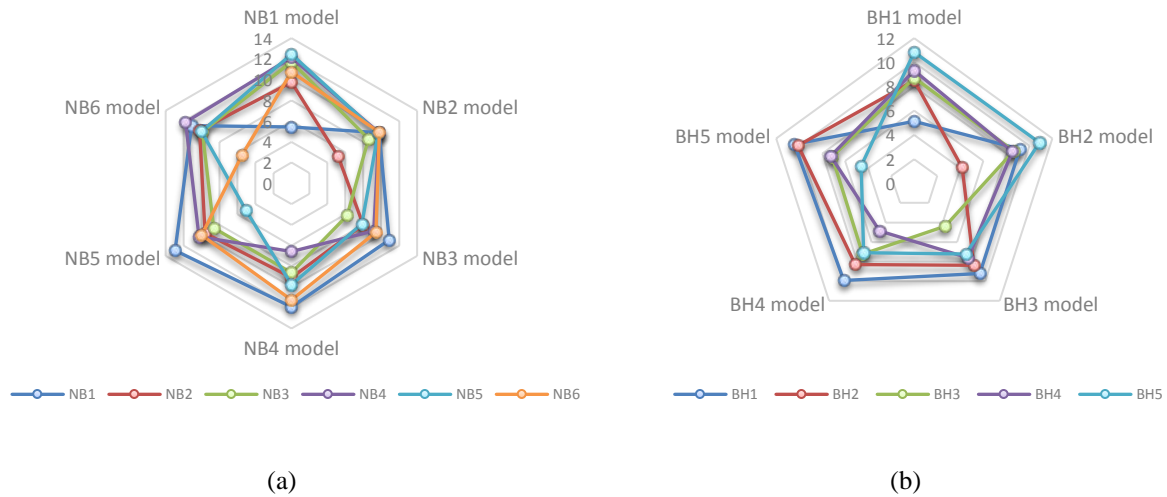
Figure 28- Standard deviation of errors for CBFP in a) NB intervals b) BH intervals

(a)   (b)
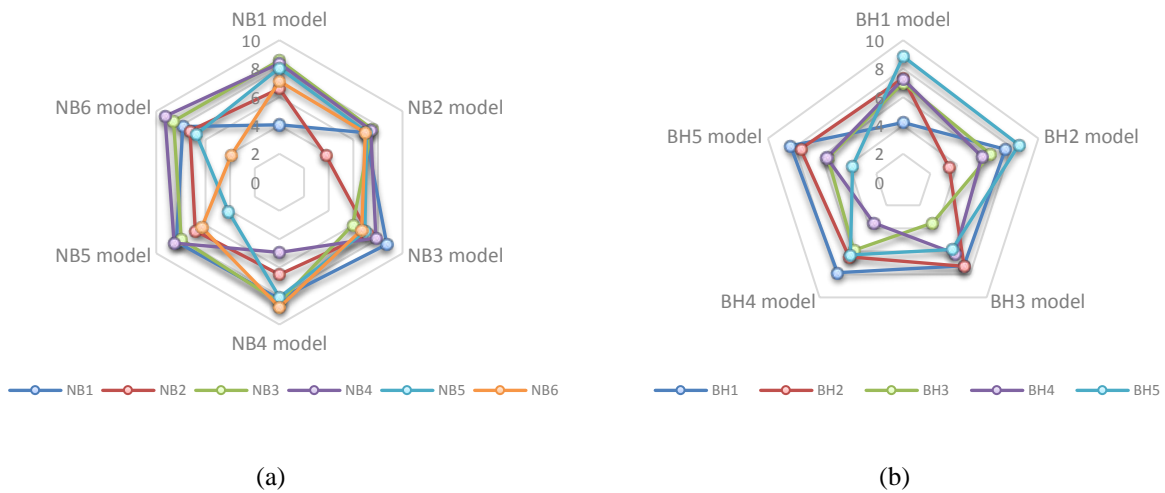
Figure 29- Standard deviation of errors for CBFT in a) NB intervals b) BH intervals

Similar to BP modeling, the results of averaging the rMSE values derived from the model errors for all subjects and for BH and NB intervals are tabulated in Table 5 and 6, respectively. Likewise, to assess how a model developed from the data of one interval (e.g., BH1) predicts the corresponding CBF measures (i.e., CBFP or CBFT) of another congruent interval, we computed the rMSE of the prediction errors for NB and BH and tabulated them in Table 7 and 8.

Table 5- rMSEs for models errors of NB intervals (cm/s)

	1st NB	2nd NB	3rd NB	4th NB	5th NB	6th NB
CBFP	5.48	5.20	6.24	6.58	5.14	5.49
CBFT	4.05	3.78	5.96	4.93	4.13	3.89

Table 6- rMSEs for model errors of BH intervals (cm/s)

	1st BH	2nd BH	3rd BH	4th BH	5th BH
CBFP	5.12	4.18	4.39	4.86	4.64
CBFT	4.21	3.41	3.52	3.51	3.73

Table 7- rMSE of prediction errors of models identified for each NP interval and applied to estimating BP features for other NB intervals (cm/s)

	1st NB	2nd NB	3rd NB	4th NB	5th NB	6th NB
CBFP	10.77	9.72	9.15	10.18	10.41	10.69
CBFT	8.34	7.37	7.63	8.16	7.85	8.12

Table 8- rMSE of prediction errors of models identified for each BH interval and applied to estimating BP features for other BH intervals (cm/s)

	1st BH	2nd BH	3rd BH	4th BH	5th BH
CBFP	9.66	9.50	8.18	8.25	8.86
CBFT	7.70	7.22	6.69	6.69	6.86

4.2   Sleep study results

ARMA models were calculated for 6 longest apnea episodes for each subject separately. A sample of distribution of apnea episodes duration is displayed in . This plot can help visualize distribution of apnea durations over the entire sleep period for subject number 1. Similar plots for

56

the rest of the subjects can be found in Appendix B. For BP modeling, we used all 15 subjects, but in CBF, modeling 2 subjects had poor signals and could not be included in the analysis. Therefore, we only analyzed 13 subjects (9 males, 4 females, aged 52.92 ± 7.2 years, BMI 34.1 ± 7.3 kg/m^2) in CBF modeling.
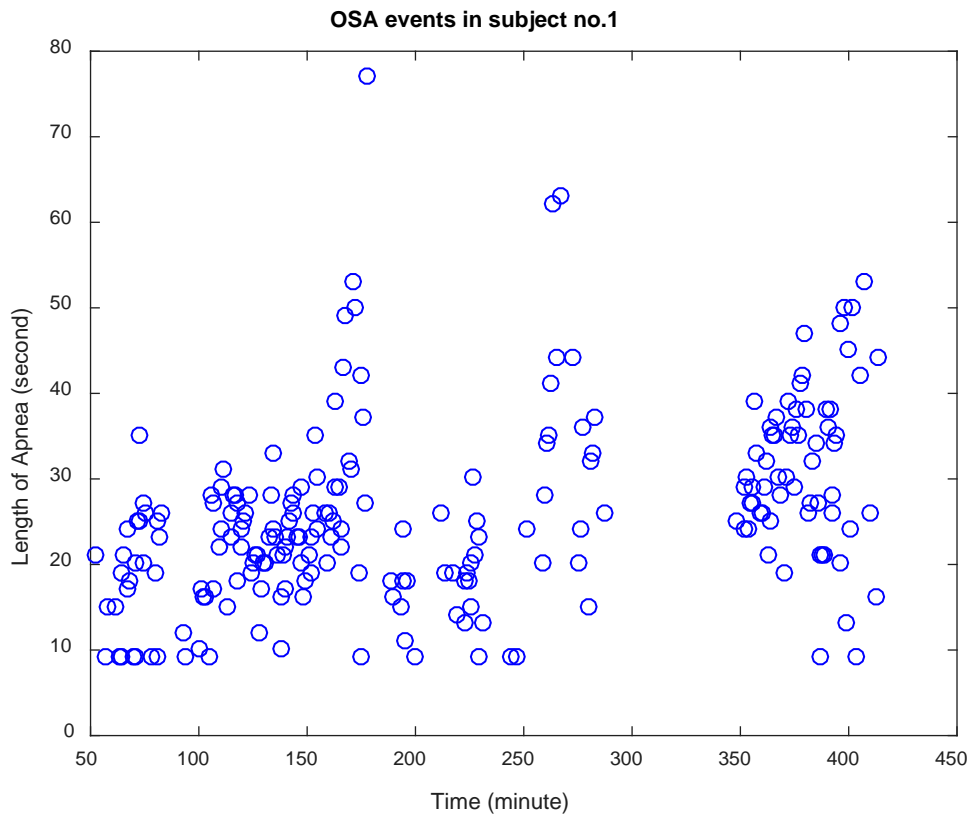
Figure 30- Apnea episode durations over the entire sleep study for subject no. 1

4.2.1 *Blood pressure modeling results in sleep study*

Figure 31 shows an example of estimated systolic and diastolic BP – obtained from PPG signal – superimposed on their respective measured values for the same apnea episode from one of the subjects.

(a)   (b)
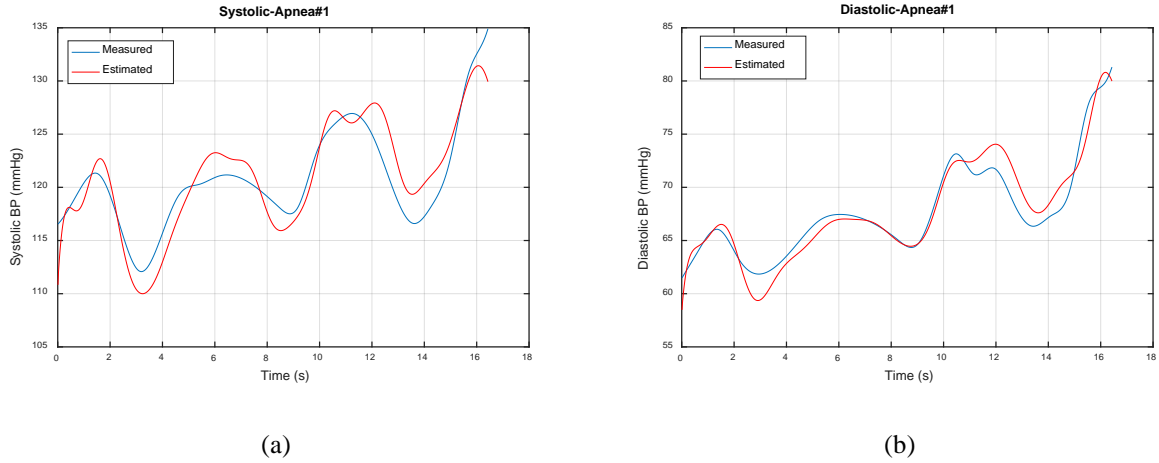
Figure 31- a) Measured SBP signal versus estimated SBP from modeling b) Measured DBP signal versus estimated DBP from modeling

Figure 32, Figure 33 and Figure 34 show the mean of the Model Errors as well as the mean of the Prediction Errors for systolic, diastolic and MAP in sleep study. Means of errors are calculated across the all 15 subjects.
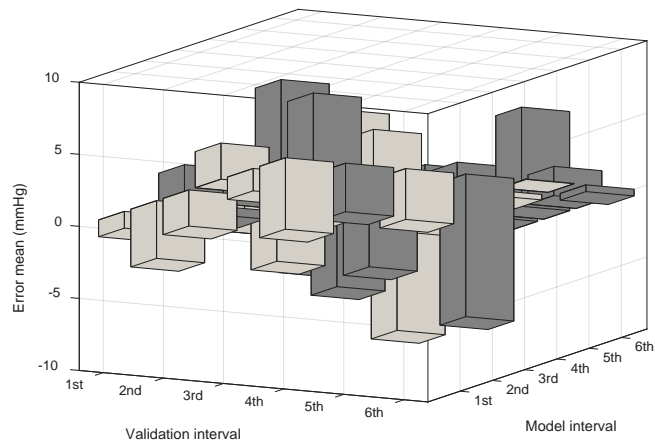
Figure 32- Mean of errors for SBP in apnea episodes

Figure 33- Mean of errors for DBP in apnea episodes

Figure 34- Mean of errors for MAP in apnea episodes

In addition to mean of errors, standard deviation of the errors are calculated and displayed in Figure 35 and Figure 36. These plots reflect the level of dispersion in these errors around their mean values for both modeling and prediction errors.

Figure 35- Standard deviation of errors for SBP in apnea episodes

Figure 36- Standard deviation of errors for DBP in apnea episodes
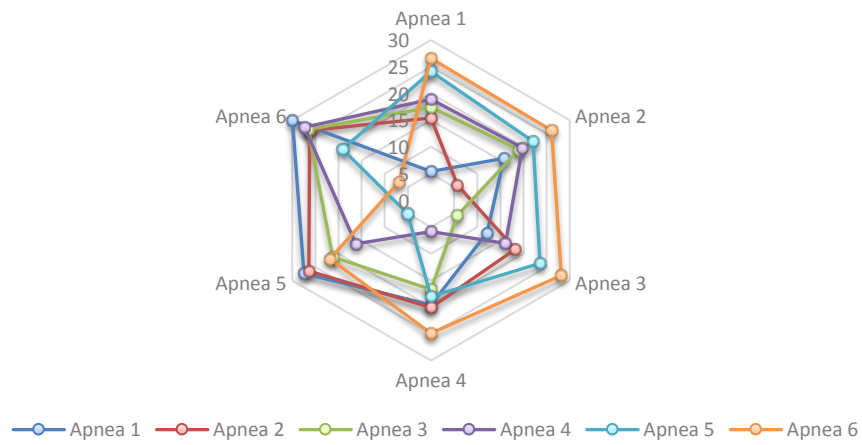
Figure 37- Standard deviation of errors for MAP in apnea episodes

Similar to breath-hold study, the results of averaging the rMSE values derived from the model errors for all subjects are tabulated in Table 9, respectively. Likewise, to assess how a model developed from the data of one apnea episode predicts the corresponding BP measures (i.e., SBP, DBP or MAP) of another apnea episode, we computed the rMSE of the prediction errors and tabulated them in Table 10.

Table 9- rMSEs for models errors of apnea episodes (mmHg)

	1st apnea	*2nd apnea*	*3rd apnea*	*4th apnea*	*5th apnea*	*6th apnea*
Systolic	6.16	7.03	6.44	7.43	6.23	7.81
Diastolic	4.27	3.14	4.39	2.74	2.64	5.07
MAP	5.65	6.45	4.75	5.93	4.54	6.17

Table 10- rMSE of prediction errors of models identified for each apnea episode and applied to estimating BP features for other apnea episodes (mmHg)

	1st apnea	*2nd apnea*	*3rd apnea*	*4th apnea*	*5th apnea*	*6th apnea*
Systolic	17.26	18.03	20.12	17.45	21.05	16.85
Diastolic	13.96	11.55	7.39	11.07	9.26	21.13
MAP	14.97	14.25	11.55	12.44	14.68	17.89

4.2.2   *Cerebral blood flow modeling results in sleep study*

CBFP and CBFT during apnea episodes were modeled in the same way as modeling systolic and diastolic BP. A sample result of this modeling is shown in Figure 38 obtained from the same apnea episode (apnea no. 5) from one of the subjects (subject no. 3).
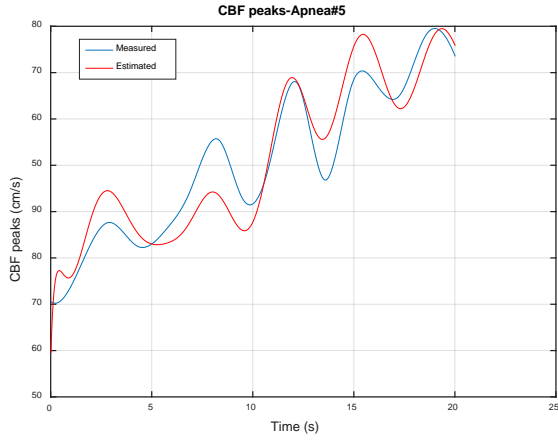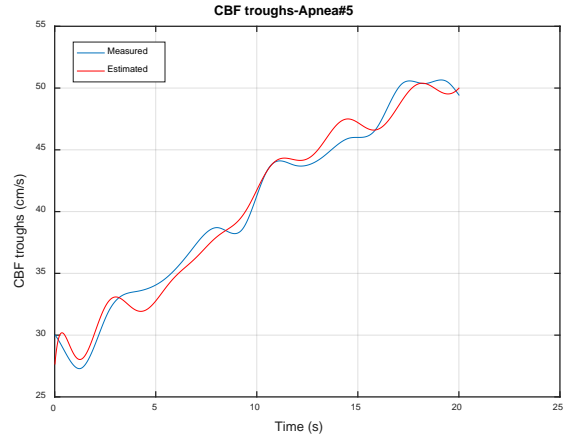
(a)   (b)

Figure 38- a) Measured CBFP signal versus estimated CBFP from modeling and b) Measured CBFT signal versus estimated CBFT from modeling

The mean of the Prediction Errors for CBFP and CBFT in sleep study are illustrated in Figure 39 and Figure 40. Means of errors are calculated across the 13 subjects as explained in 4.2.
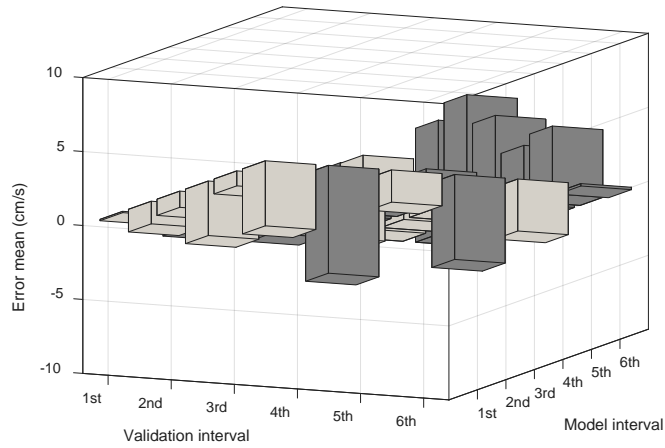
Figure 39- Mean of errors for CBFP in apnea episodes
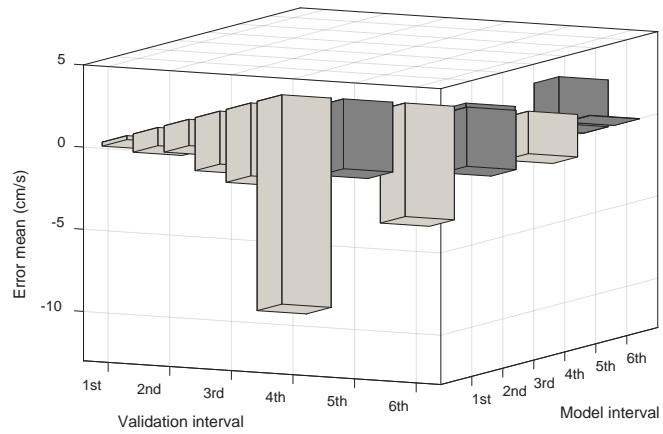
Figure 40- Mean of errors for CBFT in apnea episodes

In addition to mean of errors, standard deviation of the errors are calculated and displayed in Figure 41 and Figure 42. These plots reflect the level of dispersion in these errors around their mean values for both modeling and prediction errors.
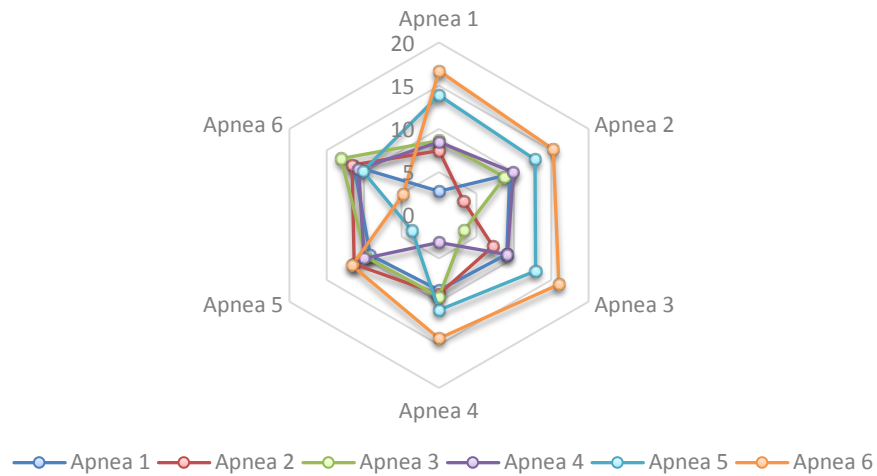
Figure 41- Standard deviation of errors for CBFP in apnea episodes
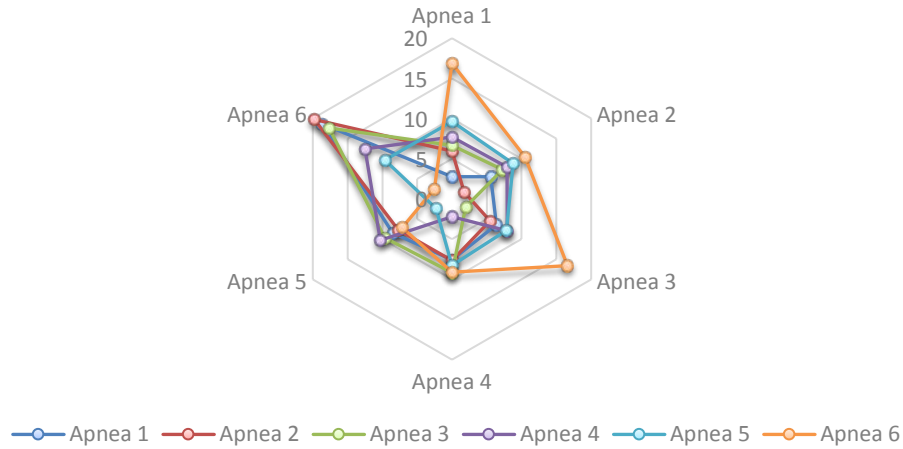
Figure 42- Standard deviation of errors for CBFT in apnea episodes
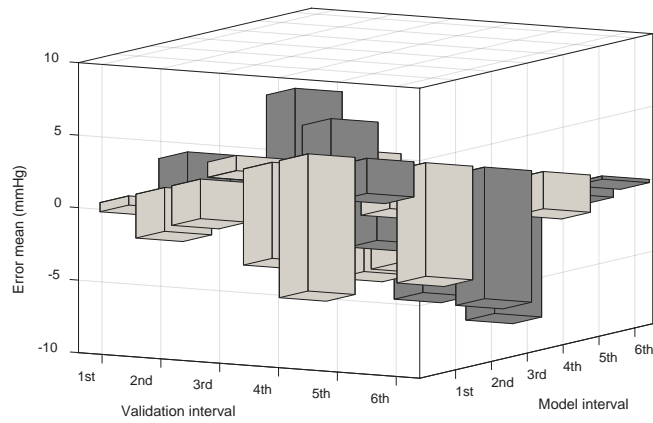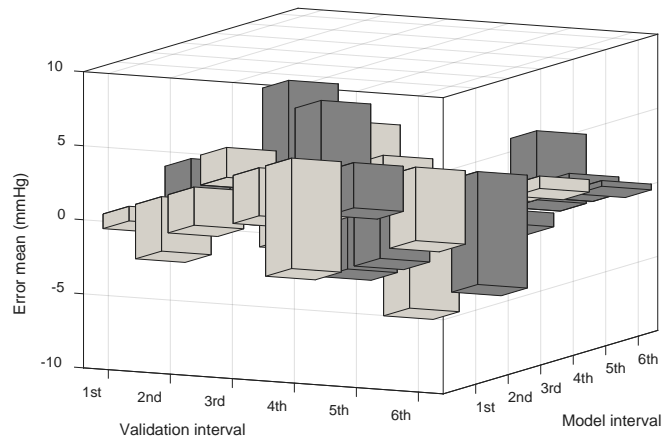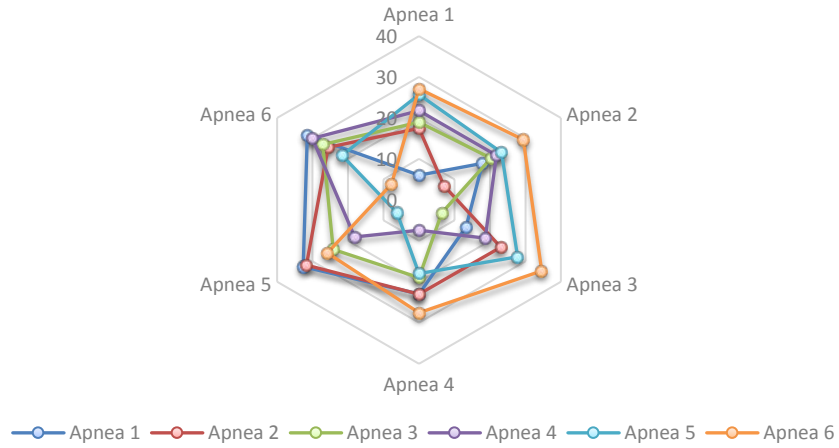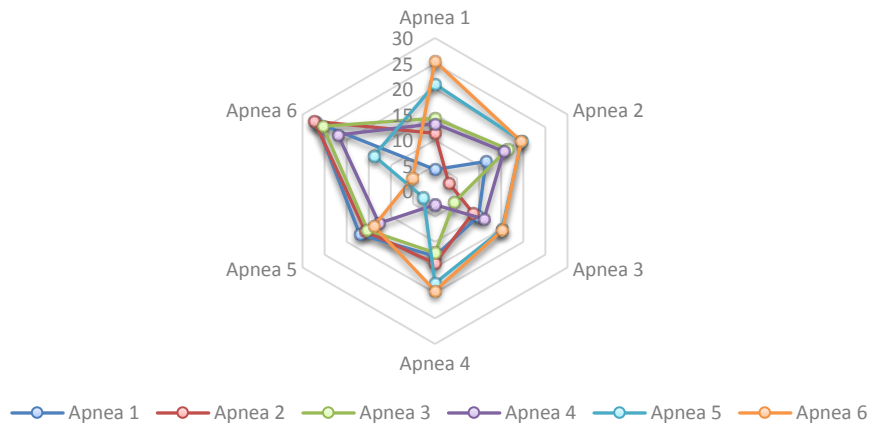
Similar to breath-hold study, the results of averaging the rMSE values derived from the model errors for all subjects are tabulated in Table 11, respectively. Likewise, to assess how a model developed from the data of one apnea episode predicts the corresponding CBF measures (i.e., CBFP or CBFT) of another apnea episode, we computed the rMSE of the prediction errors and tabulated them in Table 12.

Table 11- rMSEs for model errors of apnea episodes (cm/s)

	1ˢᵗ apnea	*2ⁿᵈ apnea*	*3ʳᵈ apnea*	*4ᵗʰ apnea*	*5ᵗʰ apnea*	*6ᵗʰ apnea*
CBFP	2.79	3.29	3.40	3.16	3.60	4.79
CBFT	2.77	1.75	1.99	2.20	2.33	2.52

Table 12- rMSE of prediction errors of models identified for each apnea episode and applied to estimating CBF features for other apnea episodes (cm/s)

	1ˢᵗ apnea	*2ⁿᵈ apnea*	*3ʳᵈ apnea*	*4ᵗʰ apnea*	*5ᵗʰ apnea*	*6ᵗʰ apnea*
CBFP	12.47	12.63	12.01	11.69	10.91	13.39
CBFT	12.87	8.77	11.13	8.76	8.78	14.33

64

For illustrative purposes, some samples of validation plots for both studies, BH and sleep study can be seen in Figure 43 through Figure 46:
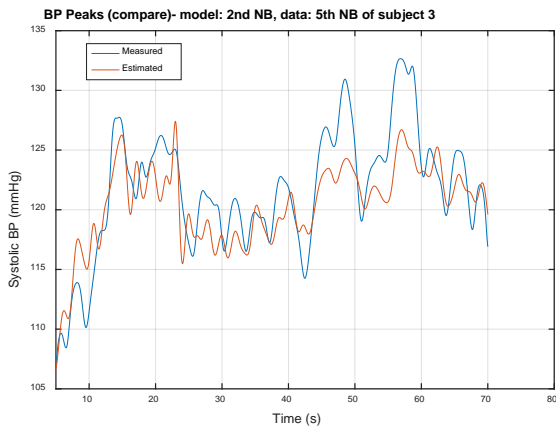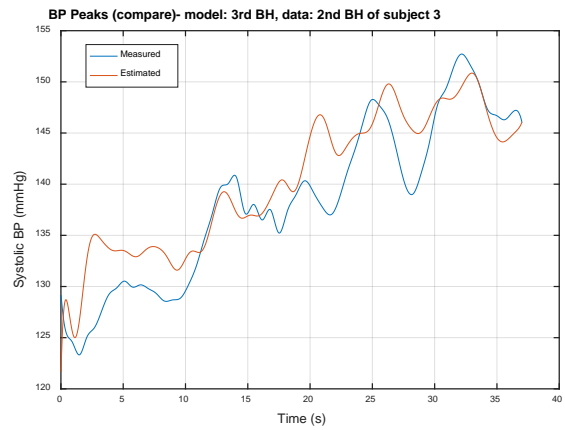
(a)   (b)

Figure 43- Estimated systolic BP and measured systolic BP in an interval using model obtained from another interval, both in simulated sleep study: a) in NB interval b) in BH interval
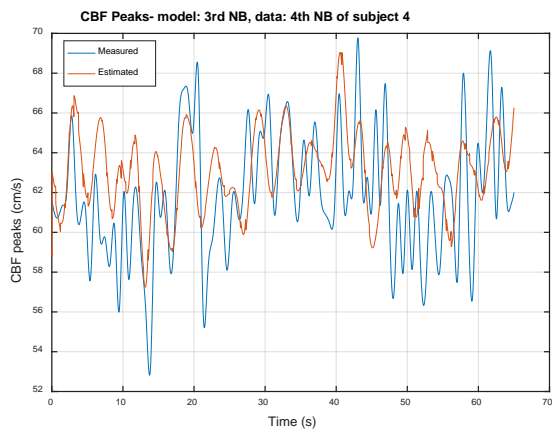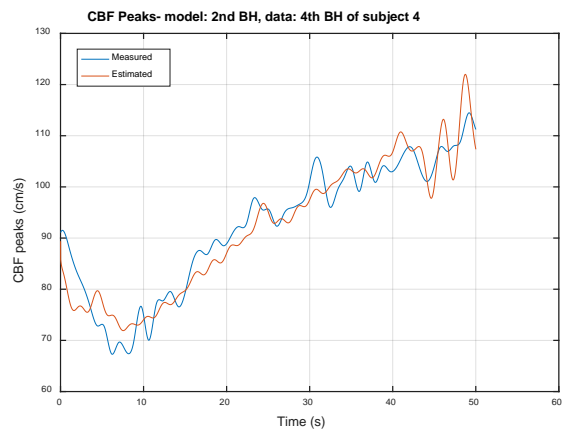
(a)   (b)

Figure 44- Estimated CBFP and measured CBFP in an interval using model obtained from another interval, both in simulated sleep study: a) in NB interval b) in BH interval
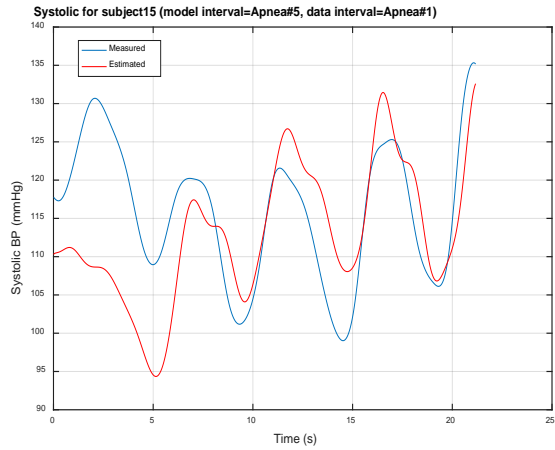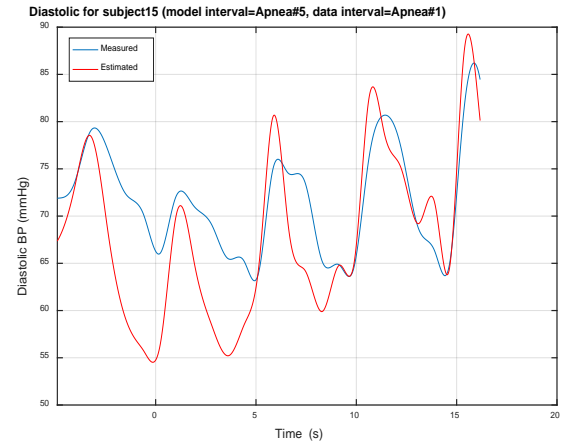
Figure 45- Estimated and measured values in an apnea using model obtained from another apnea from sleep study:
a) Estimated systolic BP and measured systolic BP b) Estimated diastolic BP and measured diastolic BP
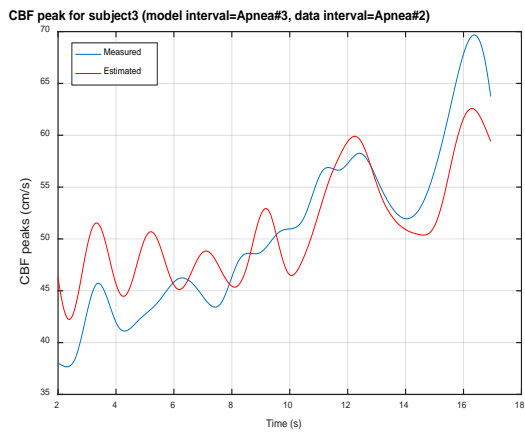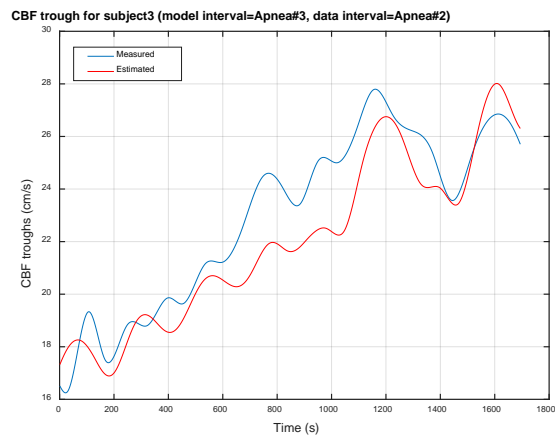
Figure 46- Estimated and measured values in an apnea using model obtained from another apnea from sleep study:
a) Estimated CBFP and measured CBFP b) Estimated CBFT and measured CBFT

CHAPTER 5

Discussion

5.1   Breath-hold modeling

As explained in 4, ARMA models for each BH and NB intervals were calculated separately for both CBF/BP peaks and CBF/BP troughs in all subjects. Results of BP modeling and CBF modeling are discussed separately in following sections.

5.1.1   Blood pressure modeling results

Subplot (a) of Figure 15, Figure 16 and Figure 17 show that the $\hat{S}BP$, $\hat{D}BP$, and $\hat{M}AP$ track the overall rising trends of the DBP, SBP, and MAP signals during the BH intervals. As shown, there is an upward trend in BH intervals indicating that BP is increasing during BH intervals which is a direct result of the sympathetic nerve response to breath hold maneuvers [127]. Further, these subplots illustrate the ability of the models in tracking the higher frequency modulations present in the measured BH signals. Similar observations can be made about the results plotted in the subplot (b) of Figure 15, Figure 16 and Figure 17. As can be seen from these sample plots, the ARMA models developed can track the measured values of the BP parameters of interest for both modes of NB and BH with relatively high level of fidelity.

However, it can be seen that modelling results shown in Figure 15 (b) does not track all the oscillations of the measured SBP as closely as in the other subplots. This is due to the fact that we have selected the maximum model orders for all experimental conditions to be 5, based on evaluation of a sample number of records. This was done to avoid custom fitting the data for each experimental setting and to achieve some degree of uniformity in the derived models. Hence, some instantaneous estimates of the BP features may follow the measured values more closely than the

67

others, but, as shown in all subplots of Figure 15, Figure 16 and Figure 17, the estimates do follow the longer term trends of the measured values. Some models may perform better than the others depending on the frequency content of that specific interval or baseline trend.

The plots of the means of the model errors and prediction errors in Figure 18, Figure 19 and Figure 20 provide a visual assessment of the level of accuracy of estimation of the SBP, DBP, and MAP. As can be seen from the subplots (a) and (b) of these figure, the estimation errors for NB interval in all cases have a mean that is well within ±3 mmHg. Indeed, a majority of the cases have error means that are within ±2 mmHg. With taking the level of dispersion of the model errors in Figure 21, Figure 22 and Figure 23 into consideration, it can be seen that the standard deviations for the modeling errors for BH intervals are all below 5 mmHg. This relatively small window of variation is also corroborated by congruent rMSE values that are shown in Table 1 through Table 4. A similar observation can be made regarding the errors for BH interval. As illustrated, the mean values of these errors fall with a tighter interval than those of NB; all fall within ±2 mmHg. Moreover, the dispersion of the errors for BH is comparable to that of NB by being below 5 mmHg. Majority of mean of the errors are negative for all SBP, DBP and MAP especially in BHs, which might be due to the fact that the initial conditions are a little deviated from the actual values and models need some time to pass the transient state and catch up with the measured values. As the rising trend of the BP and CBF is a characteristic of BH intervals, it is expected that estimated values which are falling behind, be lower than the actual values making the error term to be negative.

As can be seen from the results shown in Figure 21-23, the upper bound for the dispersion of the prediction errors is larger than dispersion for model errors (i.e. 10 vs 5 mmHg, respectively). This is somewhat expected as prediction errors reflect the ability of the models in predicting BP

under the condition different from the condition that model was derived for. In particular, the experimental protocol was designed to examine the effect of successive breath holds on the estimation of BP.

Table 1 and Table 2 show additional information about the dispersion of the estimates of SBP, DBP, and MAP. The rMSE values for the model errors for all NB and BH cases lay below 5 mmHg. This indicates that the developed models from the measured data on the average can have an accuracy of 5 mmHg when they are applied to predict the SBP, DBP, or MAP for the same interval.

The overall dispersion of the errors of a model in predicting values of SBP, DBP, and MAP by models which are derived from a given interval and applied to different, but congruent (i.e., BH to BH and NB to NB), intervals are shown in Table 3 and Table 4. Considering that the model parameters are derived from a different interval, one can expect the estimation errors to rise. Indeed, comparing the rMSE values in Table 1 and 2 with those in Table 3 and 4 shows that rMSE values have a max mean of approximately 8 mmHg. Therefore, if rMSE is used to gauge the level of the error, for both model errors and prediction errors, an overall error of less than 8 mmHg can be expected. When compared with some of the previously reported techniques, one finds that our results are comparable to techniques that used PAT in estimating BP from PPG signals [128]. The mean error reported in the previous study was 5 mmHg for DBP and 1 mmHg for SBP, while our method achieved mean error of less than 3 mmHg for all SBP, DBP and MAP [129]. PTT has been used to estimate mean SBP and mean DBP and compared to actual measurements and reported to be within 15 and 25 mmHg respectively which is much higher than our method. These findings show the ARMA model approach is capable of tracking slow frequency trend and also high frequency hemodynamic changes of the body and exhibit adequate accuracy for possible clinical

applications. Nonetheless, since the blood pressure level is influenced by a host of variables such as cardiac output and peripheral vascular resistance, introducing other measurable parameters, particularly from PPG, may increase the accuracy of estimation of the blood pressure [130]. These can include temporal features like duration of each period, amplitude of the PPG and area under curve.

5.1.2   Cerebral blood flow modeling results

As shown in Figure 24 and Figure 25, the CBF generally follows a rising trend during BHs, along with the PPG amplitude. It is noted that irrespective of the duration of each breath hold, the CBF and the level of PPG tended to rise and reach the highest level when BH was ended or shortly afterwards. This is the motive behind this study, indicating CBF might be modeled from PPG as blood perfusion is reflected in both signals.

In subplot (a) of Figure 24 and Figure 25, it can be seen that $\widehat{CBFP}$ and $\widehat{CBFT}$ track the overall rising trends of the CBFP and CBFT signals during the BH intervals. As shown, there is an upward trend in BH intervals indicating CBF is increasing during BH intervals. Such a rise is a direct result of the sympathetic nervous system response to breath-hold maneuvers [127]. Additionally, these subplots illustrate the ability of the models to track the higher frequency modulations present in the measured CBF signals. Similar observations can be made about the results plotted in the subplots (b) of Figure 24 and Figure 25. As can be seen from these sample plots, the ARMA models developed can track the measured values of the CBF parameters of interest for both modes of NB and BH with a relatively high degree of fidelity. From these plots, one can see that some instantaneous estimates of the CBF features may follow the measured values more closely than the others, but, as presented in all subplots of these figures, the estimates do follow the longer term trends of the measured values.

70

Table 5 and Table 6 give additional information about the dispersion of the estimates of CBFP and CBFT. The rMSE values for the model errors for all NB and BH cases were equal or less than 6.58 cm/s with the average of 4.65 cm/s. The overall errors associated with predicting values of CBFP and CBFT using models derived from a given interval and applied to different but congruent intervals (i.e. BH to BH and NB to NB) are shown in Table 7 and Table 8. Considering the model parameters were derived from a different interval, a rise in errors is expected. Indeed, comparing the rMSE values in Table 5 and Table 6 with those in Table 7 and Table 8 shows that rMSE values of prediction errors have a max mean of 10.77 cm/s as compared to a max mean value of 6.58 cm/s for modeling error. Therefore, using rMSE as an indicator of error level, for both model errors and prediction errors, an overall error of less than 11 cm/s can be expected. These findings show the ARMA model approach capable of tracking slow frequency trends and also high frequency hemodynamic changes of the body along with exhibiting adequate accuracy for possible clinical applications [131] [132]. However, since the cerebral blood flow is influenced by a host of variables such as cardiac output, cerebral vascular resistance, intracranial pressure, and more importantly, the cerebral autoregulation mechanism [133], future introduction of other measurable parameters, in addition to PPG features, may increase the accuracy of cerebral blood flow estimation. These features can be amplitude, duration of the period or area under PPG signal.

The plots of the means of the model errors and prediction errors in Figure 26 and Figure 27 provide a visual assessment of the level of accuracy of estimation of the CBFP and CBFT. As can be seen from the subplot (a) of Figure 26 and Figure 27 the estimation errors for NB interval in all cases had a mean that was well within +3 and -4 cm/s. Indeed, a majority of the cases had error means within $\pm$ 3 cm/s. With taking the level of dispersion of the model errors in Figure 28 and Figure 29 into consideration, it can be seen that the standard deviations for the modeling errors

71

for NB intervals were all below 13 cm/s. This relatively small window of variation was also corroborated by the consistent rMSE values that are shown in Table 5.

A similar observation can be made regarding the errors for BH interval. As illustrated in subplot (b) of Figure 26 and Figure 27, the mean values of these errors fell within a tighter interval than those of NB, approximately between +2 and -3, with the majority falling within ± 2 cm/s. Moreover, the dispersion of the errors for BH was also smaller than that of NB by being below 11 cm/s. This greater accuracy level for CBF modeling from PPG during BH may be attributable to the BH-induced excitations into the PPG (model input) and CBF (model output). Similar observation regarding the negative mean of errors can be made as well, which is due to the initial condition and rising trend of CBF as explained in 3.1.5.

As can be seen from the results shown in Figure 28 and Figure 29, the upper boundary for the dispersion of the prediction errors was larger than the dispersion for model errors (i.e. approximately 13 vs 8 cm/s, respectively). This was somewhat expected as prediction errors reflect the ability of the models to predict CBF from the input (PPG signal) that in general would be different from the input that was used in deriving the model.

By studying models derived for different intervals separately, it was revealed that no interval is showing any superior performance in predicting values of BP and CBF from PPG signal.

5.2 Sleep study modeling

Similar to breath-hold study, each apnea episode was modeled separately and used to evaluate both modeling and validation error. Results of the BP modeling and CBF modeling during nocturnal apnea episodes are presented in 4.2 and discussed separately in following sections. As can be seen in Figure 30 and figures in Appendix B, the apnea episodes, which have been selected

for sleep study, are occurring at different time and stages of sleep and can affect the modeling which is further discussed in 5.4.

5.2.1 Blood pressure modeling for sleep study results

As shown in Figure 31, BP exhibits a rising trend during apnea interval which is due to the sympathetic nervous activity and ARMA model is capable of following this slow frequency rising trend. However, while the trend is followed, the accuracy and precision may not be as good as BH maneuver study. This is further illustrated in Table 9 and Table 10. Furthermore, as displayed in Figure 45, validation results are not as good as the modeling results. This arises from the fact that the initialization for the estimation affects the transient part of the estimated signal which would diminish as the model response tends toward the steady state. However, if apnea episode is extends to pass the transient part of the response, then the estimated signal is closer to the actual measured value. Hence, in the validation study, the observed discrepancy between the measured and estimated BP during the transient phase of the response is partially due to how close the estimated initial conditions (please see section 3.1.5) are to the values that would have been obtained if one had access to the measured output for their estimation.

The mean of the errors which are illustrated in Figure 32, Figure 33 and Figure 34, are all approximately between 8 to -8 mmHg; with the max absolute mean of 7.62 mmHg. By careful observation it can be seen that more than 90 percent of the mean of errors actually fall within ±6 mmHg. Assuming the baseline of systolic to be around 110-130 cm/s and diastolic to be around 80-100 cm/s, this is equivalent to less than 10 percent deviation from the actual values, which is slightly higher than the breath-hold result of ±3 mmHg, as is discussed in 5.3 below.

Figure 35, Figure 36 and Figure 37 display the level of standard deviation of the errors, a measure of the dispersion in the estimation of the BP features during apnea episodes. These figures

show both modeling and validation error standard deviations. The maximum level of dispersion is around 34 mmHg which indicates that the estimates may not be useful for clinical applications. The average of the standard deviation of the errors calculated to be 15.83 mmHg. By a closer examination of these values, it can be seen that the standard deviations of the modeling errors are all below 8mmHg with more than 50 percent of them being below 6mmHg. This indicates that the modeling has performed well in each apnea episode, but it cannot exhibit the same performance in other intervals when used for validation purpose. This divergence in the results are further discussed in section 5.3 and some future modifications are proposed to improve it.

Quantitative evaluation of the results in Table 9 and Table 10 confirms the illustrative results of previously discussed figures. The rMSE values for modeling errors are all below 8 mmHg and rMSE of the validation errors are below 22 mmHg. Same discussion applies to the validation interval and needs to be improved to be practically useable. However, an interesting observation can be made that the maximum error, in either mean or standard deviation or even in rMSE values, usually occurs in last intervals. Considering the fact that the apnea episodes are sorted based on their occurrence during the sleep, this suggests that temporal incidence of an apnea episode may influence the outcome of modeling.

5.2.2   *Cerebral blood flow modeling for sleep study results*

Samples of modeling results for both CBFP and CBFT that are illustrated in Figure 38 show that ARMA model can track the overall rising trend of the CBF during the apnea interval, while missing high frequency fluctuations, which has resulted in poorer accuracy. This is reflected in Table 11 and Table 12 where quantitative evaluations of the modeling show that modeling accuracy is not as good as BH study. It is important to note the PPG signal reflects both blood oxygenation and volume changes; however, the main effect is dominated by volume changes [134]

74

[135]. Previous studies have shown that apnea episodes elicit a significant rise in the beat-by-beat blood pressure [34] [58]. When the rise in BP is concomitant with the rise in CBF [54] [55], the CBF and PPG changes tend to follow the same trend.

The plots of the mean of errors are displayed in Figure 39 and Figure 40 and provide a visual assessment of the level of accuracy for both CBFP and CBFT. As can be seen, all the mean of the errors fall within 13 cm/s with the maximum of 12.73 cm/s, while more than 90% of them are within ±6 cm/s. Indeed, it seems that some interval errors are outliers, like apnea no. 1 validated with apnea no. 6 in CBFT modeling. If this outlier, for example, removed, the means of the errors for CBFT will be all less than 5 cm/s.

Figure 41 and Figure 42 illustrate the standard deviation of the errors in both validation and modeling errors for CBFP and CBFT. As can be seen, the standard deviation values fall within ±20 cm/s with average of 7.28 cm/s. Indeed, more than 60 percent of the standard deviation of errors are within ±10 cm/s. The dispersion of the errors is less than that of BP modeling for sleep studies. This may be attributable to the cerebral autoregulation which governs CBF modulations and attempts to temper the effect of BP fluctuations.

Table 11 and Table 12 present the rMSE values calculated for quantitative evaluation of the estimations. The rMSE values for modeling errors are all less than 5 cm/s. However, the rMSE of the validation errors are less than 15 cm/s. These seem to be better results compared with BP modeling results, but taking the baseline of the CBF and BP into consideration, it shows that the percentage of the error is lower in BP compared to those of CBF. This was expected due to the effect of CA as discussed above.

5.3 Comparison of Sleep Study and Breath Hold Study Results

First thing to mention is the subject population of both studies as the BH subjects were much younger with their age being 28.9 ± 5.0 years while sleep study subject's age were 53.8 ± 7.4 years. Also, quality of the signals were much better in BH study as it was more controlled and shorter. Subjects did not move much as the duration of the whole experiment was shorter and also study was thoroughly observed, while in sleep study, sometimes the probe were removed during the study and reattached a few minutes later when the observer noticed it.

Another important point which makes the comparison harder is the duration of the apneas which that are not fixed compare to BH study. It can affect both percentage rise in BP or CBF and also results of validations to be poor, because the two intervals being evaluate do not have the same length. The average duration of the BH across all the subjects were was 53.9 seconds, while the apnea episodes average across all the subjects was only 22.6 seconds. Standard deviation of the duration of the apnea intervals was 10.17 seconds compared to that of BH study which was 21.8 seconds. This reveals the difference in nature of both studies and make the comparison even harder.

In breath-hold study, the changes in BP and CBF during BH intervals are higher than NB due to the sympathetic nervous system response to breath hold. Further, the intensity of these variations induced by breath hold varies among subjects. The same effect can be seen in apnea episodes in sleep study, where the sympathetic nervous system response to hypercapnia and hypoxia causes the rise in BP and, in most instances, in CBF.

As discussed in 5.1 and 5.2, errors of BP modeling are in general lower than CBF modeling in BH study. The same applies to sleep study where the results of the BP modeling are closer to measured values than the CBF modeling. Comparing BP modeling results in BH with those from

sleep study, we can observe that BP modeling performed better in BH study. The same holds true for CBF modeling where the results of sleep study are poorer. These are due the facts that are discussed in 5.2.2. Moreover, it should be considered that the BH subject were awake during the study versus being sleep in apnea study. Other factors like sleep stage and CA malfunctioning due to the apnea can affect the response of the subject to systemic perturbation.

5.4   Pitfalls and limitations

One of the limitations of these studies is that the age and health situation of subjects in breath-hold study and sleep study are different. Subjects participated in breath-hold study are chosen to be healthy and relatively young (28.9 ± 5.0 years) so with no known medical condition. On the other side, the subjects of sleep study are pre-diagnosed to have sleep disordered breathing and are much older (53.8 ± 7.4 years). This difference may affect how the systemic or cerebral hemodynamic responds to the apnea or BH intervals due to the change in vasculature stiffness, cerebral autoregulation, and other age-related effects.

By choosing 6 longest apnea episodes from each subject for analysis in sleep study, it was attempted to unify the modeling, but this could only be done to a limited extent, as duration of apneas are naturally variable both within subjects and across subjects (22.6±10.6 seconds) . The duration of the apnea affects the impact of initial condition on the response, but the selection of the apneas for analysis did not take that into account. It can be further improved by taking more episodes into modeling and defining other criteria to avoid deviations in interval lengths.

Moreover, it seems that the time of occurrence of an apnea seems to affect the modeling, but this was not considered. Factors like sleep stage can be considered in addition to time of occurrence as well. Sleep stage, particularly REM versus non-REM may affect both the sympathetic nervous response affecting BP and CA, which were not studied here. Last but not least is that the range of

77

AHI may affect the efficacy of the model. The present subject group has a broad range with their mean and standard deviation to be 61.1±27.6, compared to BH study with 31.1±4.9.

5.5   Conclusions

These studies conducted reveal that we can now model both BP and CBF in healthy subjects in BH study with acceptable accuracy. Results of BH study suggest that with further development it may be possible to get reasonable estimates of key features of beat-to-beat blood pressure or cerebral blood flow from PPG, creating opportunities for improvement in monitoring cerebrovascular and cardiovascular system health in healthy subjects. This can lead to applications including health monitoring and activity tracking devices.

The modeling in SDB patients is not as good as BH modeling and needs further modifications to be capable of predicting the BP and CBF in SDB subjects or in general subjects with impaired CA.

Moreover, aside from aims of these studies, we achieved all the innovations discussed in 1.2.3 and discussed them in discussion chapter of this work.

5.6   Future works

While the aim of this study was to present a method of estimating BP/CBF from PPG, future development of the methods presented here provides an opportunity for implementation in wearable health monitoring devices. Such implementation could bring about a positive impact for near-continuous monitoring of BP/CBF in a large sector of the population ranging from athletes to hypertensive patients. If such applications are considered, then steps need to be taken to eliminate or minimize the effect of any motion artifact [136] [137] [138].

Among many possible applications, such as the examples mentioned here, the methodology for a person-specific model calculation and validation needs to be developed. The likely need for

person-specific models stems from the fact that there is a wide variation in the physiological systems involved in the control of blood pressure, which includes responsiveness of the sympathetic nervous system, mechanical, fluid mechanics, dynamical properties of the cardiovascular system, and metabolic rate.

In this study, we explored only the linear single-input single-output ARMA models since they provide distinct advantages in analyzing the dynamic characteristic of the modeled system (e.g., stability, frequency response assessment, etc.) and existence of a well-stablished body of knowledge about linear systems. Further development can involve expansion of this method to include the use of nonlinear modeling, as it may increase the accuracy of the results. Also MIMO (Multi-Input-Multi-Output) ARMA model can take into account multiple features of the PPG and may result in higher accuracy, as it can have temporal information in addition to blood volume change reflected in peaks and troughs of PPG signal. Suggested features can be peak to peak interval, amplitude of PPG (trough to peak) as well as the area under PPG signal for each period.

In case there are more subjects available either from sleep lab or from any other source of data, providing enough data to train machine learning methods specifically deep learning techniques, it might be helpful to try these techniques as well. These techniques are useful in terms of being self-learning and they can reveal more sophisticated relationship between PPG and BP/CBF without the need for any preliminary assumptions.

Moreover, the effect of shorter time between breath-holds as well as the posture effect on the modeling of the BH can be studied later. It can be further compared with the modeling of comparable AHI levels in apnea subjects. As less normal breathing time can help simulate the repetitive apnea-hypopnea event which occurs in patients with severe SDB, one can investigate

the effect of intense BH and the residuals from the previous BH in future. Such study may provide more insight about whether the modeling is better for BH's that mimic higher AHI or lower AHI.

Also effect of different postures can help us figure out if the elevation of the head with respect to the heart can affect the CBF autoregulation and/or propagation of pulse wave during apnea. This can be another tentative hypothesis to be investigated in future.

Appendices

6.1 Appendix A
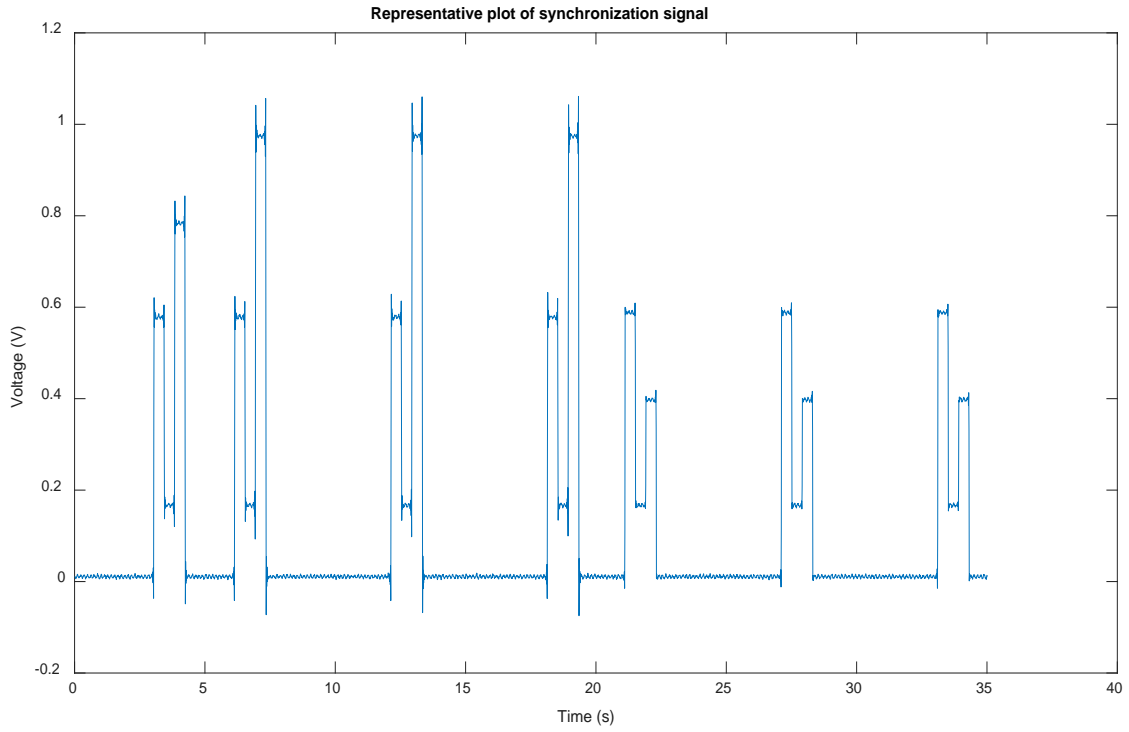
Figure 47- Representative plot of synchronization signal

6.2 Appendix B

Figure 48- Apnea episode duration over the entire sleep study for subject no. 2

Figure 49- Apnea episode duration over the entire sleep study for subject no. 3

Figure 50- Apnea episode duration over the entire sleep study for subject no. 4

Figure 51- Apnea episode duration over the entire sleep study for subject no. 5

83
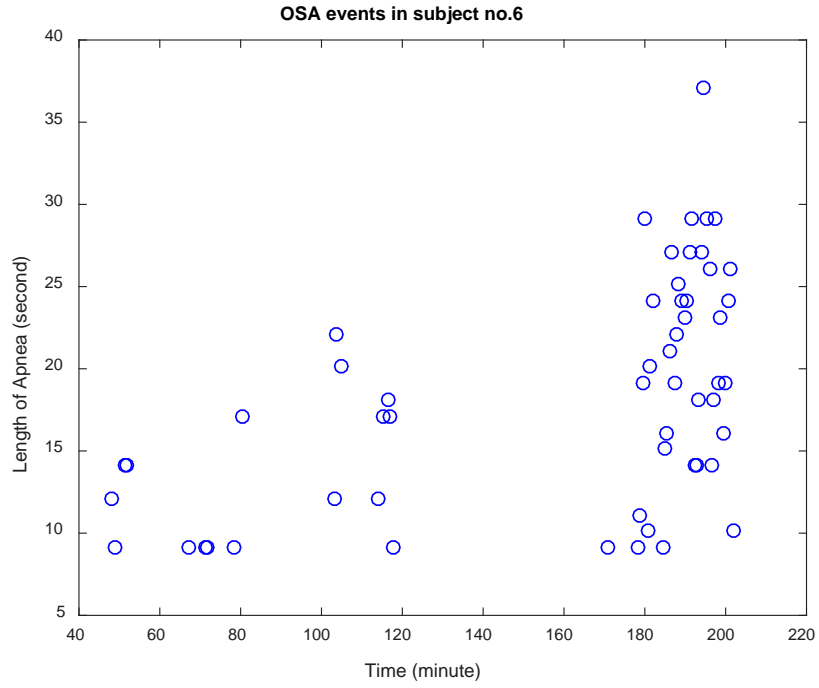
Figure 52- Apnea episode duration over the entire sleep study for subject no. 6
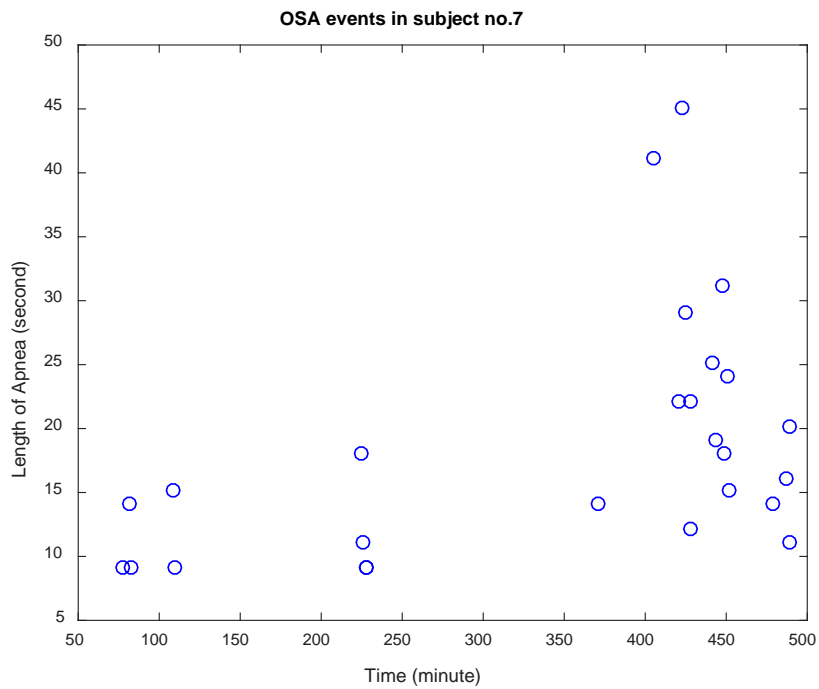
Figure 53- Apnea episode duration over the entire sleep study for subject no. 7
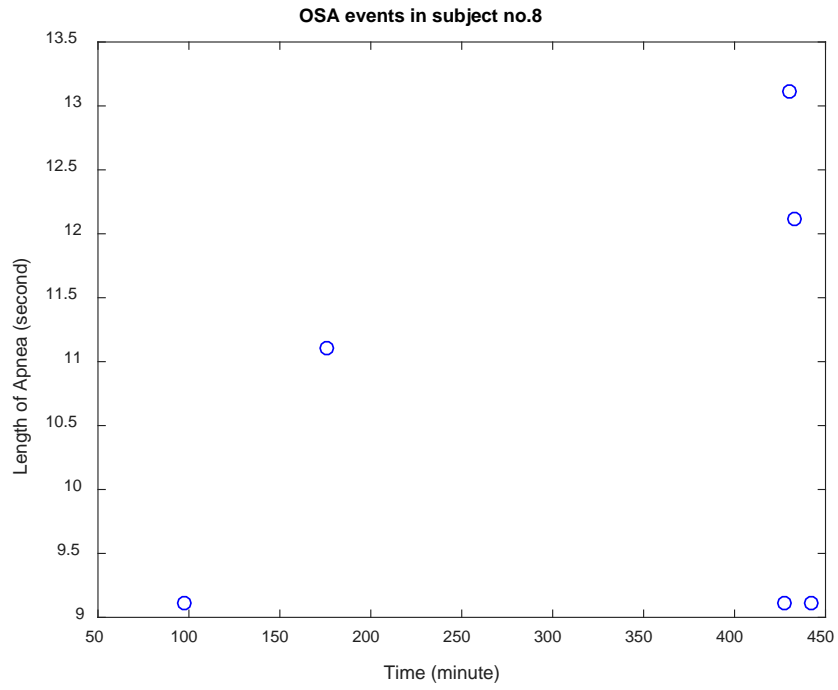
Figure 54- Apnea episode duration over the entire sleep study for subject no. 8
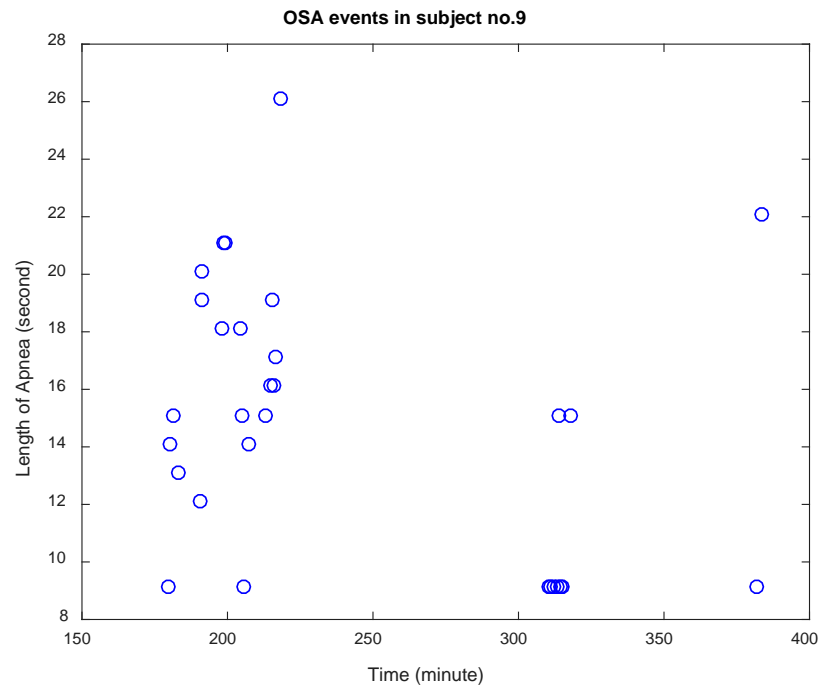
Figure 55- Apnea episode duration over the entire sleep study for subject no. 9
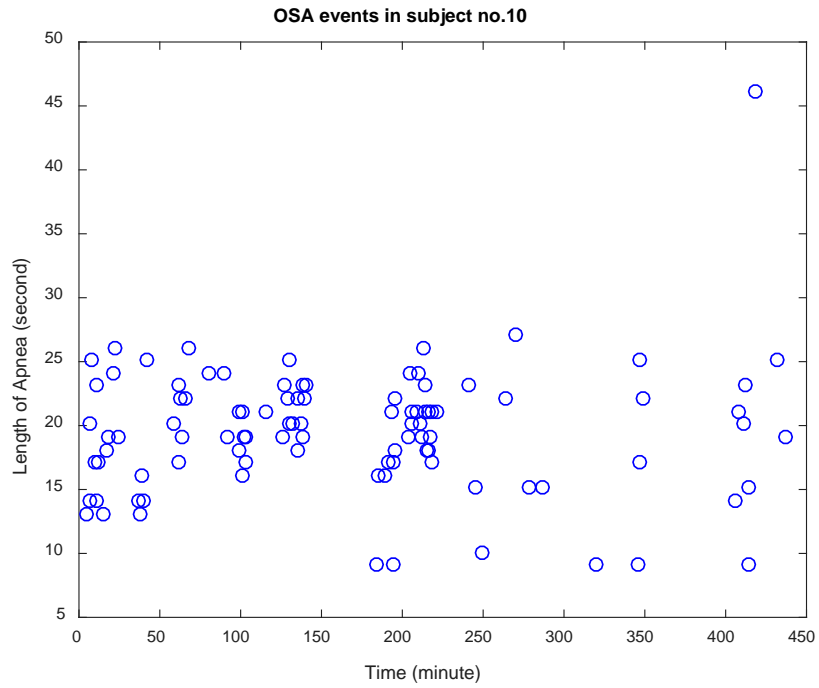
Figure 56- Apnea episode duration over the entire sleep study for subject no. 10
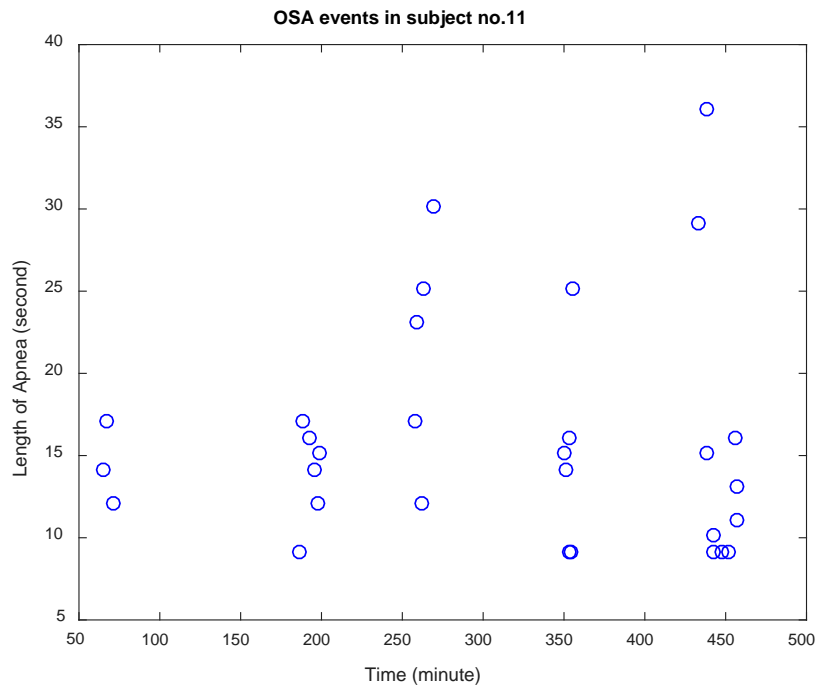
Figure 57- Apnea episode duration over the entire sleep study for subject no. 11
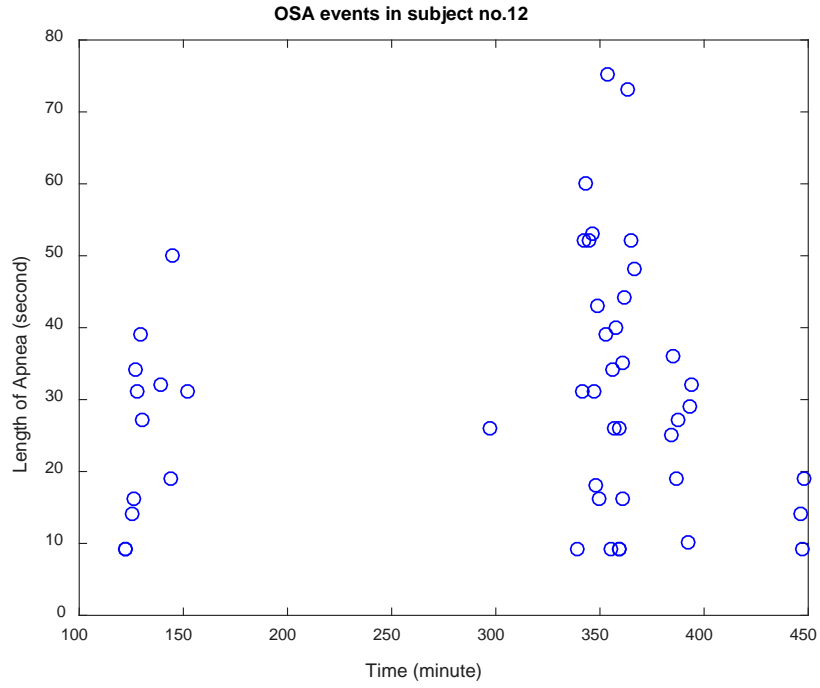
Figure 58- Apnea episode duration over the entire sleep study for subject no. 12
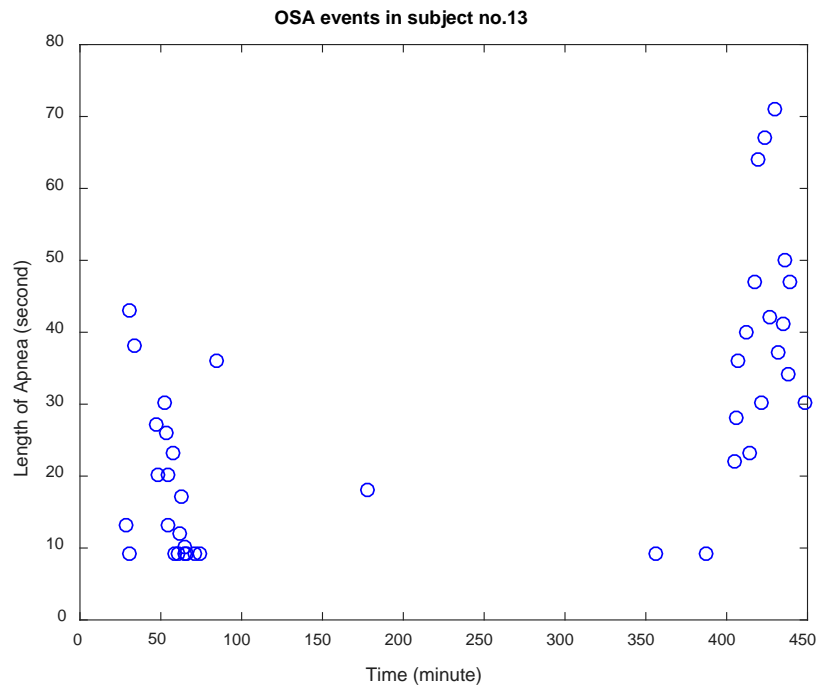
Figure 59- Apnea episode duration over the entire sleep study for subject no. 13
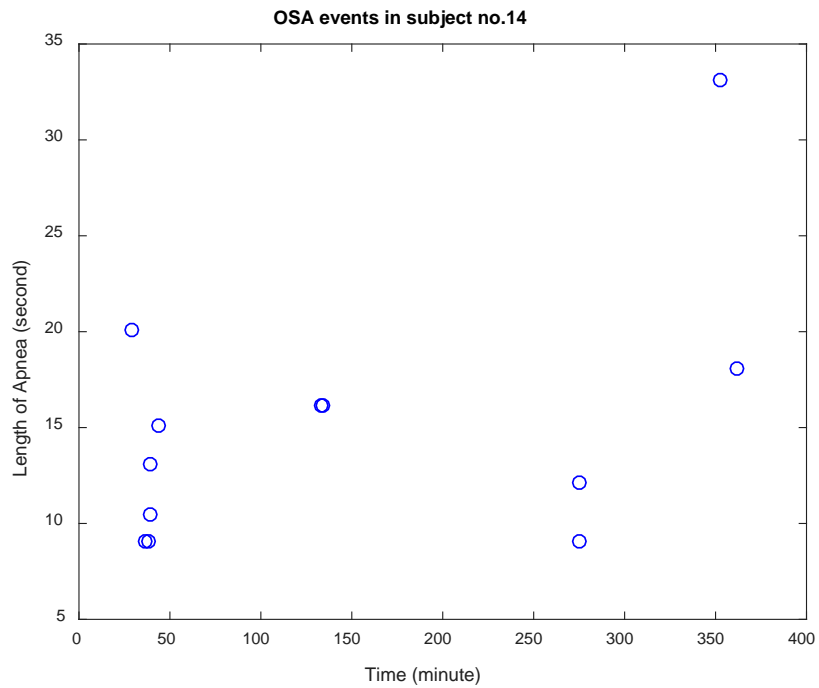
Figure 60- Apnea episode duration over the entire sleep study for subject no. 14
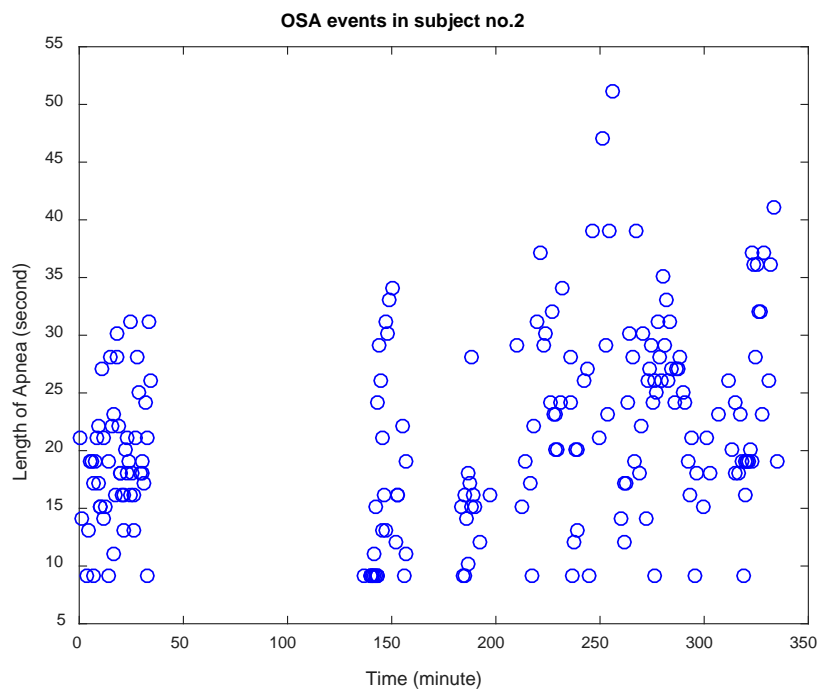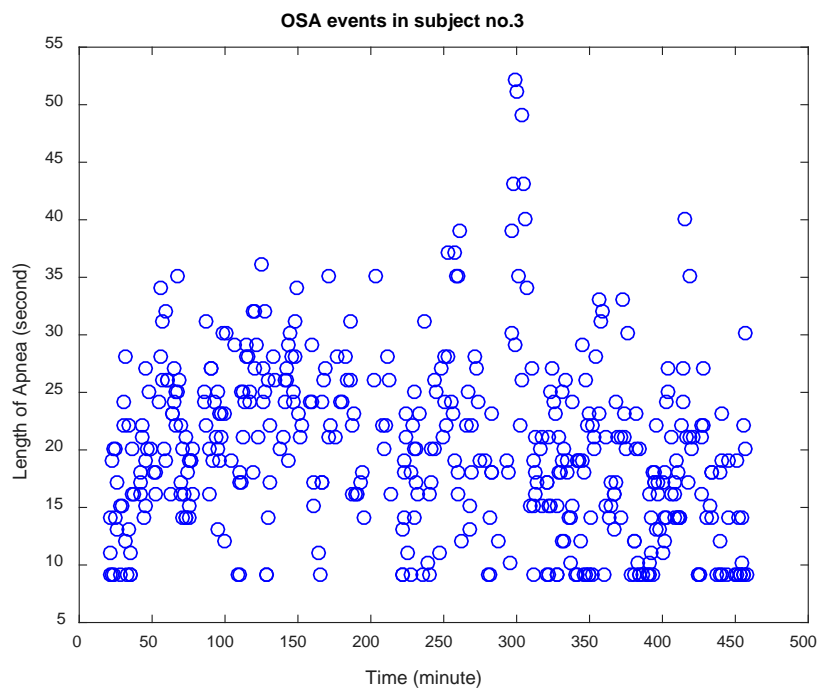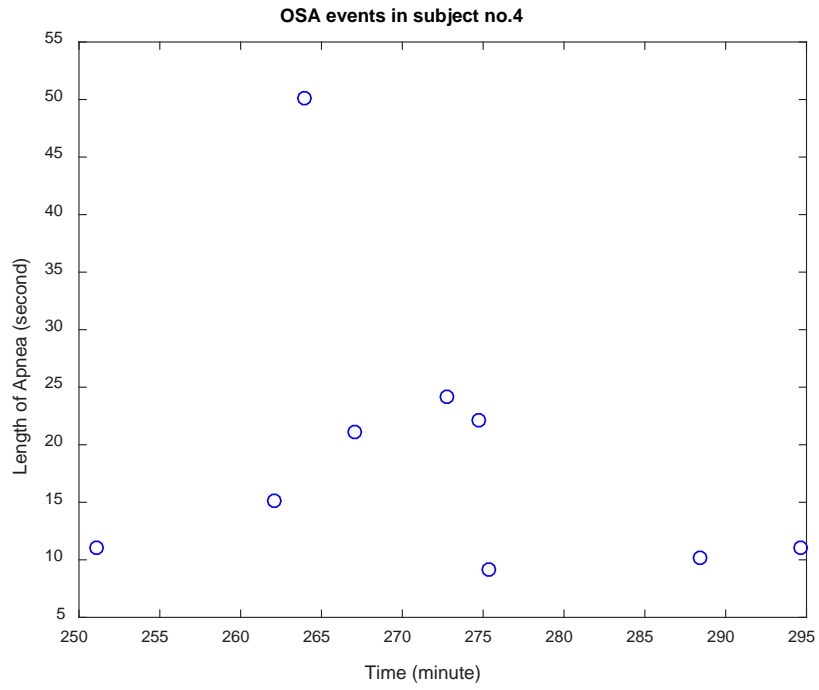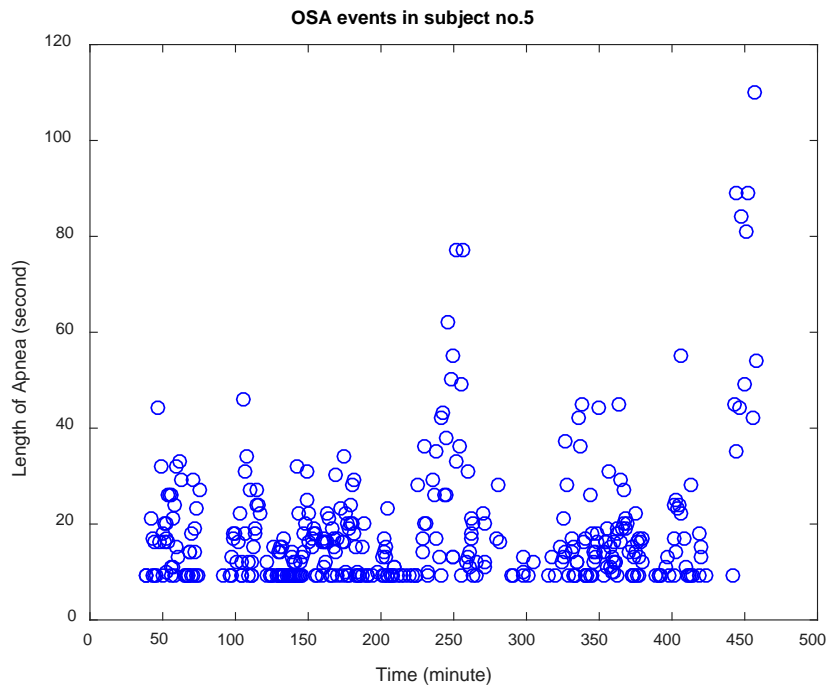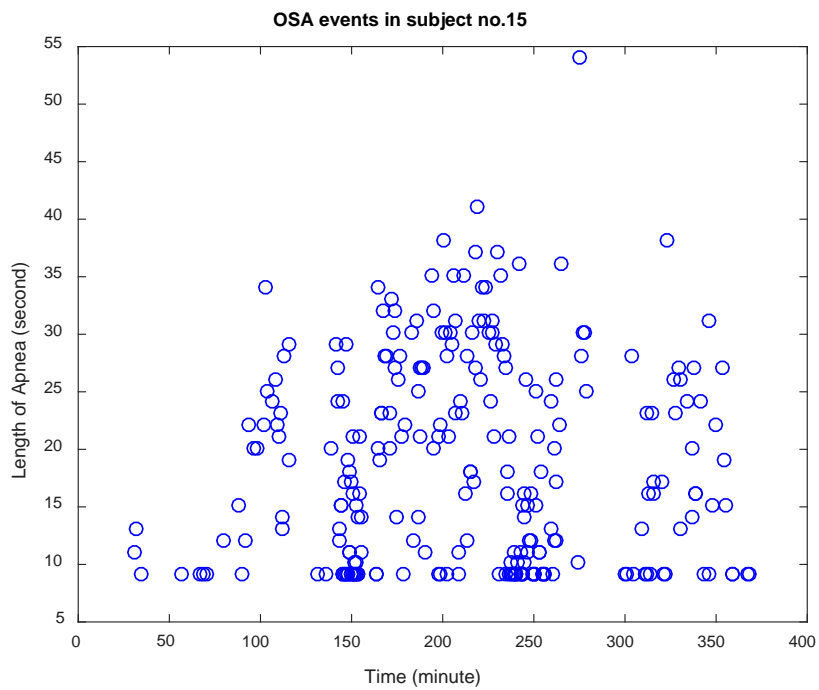

Figure 61- Apnea episode duration over the entire sleep study for subject no. 15

88

References

[1] T. Young, P. E. Peppard, and D. J. Gottlieb, "Epidemiology of obstructive sleep apnea: a population health perspective," *Am J Respir Crit Care Med,* vol. 165, pp. 1217-39, 2002.

[2] R. Wolk, T. Kara, V.K. Somers, "Sleep-Disordered Breathing and Cardiovascular Disease," *Ciculation,* vol. 108, pp. 9-12, 2003.

[3] American Academy of Sleep Medicine Task Force, "Sleep-Related Breathing Disorders in Adults: Recommendations for Syndrome Definition and Measurement Techniques in Clinical Research," *sleep,* vol. 22, no. 5, pp. 667-689, 1999.

[4] T.D. Bradly and J.S. Floras, Sleep Apnea: Implications in Cardiovascular and Cerebrovascular Disease, vol. 146, New york: Marcel Dekker Inc., 2000.

[5] S. G. Pearse, M. R. Cowie, "Sleep-disordered breathing in heart failure," *European J. of Heart Failure,* vol. 18, no. 4, pp. 353-361, 2016.

[6] M. R.Cowie, "Sleep apnea:State of the art," *TRends in Cardiovascular Medicine,* vol. 27, pp. 280-289, 2017.

[7] T. Young, L. Evans, L. Finn and M. Palta, "Estimation of the clinically diagnosed proportion of sleep apnea syndrome in middle-aged men and women," *Sleep,* vol. 20, pp. 705-706, 1997.

[8] N. M.Al Lawati, S. R.Patel, N. T. Ayas, "Epidemiology, Risk Factors, and Consequences of Obstructive Sleep Apnea and Short Sleep Duration," *Progress in Cardiovascular Diseases,* vol. 51, no. 4, pp. 285-293, 2009.

[9] V. K. Somers, D. P. White, R. Amin, W. T. Abraham, F. Costa, A. Culebras, et, "Sleep apnea and cardiovascular disease: an American Heart Association/american College Of Cardiology Foundation Scientific Statement from the American Heart Association Council for High Blood Pressure Research Professional Education Committee, Council on," *Circulation,* vol. 118, no. 10, pp. 1080-1111, 2008.

[10] Romero-Corral A, Caples SM, Lopez-Jimenez F, Somers VK, "Interactions between obesity and obstructive sleep apnea: implications for treatment," *Chest,* vol. 137, no. 3, pp. 711-9, 2010.

[11] T. Young, M. Palta, J. Dempsey, J. Skatrud, S. Weber, S. Badr, "The occurrence of sleep-disordered breathing among middle-aged adults.," *N Engl J Med.,* vol. 328, no. 17, pp. 1230-5, 1993.

[12] E. O. Bixler, A. N. Vgontzas, H. M. Lin, T. Ten Have, J. Rein, A. Vela-Bueno A, A. Kales, "Prevalence of sleep-disordered breathing in women: effects of gender," *Am J Respir Crit Care Med.,* vol. 163, pp. 608-613, 2001.

[13] H. Bearpark, L. Elliott, R. Grunstein, S. Cullen, H. Schneider, W. Althaus, C. Sullivan, "Snoring and sleep apnea. A population study in Australian men," *Am J Respir Crit Care Med.,* vol. 151, no. 5, pp. 1459-65, 1995.

[14] J. Durán, S. Esnaola, R. Rubio, A. Iztueta, "Obstructive sleep apnea-hypopnea and related clinical features in a population-based sample of subjects aged 30 to 70 yr," *Am J Respir Crit Care Med.,* vol. 163, pp. 685-689, 2001.

[15] J. Kim, K. In, J. Kim, S. You, K. Kang, J. Shim, S. Lee, J. Lee J,S. Lee, C. Park, C. Shin, "Prevalence of sleep-disordered breathing in middle-aged Korean men and women," *Am J Respir Crit Care Med.,* vol. 170, no. 10, pp. 1108-13, 2004.

[16] Z. F. Udwadia, A. V. Doshi, S. G. Lonkar, C. I. Singh, "Prevalence of sleep-disordered breathing and sleep apnea in middle-aged urban Indian men," *Am J Respir Crit Care Med.,* vol. 169, no. 2, pp. 168-173, 2004.

[17] S. Batool-Anwar, J. L. Goodwin, C. A. Kushida, J.A. Walsh, R. D. Simon, D. A. Nichols, S. F. Quan, "Impact of continuous positive airway pressure (CPAP) on quality of life in patients with obstructive sleep apnea (OSA)," *J Sleep Res.,* vol. 25, no. 6, pp. 731-738, 2016.

[18] J. H. Ng, M. Yow, "Oral Appliances in the Management of Obstructive Sleep Apnea," *Sleep Med Clin,* vol. 14, no. 1, pp. 109-118, 2019.

[19] C. C. Dicus Brookes, S. B. Boyd, "Controversies in Obstructive Sleep Apnea Surgery," *Oral Maxillofac Surg Clin North Am.,* vol. 29, no. 4, pp. 503-513, 2017.

[20] P. L. Smith, J. P. Kirkness, S. Patil, H. Schneider, & A. R. Schwartz, "Biomechanics of the upper airway during sleep," in *Sleep apnea: Pathogenesis, diagnosis, and treatment*, New York, CRC Press, 2011.

[21] J. P. Kirkness, M. Sowho and E. Murano, "The Interplay between Tongue Tissue Volume, Hyoid Position, and Airway Patency," *Sleep,* vol. 37, no. 10, pp. 1585-86, 2014.

[22] W. S. Mezzanotte, D. J. Tangel, D. P. White, "Waking genioglossal electromyogram in sleep apnea patients versus normal controls (a neuromuscular compensatory mechanism)," *J Clin Invest.,* vol. 89, no. 5, pp. 1571-79, 1992.

[23] L. V. Pham and A. R. Schwartz, "The pathogenesis of obstructive sleep apnea," *J Thorac Dis.,* vol. 7, no. 8, pp. 1358-72, 2015.

[24] David J. Durgan, Robert M. Bryan, "Cerebrovascular Consequences of Obstructive Sleep Apnea," *Journal of the American Heart Association,* vol. 1, no. 4, p. e000091, 2012.

[25] Somers VK, Mark AL, Abboud FM, "Sympathetic activation by hypoxia and hypercapnia--implications for sleep apnea," *Clin Exp Hypertens A.,* vol. 1, pp. 413-22, 1988.

[26] J. S.Floras, "Sleep apnea and cardiovascular risk," *Journal of Cardiology,* vol. 63, no. 1, pp. 3-8, 2014.

[27] Bradley TD, Floras JS, "Sleep apnea and heart failure: Part I: obstructive sleep apnea," *Circulation,* vol. 107, no. 12, pp. 1671-8, 2003.

[28] Torelli F, Moscufo N, Garreffa G, Placidi F, Romigi A, Zannino S, Bozzali M, Fasano F, Giulietti G, Djonlagic I, Malhotra A, Marciani MG, Guttmann CR., "Cognitive profile and brain morphological changes in obstructive sleep apnea," *Neuroimage.,* vol. 54, no. 2, pp. 787-93, 2011.

[29] Urbano F, Roux F, Schindler J, Mohsenin V., "Impaired cerebral autoregulation in obstructive sleep apnea," *Journal of Applied Physiology,* vol. 105, no. 6, pp. 1852-1857, 2008.

[30] T. Kasai, J.S. Floras, T.D. Bradley, "Sleep apnea and cardiovascular disease: a bidirectional relationship," *Circulation,* vol. 126, pp. 1495-1510, 2012.

[31] V. K. Somers, A. L. Mark, and F. M. Abboud, "Sympathetic activation by hypoxia," *Clin Exp Hypertens A,* vol. 10, no. 1, pp. 413-422, 1988.

[32] F. Urbano, F. Roux, J. Schindler, and V. Mohsenin, "Impaired cerebral autoregulation in obstructive sleep apnea," *J Appl Physiol,* vol. 105, pp. 1852-1857, 2008.

[33] K. J. Reichmuth, J. M. Dopp, S. R. Barczi, J. B. Skatrud, P. Wojdyla, D. Hayes Jr, B. J. Morgan, "Impaired vascular regulation in patients with obstructive sleep apnea: effects of continuous positive airway pressure treatment," *Am J Respir Crit Care Med.,* vol. 180, no. 11, pp. 1143-1150, 2009.

[34] R. M. Alex, "An investigation of the effect of obstructive sleep apnea," UTA library, Arlington, 2015.

[35] N. Canessa, V. Castronovo, S. F. Cappa, M. S. Aloia, S. Marelli, A. Falini, et al., "Obstructive sleep apnea: brain structural changes and neurocognitive function before and after treatment," *Am J Respir Crit Care Med,* vol. 183, no. 10, pp. 1419-26, May 2011.

[36] A. Daurat, J. Foret, J. Bret-Dibat, C. Fureix, M. & Tiberge, "Spatial and temporal memories are affected by sleep fragmentation in obstructive sleep apnea syndrome," *Journal of Clinical and Experimental Neuropsychology,* vol. 30, no. 1, pp. 91-101, 2008.

[37] P. M. Macey, M. K. Sarma, J. P. Prasad, J. A. Ogren, R. Aysola,R. M. Harper, and M. A. Thomas, "Obstructive sleep apnea is associated with altered midbrain chemical concentrations," *Neuroscienc,* vol. 363, pp. 76-86, 2017.

[38] E. Y. Joo, W. S. Tae, M. L. Lee, J. W. Kang, H. S. Park, J. Y. Lee, M. Suh, S. B. Hong, "Reduced brain gray matter concentration in patients with obstructive sleep apnea syndrome," *Sleep,* vol. 33, no. 2, pp. 235-41, 2010.

[39] C. Lal, C. Strange, D. Bachman, "Neurocognitive impairment in obstructive sleep apnea," *Chest,* vol. 141, no. 6, pp. 1601-1610, 2012.

[40] Parati G, Ochoa JE, Lombardi C, Salvi P, Bilo G, "Assessment and interpretation of blood pressure variability in a clinical setting," *Blood press,* vol. 22, no. 6, pp. 345-354, 2013.

[41] Campbell NR, Chockalingam A, Fodor JG, McKay DW, "Accurate, reproducible measurement of blood pressure," *CMAJ(Canadian Medical Association Journal),* vol. 143, no. 1, pp. 19-24, 1990.

[42] J Penaz, A. Voigt, W. Teichmann, "Beitrag zur fortlaufenden indirekten Blutdruckmessung," *Z Inner Med,* vol. 31, no. 24, pp. 1030-1033, 1976.

[43] K.H. Wesseling, B. de Wit, G.M.A. van der Hoeven, J. van Goudoever, J.J. Settels, "Physiocal, calibrating finger vascular physiology for finapres," *Homeostasis in health and disease,* vol. 36, pp. 67-82, 1995.

[44] Kurki T, Smith NT, Head N, Dec-Silver H, Quinn A, "Noninvasive continuous blood pressure measurement from the finger: optimal measurement conditions and factors affecting reliability," *J Clin Monit,* vol. 3, no. 1, pp. 6-13, 1987.

[45] M. Nakagawara, K. Yamakoshi, "A portable instrument for non-invasive monitoring of beat-by-beat cardiovascular haemodynamic parameters based on the volume-compensation and electrical-admittance method," *Medical and Biological Engineering and Computing,* vol. 38, no. 1, pp. 17-25, 2000.

[46] J. Fortin, W. Marte, R. Grüllenberger, A. Hacker, W. Habenbacher, A. Heller,CH. Wagner, P. Wach, F. Skrabal, "Continuous non-invasive blood pressure monitoring using concentrically interlocking control loops," *Computers in Biology and Medicine,* vol. 36, pp. 941-957, 2006.

[47] K. Matsumura, T. Yamakoshi, P. Rolfe, and K. I. Yamakoshi, "Advanced Volume-Compensation Method for Indirect Finger Arterial Pressure Determination: Comparison with Brachial Sphygmomanometry," *IEEE Trans Biomed Eng,* vol. 64, no. 5, pp. 1131-1137, 2017.

[48] G. Drzewiecki, "Deformational forces in arterial tonometry," *IEEE press,* vol. 28, pp. 642-645, 1984.

[49] O'Rourke MF, Seward JB., "Central arterial pressure and arterial pressure pulse: new views entering the second century after Korotkov," *Mayo Clin Proc.,* vol. 81, no. 8, pp. 1057-1068, 2006.

[50] H. M. Cheng, D. Lang, C. Tufanaru , A. Pearson, "Measurement accuracy of non-invasively obtained central blood pressure by applanation tonometry: a systematic review and meta-analysis," *Int J Cardiol. ,* vol. 167, no. 5, pp. 1867-76, 2013.

[51] S. Sarkar, S Ghosh, S. K. Ghosh, A. Collier, "Role of transcranial doppler ultrasonography in stroke," *Postgraduate Medical Journal,* vol. 83, pp. 683-689, 2007.

[52] M. Furtner , M. Staudacher , B. Frauscher, E. Brandauer, M. M. E. Rojas, V. Gschliesser, W. Poewe, C. Schmidauer, M. Ritsch-Marte, B. Högl, "Cerebral vasoreactivity decreases overnight in severe obstructive sleep apnea syndrome: A study of cerebral hemodynamics," *Sleep Medicine,* vol. 10, pp. 875-881, 2009.

[53] A. Nachtmann, A. Stang, Y.M. Wang, E. Wondzinski, A. F. Thilmann, "Association of obstructive sleep apnea and stenotic artery disease in ischemic stroke patients.," *Atherosclerosis,* vol. 169, no. 2, pp. 301-307, 2003.

[54] R. G. Berg, R. R. Plovsing, D. M. Bailey, N. Holstein-Rathlou and K. Møller, "Dynamic cerebral autoregulation to induced blood pressure changes in human experimental and clinical sepsis," *Clin Physiol Funct Imaging,* vol. 36, pp. 490-496, 2016.

[55] R. Zhang, Kh. Behbehani and B. D. Levine, "Dynamic pressure–flow relationship of the cerebral circulation during acute increase in arterial pressure," *J Physiol,* vol. 587, no. 11, pp. 2567-2577, 2009.

[56] V. Novak, A. C. Yang, L. Lepicovsky, A. L. Goldberger, L. A. Lipsitz and C. K. Peng, "Multimodal pressure-flow method to assess dynamics of cerebral autoregulation in stroke and hypertension," *BioMedical Engineering OnLine,* vol. 3, no. 39, 2004.

[57] E.C. Chua, S.J. Redmond, G. McDarby and C. Heneghan, "Towards using photoplethysmogram amplitude to measure blood pressure during sleep," *Annals of Biomedical Engineering,* vol. 38, no. 3, pp. 945-954, 2010.

[58] A. Soltan Zadi, R. Alex, R. Zhang, D. E. Watenpaugh, K. Behbehani, "Arterial Blood Pressure Feature Estimation Using Photoplethysmography," *Computers in Biology and Medicine,* vol. 102, pp. 104-111, 2018.

[59] Gesche H, Grosskurth D, Kuchler G, Patzak A, "Continuous blood pressure measurement by using the pulse transit time: comparison to a cuff-based method," *European Journal of Applied Physiology,* vol. 112, no. 1, pp. 309-315, 2012.

[60] R. Smith, J. Argod, J. Pepin, and P. Levy, "Pulse transit time: an appraisal of potential clinical applications," *Thorax,* vol. 54, no. 5, pp. 452-457, 1999.

[61] X. Xing and M. Sun, "Optical blood pressure estimation with photoplethysmography and FFT-based neural networks," *BIOMEDICAL OPTICS EXPRESS,* vol. 7, no. 8, pp. 3007-3020, 2016.

[62] X. F. Teng and Y. T. Zhang, "Continuous and Noninvasive Estimation of Arterial Blood Pressure Using a Photoplethysmographic Approach," in *Praceedings of the 25* Annual lnlematianal Conference of the IEEE EMBS*, Cancun, Mexico, 2003.

[63] D. B. McCombie, A. T. Reisner, H. H. Asada, "Adaptive blood pressure estimation from wearable PPG sensors using peripheral artery pulse wave velocity measurements and multi-channel blind identification of local arterial dynamics," in *Proceedings of the 28th IEEE EMBS Annual International Conference*, New York City, USA, Aug 30-Sept 3, 2006.

[64] E. M, "On the analysis of fingertip photoplethysmogram signals," *Current Cardiology Reveiews,* vol. 8, no. 1, pp. 14-25, 2012.

[65] A. J, "Photoplethysmography and its application in clinical physiological measurement," *Physiological Measurement,* vol. 28, no. 3, pp. R1-39, 2007.

[66] Hiromitsu Sekizuka, Keisuke Kida, Yoshihiro J.Akashi, Kihei Yoneyama, Naohiko Osada, Kazuto Omiya, Fumihiko Miyak, "Relationship between sleep apnea syndrome and sleep blood pressure in patients without hypertension," *Journal of Cardiology,* vol. 55, no. 1, pp. 92-98, 2010.

[67] V.L. Burt, P. Whelton, E.J. Roccella, C. Brown, J.A. Cutler, M. Higgins, M.J. Horan, D. Labarthe, "Prevalence of hypertension in the US adult population, results from the," *Hypertension,* vol. 25, no. 3, pp. 305-313, 1995.

[68] E. Dolan, A. Stanton, L. Thijs, K. Hinedi, N. Atkins, S. McClory, E. Den Hond, P. McCormack, J. A. Staessen, E. O'Brien, "Superiority of Ambulatory Over Clinic Blood Pressure Measurement in Predicting Mortality," *Hypertension,* vol. 46, no. 1, pp. 156-161, 2005.

[69] A. L. Fortmann and L. C. Gallo , "Social Support and Nocturnal Blood Pressure Dipping: A Systematic Review," *Am J Hypertens.,* vol. 26, no. 3, pp. 302-310, 2013.

[70] G. Torres, M. Sanchez-de-la-Torre, F. Barbe, "Relationship Between OSA and Hypertension," *Chest,* vol. 148, no. 3, pp. 824-832, 2015.

[71] F. J. Nieto, T. B. Young, B. K. Lind, "Association of Sleep-Disordered Breathing, Sleep Apnea, and Hypertension in a Large Community-Based Study," *JAMA.,* vol. 283, no. 14, pp. 1829-1836, 200.

[72] L. Bathala, M. M. Mehndiratta and V. K. Sharma, "Transcranial doppler: Technique and common findings (Part 1)," *Ann Indian Acad Neurol.,* vol. 16, no. 2, pp. 174-179, 2013.

[73] J. Naqvi,K. Hooi Yap,G. Ahmad and J. Ghosh, "Transcranial Doppler Ultrasound: A Review of the Physical Principles and Major Applications in Critical Care," *International Journal of Vascular Medicine,* 2013.

[74] A. E. Roher, Z. Garami, S. L. Tyas, C. L. Maarouf, T. A. Kokjohn, M. Belohlavek, L. J. Vedders, Donald Connor, Marwan N. Sabbagh, T. G. Beach, M. R. Emmerling, "Transcranial Doppler ultrasound blood flow

velocity and pulsatility index as systemic indicators for Alzheimer's disease," *Alzheimers Dement.,* vol. 7, no. 4, pp. 445-455, 2011.

[75] F. Urbano, F. Roux, J. Schindler, and V. Mohsenin, "Impaired cerebral autoregulation in obstructive sleep apnea," *J Appl Physiol,* vol. 105, pp. 1852-7, Dec 2008.

[76] Mario Siebler, Andreas Nachtmann, "Cerebral Hemodynamics in Obstructive Sleep Apnea," *Chest,* vol. 103, no. 4, pp. 1118-1119, 1993.

[77] A. B. Hertzman, "The blood supply of various skin areas as estimated by the photoelectric plethysmograph," *Am. J. Physiol.,* vol. 124, pp. 328-340, 1938.

[78] P. D. Mannheimer, N. A. Asbaugh, and N. T. Staff, "Nellcor™ OxiMax Pulse," Covidien, Boulder, CO, 2011.

[79] T. S. Ahrens, K. Ott, "Comparison of three new generation pulse oximeters in a medical intensive care unit.," *Critical Care Medicine,* vol. 34, no. 12, 2006.

[80] Aymen A. Alian, Kirk H. Shelley, "Photoplethysmography," *Best Practice & Research Clinical Anaesthesiology,* vol. 28, pp. 395-406, 2014.

[81] J. L. Moraes, M. X. Rocha, G. G. Vasconcelos, J. E. Vasconcelos Filho ,V. C. de Albuquerqueand A. R. Alexandria, "Advances in Photopletysmography Signal Analysis for Biomedical Applications," *Sensors,* vol. 18, no. 6, p. 1894, 2018.

[82] J. Spigulis, "Optical noninvasive monitoring of skin blood pulsations," *Applied Optics,* vol. 44, no. 10, pp. 1850-1857, 2005.

[83] H Hsiu, C-L Hsu, and T-L Wu, "Effects of different contacting pressure on the transfer function between finger photoplethysmographic and radial blood pressure waveforms," *J. Engineering in Medicine,* vol. 225, 2010.

[84] M. E. Safar, "Peripheral Pulse Pressure, Large Arteries, and Microvessels," 2004.

[85] K.P. Clark, R. G. Mark, "Extracting new information from the shape of the blood pressure pulse," in *IEEE Xplore*, Los Alamitos, CA, 1990.

[86] J K-J Li, Tangbing Cui, Gary M. Drzewiecki, "A nonlinear model of the arterial system incorporating a pressure-dependent compliance," *IEEE transactions on bio-medical engineering,* vol. 37, no. 7, pp. 673-678, 1990.

[87] Pochet T, Gerard P, Lambermont B, Detry O, D'Orio V, Defraigne J-O, Fossion A and Limet R, "Selection and," in *Proc. 10th Nordic–Baltic Conf. on Biomedical Engineering*, Tampere, 1996.

[88] K.P. Clark, R.G. Mark, "Extracting new information from the shape of the blood pressure pulse," in *Computers in Cardiology 1990, Proceedings.*, 1990.

[89] Singaram, M., Webb, J.A.C. , Finlay, C. , Mitchell, R.H. , "The application of PSPICE in the assessment of blood pressure pulse contour models based on windkessel networks," *Automedica,* vol. 16, pp. 127-138, 1994.

[90] John Allen and Alan Murray, "Modelling the relationship between peripheral blood pressure and blood volume pulses using linear and neural network system identification techniques," *Physiol. Meas.,* vol. 20, no. 3, pp. 287-301, 1999.

[91] Sandrine C. Millasseau, Franck G. Guigui, Ronan P. Kelly, Krishna Prasad, John R. Cockcroft, James M. Ritter, Philip J. Chowienczyk, "Noninvasive Assessment of the Digital Volume Pulse Comparison With the Peripheral Pressure Pulse," *Hypertension,* vol. 36, pp. 952-956, 2000.

[92] Eric C Chua, Stephen J. Redmond, Gary McDarby, and Conor Heneghan, "Toward using photo-plethysmogram amplitude to measure blood pressure during sleep," *Annals of Biomedical Engineering,* vol. 38, no. 3, pp. 945-954, 2010.

[93] J. A. van Waes, W. A. van Klei, D. N. Wijeysundera, L. van Wolfswinkel, T. F. Lindsay, W. S. Beattie, "Association between Intraoperative Hypotension and Myocardial Injury after Vascular Surgery," *Anesthesiology,* vol. 124, no. 1, pp. 35-44, 2016.

[94] J. C. Petrie, E. T. O'Brien, W. A. Littler, M. de Swiet, "Recommendations on blood pressure measurement," *Br Med J (Clin Res Ed),* vol. 293, pp. 611-15, 1986.

[95] J. Penáz, A. Voigt, W. Teichmann, "Contribution to the continuous indirect blood pressure measurement," *Z Gesamte Inn Med,* vol. 31, no. 243, pp. 1030-33, 1976.

[96] B. Scheer, A. Perel, U. J. Pfeiffer, "Clinical review: complications and risk factors of peripheral arterial catheters used for haemodynamic monitoring in anaesthesia and intensive care medicine," *Crit Care.,* vol. 6, no. 3, pp. 199-204, 2002.

[97] K. H. Wesseling, "Finapres, continuous noninvasive finger arterial pressure based on the method of Peñáz," in *Blood pressure measurement*, Steinkopff, 1990, pp. 161-172.

[98] J. Penaz, "Photoelectric measurement of blood pressure, volume and flow in the finger," in *Digest of the 10th International Conference on Medical and Biological Engineering*, Dresden, 1973.

[99] J. R. Martina, B. E. Westerhof, J. van Goudoever et al., "Noninvasive continuous arterial blood pressure monitoring with Nexfin," *Anesthesiology,* vol. 116, pp. 1092-1103, 2012.

[100] J. F. Stover, R. Stocker, R. Lenherr, T. A. Neff, S. R. Cottini, B. Zolle, M. Béchir, "Noninvasive cardiac output and blood pressure monitoring cannot replace an invasive monitoring system in critically ill patients," *BMC Anesthesiol.,* vol. 9, no. 6, 2009.

[101] W. J. Bos ,J. van Goudoever, G. A. van Montfrans, A. H. van den Meiracker, K. H. Wesseling, "Reconstruction of brachial artery pressure from noninvasive finger pressure measurements," *Circulation,* vol. 94, no. 8, pp. 1870-5, 1996.

[102] Imholz BP, Wieling W, van Montfrans GA, Wesseling KH, "Fifteen years experience with finger arterial pressure monitoring: assessment of the technology," *Cardiovasc Res.,* vol. 28, no. 3, pp. 605-616, 1998.

[103] A. M. Harper, "Autoregulation of cerebral blood flow: influence of the arterial blood pressure on the blood flow through the cerebral cortex," *J Neurol Neurosurg Psychiatry,* vol. 29, no. 5, pp. 398-403, 1966.

[104] N. A. Lassen and M. S. Christensen, "Physiology of Cerebral Blood Flow," *Br. J. Anaesth.,* vol. 48, pp. 719-734, 1976.

[105] S. J. Phillips, J. P. Whisnant, "Hypertension and the brain. The National High Blood Pressure Education Program," *Arch Intern Med.,* vol. 152, no. 5, pp. 938-945, 1992.

[106] R. M. Alex, "AN INVESTIGATION OF THE EFFECT OF OBSTRUCTIVE SLEEP APNEA ON CEREBRAL HEMODYNAMICS IN RELATION WITH SYSTEMIC HEMODYNAMICS," UTA, Arlington, 2015.

[107] S. Purkayastha and F. Sorond, "Transcranial Doppler Ultrasound: Technique and Application," *Semin Neurol. ,* vol. 32, no. 4, pp. 411-420, 2012.

[108] R Aaslid, K. F. Lindegaard, W. Sorteberg, and H. Nornes, "Cerebral Autoregulation Dynamics in Humans," *Stroke,* vol. 20, no. 1, pp. 45-53, 1989.

[109] S. S. Kety and C. F. Schmidt, "The Nitrous Oxide Method For The Quantitative Determination Of Cerebral Blood Flow In Man: Theory, Procedure And Normal Values," *J Clin Invest.,* vol. 27, no. 4, pp. 476-483, 1948.

[110] W. D. Obrist, H. K. Jr Thompson, H. S. Wang, W. E. Wilkinson, "Regional cerebral blood flow estimated by 133-xenon inhalation.," *Stroke,* vol. 6, no. 3, pp. 245-256, 1975.

[111] E. W. Lang, Y. Mudaliar, J. Lagopoulos, N. Dorsch, A. Yam, J. Griffith and J. Mulvey, "A Review of Cerebral Autoregulation: Assessment and Measurements," *Australasian Anaesthesia,* pp. 161-172, 2005.

[112] F. P. Tiecks, C. Douville, S. Byrd, A. M. Lam, D. W. Newell, "Evaluation of impaired cerebral autoregulation by the Valsalva maneuver.," *Stroke,* vol. 27, no. 7, pp. 1177-1182, 1996.

[113] P. M. Venturelli, A. M. Brunser, J. Gaete, S. Illanes, J. López, V. V.Olavarría, A. Reccius, P. Brinck, F. González, G. Cavada, P. M. Lavados, "Reliability of Hand-Held Transcranial Doppler with M-mode Ultrasound in Middle Cerebral Artery Measurement," *Journal of Medical Ultrasound,* vol. 25, no. 2, pp. 76-81, 2017.

[114] B. Sedighi, H. A. Ebrahimi, S. Jabbarpour and Kaveh Shafiee, "Transcranial doppler sonography diagnostic value for the cerebral flow velocity changes in the interictal phase of classic migraine," *Caspian J Intern Med,* vol. 2, no. 1, pp. 178-182, 2011.

[115] L. Ljung, System Identification: Theory for the user, Second ed., Upper Saddle River, NJ: Printice Hall, 1999.

[116] K. Yana, J. P. Saul, R. D. Berger, M. H. Perrott, R. J. Cohen, "A time domain approach for the fluctuation analysis of heart rate related to instantaneous lung volume," *IEEE Trans Biomed Eng.,* vol. 40, no. 1, pp. 74-81, 1993.

[117] F.A. Zeiler, P. Smielewski, J Donnelly, M.Czosnyka, D. K. Menon, A. Ercole, "Estimating Pressure Reactivity Using Noninvasive Doppler-Based Systolic Flow Index," *Journal of Neurotrauma,* vol. 35, no. 4, pp. 1559-1568, 2018.

[118] J. R. Caldas, , R. B. Panerai, A. S. M. Salinet, E. Bor-Seng-Shu, F. R. Galas, G. S. R. Ferreira, L. Camara, R. H.Passos, J. P. Almeida, R. C. Nogueira, M. Oliveira, T. G. Robinson, L. A. Hajjar, "Dynamic cerebral autoregulation is impaired during sub-maximal isometric handgrip in patients with heart failure," *American Journal of Physiology-Heart and Circulatory Physiology,* vol. 315, no. 2, pp. 254-261, 2018.

[119] J. Hayano, K.Ohashi, Y. Yoshida , E. Yuda, T. Nakamura, K. Kiyono, Y. Yamamoto, "Increase in random component of heart rate variability coinciding with developmental and degenerative stages of life," *Physiological Measurement,* vol. 39, no. 5, 2018.

[120] H. Akaike, "On The Use of A Linear Model For The Identification of Feedback Systems," *Annals of the Institute of Statistical Mathematics,* vol. 20, no. 1, pp. 425-439, 1968.

[121] K. H. Chon and R. J. Cohen, "Linear and Nonlinear ARMA Model Parameter Estimation Using an Artificial Neural Network," *IEEE TRANSACTIONS ON BIOMEDICAL ENGINEERING,* vol. 44, no. 3, pp. 168-174, 1997.

[122] A. Kizilkaya, A. H. Kayran, "ARMA model parameter estimation based on the equivalent MA approach," *Digital Signal Processing,* vol. 16, no. 6, pp. 670-681, 20066.

[123] MathWorks, "PDF documnetation for system identification toolbox," 2016. [Online]. Available: https://www.mathworks.com/help/ident/index.html?s_cid=doc_ftr.

[124] H. Akaike, "Fitting Autoregressive Models For Prediction," *Annals of the Institute of Statistical Mathematics,* vol. 21, no. 1, pp. 243-247, 1969.

[125] Y.Feng, L.Liu, S.Xia, J.-F.Xu, R.Bergquist, G.J.Yang, "Chapter Seven - Reaching the Surveillance-Response Stage of Schistosomiasis Control in The People's Republic of China: A Modelling Approach," *Advances in Parasitology,* vol. 92, pp. 165-196, 2016.

[126] Mathworks, "PDF Documentation for Signal Processing Toolbox," 2016. [Online]. Available: https://www.mathworks.com/help/pdf_doc/signal/index.html. [Accessed 20 November 2018].

[127] Das AM, Khayat R., "Hypertension in obstructive sleep apnea: risk and therapy," *Expert Rev Cardiovasc Ther.,* vol. 7, no. 6, pp. 619-626, 2009.

[128] Patzak A, Mendoza Y, Gesche H, Konermann M, "Continuous blood pressure measurement using the pulse transit time: Comparison to intra-arterial measurement," *Blood press,* vol. 24, no. 4, pp. 217-221, 2015.

[129] M T G García, M F T Acevedo, M R Guzmán, R A de Montaner, B F Fernández, G. Río Camacho, N González-Mangado, "Can Pulse Transit Time Be Useful for Detecting Hypertension in Patients in a Sleep Unit?," *Arch Bronconeumol.,* vol. 50, no. 7, p. 278–284, 2014.

[130] Ruiping Wang, Wenyan Jia, Zhi-Hong Mao, Robert J. Sclabassi, and Mingui Sun, "Cuff-Free Blood Pressure Estimation Using Pulse Transit Time and Heart Rate," in *IEEE*, Hangzhou, China, 2014.

[131] C. Favilla, R. Mesquita, M. Mullen, T. Durduran, M. Kim, D. Minkoff, S. Kasner, G. Joel, A. Yodh, J. Detre, "Optical Bedside Monitoring of Cerebral Blood Flow in Acute Ischemic Stroke Patients during Head of Bed Manipulation (P4.216)," *Neurology ,* vol. 82, no. 10, 2014.

[132] H. S. Markus, "Cerebral perfusion and stroke," *Journal of Neurology, Neurosurgery & Psychiatry,* vol. 75, pp. 353-361, 2004.

[133] A. Zauner and J. P. Muizelaar, "Brain metabolism and cerebral," in *Head Injury*, London, Chapman & Hall, 1997, pp. 89-99.

[134] J. Allen, "Photoplethysmography and its application in clinical physiological measurement," *Physiological Measurement,* vol. 28, no. 3, pp. R1-39, 2227.

[135] Y. Sun and N. Thakor, "Photoplethysmography Revisited: From Contact to Noncontact, From Point to Imaging," *IEEE TRANSACTIONS ON BIOMEDICAL ENGINEERING,* vol. 63, no. 3, pp. 463-477, 2016.

[136] C. M. Lee, and Y. T. Zhang, "Reduction of motion artifacts from photoplethysmographic recordings using a wavelet denoising approach," in *IEEE*, 2003.

[137] K. W. Chan, and Y. T. Zhang, "Adaptive Reduction of Motion Artifacts from Photoplethysmography recording using a Variable Step-size LMS Filter," *Sensors Proc. IEEE,* pp. 1343-1347, 2002.

[138] H. Han, M. J. Kim, and J. Kim, "Development of real-time motion artifact reduction algorithm for a wearable photoplethysmography," *Proceedings of the 29th Annual International Conference of the IEEE EMBS,* pp. 1538-41, 2007.

[139] Aaslid R, Lindegaard KF, Sorteberg W, Nornes H, "Cerebral autoregulation dynamics in humans," *Stroke,* vol. 20, no. 1, pp. 45-52, 1989.

[140] R. Alex, G. Bhave, M. A. Al-Abed, A. Bashaboyina, S. Iyer, D. E. Watenpaugh, R. Zhang, K. Behbehani, "An Investigation of Simultaneous Variations in Cerebral Blood Flow Velocity and Arterial Blood Pressure during Sleep Apnea," in *EMBC*, San Diego, CA, 2012.

[141] Tiecks FP, Lam AM, Aaslid R and Newell DW, "Comparison of static and dynamic cerebral autoregulation measurements," *Stroke,* vol. 4, pp. 1014-1019, 1995.

[142] Rolf R. Diehl, Dieter Linden, Dorothee Lücke, Peter Berlit, "Phase Relationship Between Cerebral Blood Flow Velocity and Blood Pressure," *Stroke,* vol. 26, no. 10, pp. 1801-1804, 1995.

[143] R. Zhang, Kh, Behbehani, B. D. Levine, "Dyniamc pressure-flow relationship of the cerebral circulation during acute increase in arterial pressure," *J. Phyiol.,* vol. 587, pp. 2567-2577, 2009.

[144] Schmalgemeier H, Bitter T, Bartsch S, Bullert K, Fischbach T, Eckert S, Horstkotte D, Oldenburg O, "Pulse transit time: validation of blood pressure measurement under positive airway pressure ventilation," *Sleep and Breathing,* vol. 16, no. 4, pp. 1105-1112, 2012.

[145] J. A. J. P. a. P. L. R. Smith, "Pulse transit time: an appraisal of potential clinical applications," *Thorax,* vol. 54, no. 5, pp. 452-457, 1999.

[146] R. M. Alex, "AN INVESTIGATION OF THE EFFECT OF OBSTRUCTIVE SLEEP APNEA," UTA library, Arlington, 2015.

[147] J Pagani, MP Villa, G Calcagnini, E Lombardozzi, F Censi, S Poli, P Bartolini, V Barbaro, R Ronchetti, "Detection of Central and Obstructive Sleep Apnea in Children using Pulse," *Computers in Cardiology,* vol. 29, pp. 529-532, 2002.

[148] Nikolaus Netzer, Arn H. Eliasson, Cordula Netzer, David A. Kristo, "Overnight Pulse Oximetry for Sleep-Disordered Breathing in Adults," *Chest,* vol. 120, no. 2, pp. 625-633, 2001.

[149] R. Kahankova, R. Jaros, R. Martinek, J. Jezewski, H. Wen, M. Jezewski & A. Kawala-Janik, "Non-Adaptive Methods of Fetal ECG Signal Processing," *Advances in Electrical and Electronic Engineering,* vol. 15, no. 3, pp. 476-490, 2017.

[150] Paulson OB, Strandgaard S, Edvinsson L., "Cerebral autoregulation," *Cerebrovasc Brain Metab Rev,* vol. 2, no. 2, pp. 161-92, 1990.

[151] M. Siebler, M. Daffertshofer, M. Hennerici, H. J. Freund, "Cerebral blood flow velocity alterations during obstructive sleep apnea syndrome," *Neurology,* vol. 40, no. 9, pp. 1461-1462, 1990.

[152] M. Siebler, A. Nachtmann, "Cerebral hemodynamics in obstructive sleep apnea," *Chest,* vol. 103, no. 4, pp. 1118-1119, 1993.

Author Biography

Armin Soltan zadi was born as the first child of Pooran Nahed and Ghasem Soltan zadi in March 1982 in Tehran, Iran. He then brought up in Bandar-e-Anzali, in northern part of Iran until the end of his high school when he moved back to Tehran. After finishing his bachelor in electrical engineering, he admitted to University of Tehran, best and first inaugurated university in Iran, to pursue a Master degree in Biomedical engineering in 2006. After earning his Master degree in 2009, Mr. Soltan zadi joined a private company and earned his most valuable lessons and learned how to apply his knowledge to the field. After 6 years of work experience, he was motivated enough by his interest in medical instrument industry, to make the decision to move to US in 2014 and pursue a PhD in Biomedical engineering at University of Texas at Arlington. He has worked on modeling of vital signals during sleep and investigated different aspects of apnea and in general sleep disordered breathing diseases on systemic and cerebral hemodynamics. Mr. Soltan zadi plans to join a top tier company in eye care industry, Alcon Inc. in May 2019.